FLIGHT CHARACTERISTICS OF A TILT-WING, DISTRIBUTED-PROPULSION, VERTICAL TAKE-OFF AND LANDING AIRCRAFT CONCEPT

By

SEABROOK R. WHYTE

Bachelor of Science in Aerospace Engineering

Oklahoma State University

Stillwater, Oklahoma

2015

Submitted to the Faculty of the
Graduate College of
Oklahoma State University
in partial fulfillment of
the requirements for
the Degree of
MASTER OF SCIENCE
May 2018

FLIGHT CHARACTERISTICS OF A TILT-WING DISTRIBUTED-PROPULSION, VERTICAL TAKE-OFF AND LANDING AIRCRAFT CONCEPT

Thesis Approved:

Dr. Jamey Jacob

Thesis Adviser

Dr. Kurt Rouser

Dr. Rick Gaeta

ACKNOWLEDGEMENTS

I would like to thank Dr. Jamey Jacob for all of his advice and guidance throughout my graduate and undergraduate careers here at Oklahoma State University. His support has been invaluable in my pursuit of higher education. Additionally, my committee deserves a great deal of thanks for their advice and enthusiasm for the project. A sincere thank you to Fred Keating, Taylor Mitchell, and Dane Johnson for their help and support with autopilot issues. My gratitude also goes to Aavron Estep for help on the early building phases of the aircraft, to Allan Burba for his flexibility and willingness in lending a means of transporting equipment, to Greg Covey and Nathan Eick on the Ardupilot forum for vast clarification of VTOL fixed wing parameters and troubleshooting with the Pixhawk, and to Jordan Feight for his help with XROTOR. Thank you to all my colleagues for all of their encouragement and input.

To my parents, my unwavering gratitude, for I would not be where I am today if they had not challenged me to tackle daunting tasks. Their support throughout my life has made me who I am today. I would also like to thank Maria Yepez for her unconditional support and constancy every step of the way, and for enduring the late nights at the lab all too often. Not least of all, I am grateful for my grandmother and aunt who have been nothing but supportive in my life and scholastic endeavors.

Name: SEABROOK R. WHYTE

Date of Degree: MAY, 2018

Title of Study: FLIGHT CHARACTERISTICS OF A TILT-WING DISTRIBUTED-PROPULSION, VERTICAL TAKE-OFF AND LANDING AIRCRAFT CONCEPT

Major Field: MECHAICAL & AEROSPACE ENGINEERING

Unmanned aircraft are starting to be utilized in a diverse set of applications ranging from military surveillance to railroad inspections and natural disaster damage assessment. Given the nature of these missions, runways may not be available and long distance, high endurance flights required. Fixed wing aircraft typically have the endurance required for these missions, but require long flat areas for landing, and in some cases taking off. There have been various approaches to fixed wing aircraft taking off and landing vertically, but these systems generally have reduced endurance and efficiency. A proposed solution by to this issue is ElectraWing. This aircraft concept was designed by retired Boeing Technical Fellow Darrold Cummings and utilizes a tilting wing and horizontal stabilizer, distributed propulsion, and a twin-boom design. The goal of this project was to determine the flight characteristics of the tilt-wing distributed-propulsion vertical take-off and landing aircraft concept, ElectraWing. A base airframe was selected and modified to test the concept. The effect of tilt-wing transient weight distribution on longitudinal static stability was considered and the aircraft was determined to be statically stable. Additionally, wind effects on the aircraft in VTOL flight and the effects of VTOL flight on the wing rotation joint was examined. It was found the aircraft was susceptible to wind without appropriate compensation. It was also found that VTOL flight caused high shear stress to the point of rotation on the wings.

TABLE OF CONTENTS

LIST OF TABLES

LIST OF FIGURES

Figure Page

CHAPTER I

INTRODUCTION

1.1 MOTIVATION

Companies and government entities are utilizing unmanned aircraft for simple and inexpensive solutions to performing large tasks ranging from railroad and power line inspections to search and rescue missions in disasters and military surveillance. Due to the nature of these missions, there may not be a runway available for a conventional take-off and landing. Therefore, a vertical take-off and landing aircraft (VTOL) would be useful. However, aircraft capable of VTOL typically sacrifice range and endurance. Looking at helicopters and multi-rotors, the endurance is not very high, and most of these missions require longer flight distances and endurances. Helicopters excel when it comes to hovering efficiency due to their large rotor area, but their downfall is in forward flight. They have poor energy conversion in horizontal flight, supersonic tip speed limitations, and are very mechanically complex. For this reaon, a VTOL fixed wing aircraft would be advantageous. it would have the capability to take-off and land almost anywhere, but also have the forward flight efficiency required for the stated missions.[1]

The idea of an aircraft that can fly horizontally and take-off vertically is not a new one. There have been many aircraft throughout history that have been designed to do just that. These aircraft range from the Convair XFY-1 to the LTV XC-142A and V-22 Osprey. More recently,

the NASA GL-10 Greased Lightning, and the Joby S2. These latter aircraft employ a "blown wing" (or distributed electric propulsion/DEP) configuration due to their having multiple propellers across the leading edge of the wing. By doing this, they increase the maximum lift coefficient by increasing the dynamic pressure across the wing section at lower freestream velocities. This property enables the aircraft designers to reduce the wing's chord to achieve stall speed requirements on take-off and landing. Reducing the wing's chord, results in reduced drag in the cruise condition.2 From NACA/NASA's early attempts at VTOL capable aircraft in the 1950s and 1960s, they found that this blown wing design was needed for tilt-wing aircraft in order to keep the aircraft from stalling while in the transition phase between vertical and horizontal flight.[3]

The hypothesis proposed here is a design by Retired Boeing Technical Fellow, Darrold Cummings. This aircraft utilizes distributed hybrid electric propulsion in conjunction with vertical take-off and landing capabilities. The aircraft, called ElectraWing, will have a twin boom design with a box tail (see Figure 1, below), and be capable of conventional take-off and landing (CTOL), short take-off and landing (STOL), and VTOL. The twin boom design allows for the fuselage to be a highly customizable aerodynamic body. It will allow for an overall modular design in which the fuselage can change shape and size depending on the payload needed and for center of gravity adjustments. For this design, the entire power system would be in the booms of the aircraft, and not in the fuselage like conventional aircraft. Having the booms also allows for a wider wheel base on the main gear, as opposed to NASA's Greased Lightning, where the landing gear has to be stored in the fuselage since the entire wing rotates. The wider wheel base landing gear provides more stability while on the ground.[4]

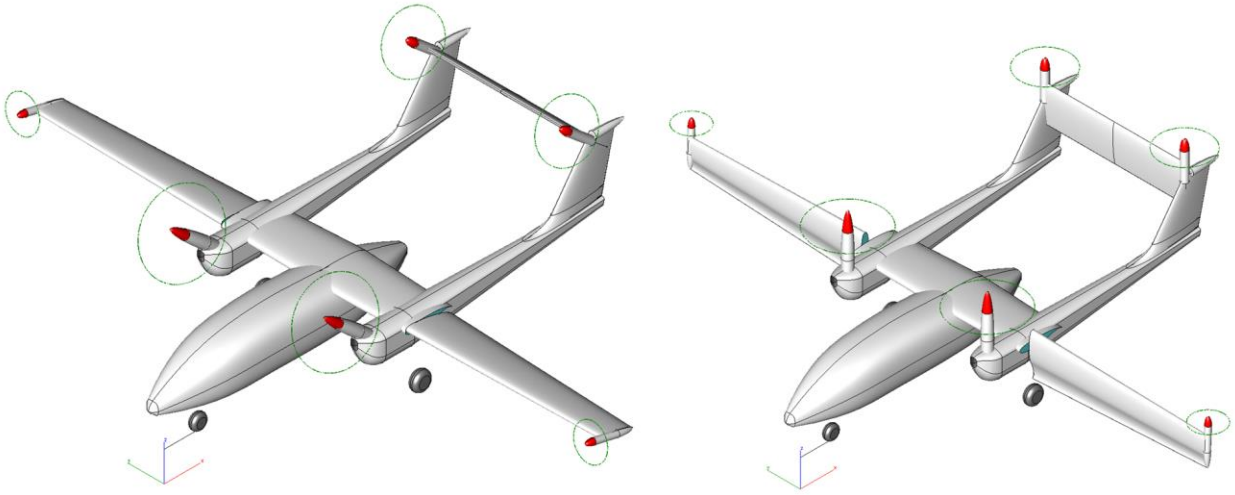

Figure 1: ElectraWing concept by Darrold Cummings in both the STOL (left) and VTOL (right) configurations.

Ideally, ElectraWing would have two turboshafts: one on each boom. These turboshafts would drive generators that would keep batteries charged to power electric motors placed in unconventional positions around the aircraft. However, for the radio controlled (RC) proof of concept version of this vehicle, there would be two gas engines, and four electric motors. Initially, the aircraft would have motors on the wingtips for vortex control. They would also provide additional lift and roll control when in the vertical flight mode. Two motors are expected to be located on the aircraft horizontal stabilizer to provide propeller wash over the stabilizer and elevator to increase control authority. They would also provide redundant lift for the aircraft in addition to pitch control when in the vertical flight mode. After considering the change in CG and structure necessary for the wing, this model could be easily scaled to a larger UAV or a large manned cargo aircraft (figures 2 and 3, below).[4]

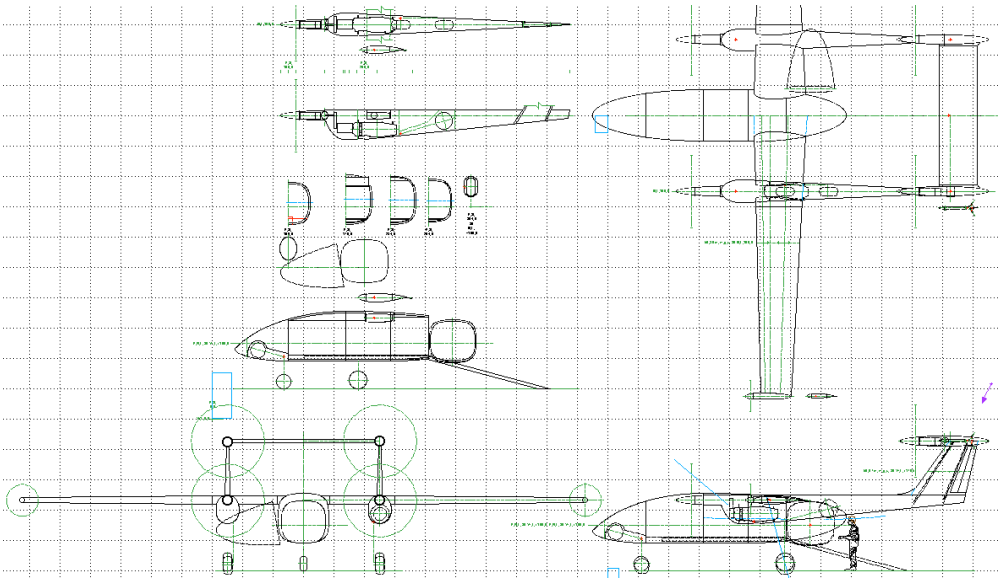

Figure 2: Larger scale cargo UAV concept by Darrold Cummings.

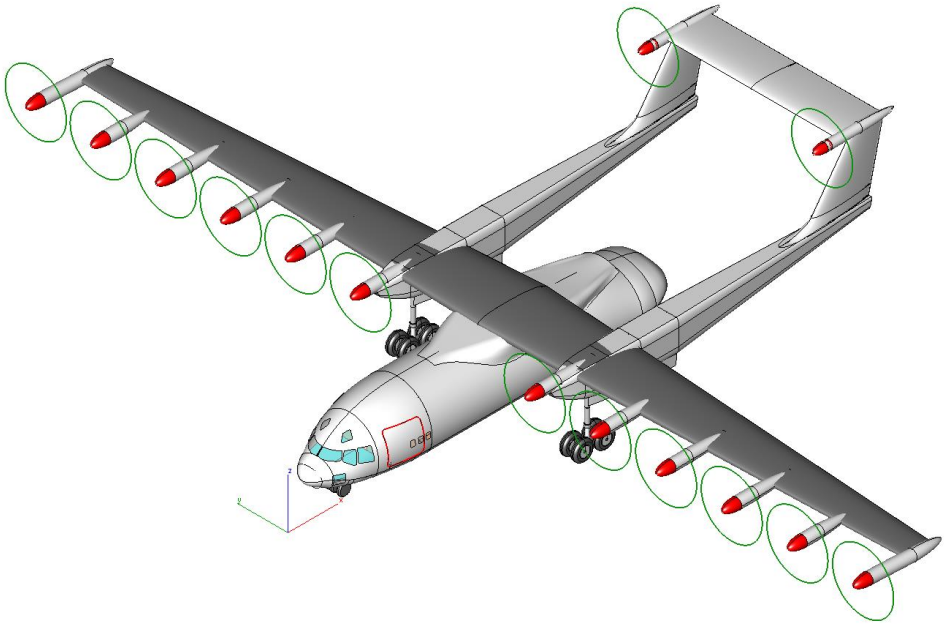

Figure 3: Large manned cargo variant of ElectraWing by Darrold Cummings.

1.2 GOALS & OBJECTIVES

The goal of this project was to evaluate the flight characteristic of the tilt-wing distributed-propulsion vertical take-off and landing aircraft concept proposed by Darrold Cummings. To evaluate the flight characteristics, three objectives were identified: 1) evaluate the effect of tilt-wing transient take-off and cruise weight distribution on flight characteristics, 2) evaluate the effect of tilt-wing transient orientation on vertical take-off characteristics, and 3) evaluate the effect of VTOL flight characteristics on tilt-wing structure. To accomplish each of these objectives, the following tasks were outlined:

- Objective 1
  - Calculate thrust and weight of the aircraft
  - Build initial test platform and estimate weight distribution
  - Test initial test platform
  - Modify the initial test platform for VTOL capabilities
  - Account for effects of intermediate wing rotation angles on center of gravity (CG) location
- Objective 2
  - Calculate flat plate force of wind on wing in vertical configuration and as wing rotates
  - Plot 2D trajectory of aircraft taking off vertically in wind and without wind
  - Test aircraft in CTOL with rotation mechanisms in place
  - Increment testing from CTOL to STOL and finally test aircraft in VTOL configuration
- Objective 3
  - Estimate maximum moment on joints between outboard and inboard wing sections while in VTOL flight configuration
  - Estimate maximum transverse shear stress on wing joint

First chapter II of this study will research past work in VTOL and distributed propulsion systems pertinent to the investigation of the ElectraWing concept. The procedures for this project, outlined in the above tasks, will then be discussed in chapter III. STOL performance will be briefly looked at as it will be utilized to test the aircraft's in-flight wing rotation capabilities and stability. Chapter IV will contain the results of all tests, and chapter V will include a discussion of the results, design conclusions and recommendations, and future work.

CHAPTER II

PREVIOUS WORK

2.1 UNMANNED AIRCRAFT CONFIGURATIONS

To achieve VTOL flight with aircraft, there are numerous approaches that can be taken. A few different methods are rotary wing aircraft (helicopters), multi-rotor aircraft (quadcopters, hexacopters, etc..), and convertible rotor aircraft which can be further broken down into two categories: tilt-rotor aircraft (V-22 Osprey and Bell Eagle Eye), and tilt-wing aircraft (XC 142A). There are many other methods to VTOL aircraft, but these four are the most relevant to this thesis.

With rotary wing aircraft, or helicopters, there is one main rotor that rotates on a horizontal plane, and one small rotor that rotates on a vertical plane, perpendicular to the main rotor. The main rotor tends to cause a torque that wants to rotate the fuselage of the aircraft. The smaller vertical rotor (tail rotor) produces thrust to counteract the yaw moment imposed by the main rotor. This tail rotor typically adds approximately 10% to the aircraft's power demands. Due to the complexity of helicopter rotor mechanisms (cyclic and collective rotor pitch) and the asymmetry they inherently have, this makes it difficult for flight controllers to handle. Additionally, the tail rotor is relatively fragile and highly susceptible to tail strikes on the ground.[5]

Multi-rotor aircraft, such as quadcopters and hexacopters, reduce the mechanical complexity problems seen by helicopters, in addition to not having a tail rotor that is prone to tail strikes. These aircraft utilize fixed pitch propellers directly mounted to electric motors. They move by producing RPM (thrust) changes to the required motors to enable the aircraft to pitch, roll, and yaw. They also generally use an even number of motor/propeller combinations and have half of them rotating clockwise and half of them rotating counter-clockwise. This makes the overall torque in the hover configuration be in equilibrium. The downside to this configuration is that they are more susceptible to wind gusts than other aircraft configurations, and in the event of one or more motors failing, the aircraft is likely to become uncontrollable and crash.[5]

Within the category of convertible rotor aircraft, there are two approaches: tilt-rotor and tilt-wing. Tilt-rotor aircraft, like the V-22 Osprey and the Bell Eagle Eye (Figure 4, below) have been widely successful in real world applications. They are fixed wing aircraft that can take-off and land vertically. They utilize two engines and rotors: one on each wingtip. The wings of the aircraft stay fixed, while the rotors are capable of rotating 90 degrees. When the engines are vertical (propeller plane parallel to the ground), the thrust is directed downward and the aircraft takes off or lands like a helicopter. When the engines rotate horizontally (propeller plane perpendicular to the ground), they act as the fixed-wing aircraft's propulsion system.[5]

Figure 4: Bell Eagle Eye in the hover/VTOL phase of flight. Picture from Drew [9].

Tilt-wing aircraft, like the XC-142A (further discussed in section 2.2.1), have also been approached a few different times throughout the history of VTOL aviation. These aircraft typically have a wing located on the top of the fuselage that rotates. Attached to the wing are multiple engine/propeller combinations across the length of the wing. Additionally, a horizontal rotor is needed in the tail of the aircraft for stability and/or additional lift. Traditionally, tilt-rotor aircraft are more efficient in the hover/VTOL phase of flight than tilt-wing aircraft, but tilt-wing aircraft are more efficient in the horizontal flight phase.[5]

2.1.2 ADVANTAGES OF DISTRIBUTED PROPULSION

Distributed propulsion is a system in which instead of having one or two main sources of propulsion, it is broken up into multiple smaller sources. The benefits include noise reduction, shorter distances required for conventional take-off and landings, and increased efficiency.[6] The shorter take-off distances are due to inducing a higher velocity across the wing by means of the propeller at lower freestream airspeeds. This induced airspeed also allows the air to remain

attached to the wing at higher angles of attack. Another result of induced velocity is that it increases the maximum lift coefficient across the wing section which enables the aircraft to have a smaller chord length, which will reduce drag on the aircraft.[2] Additionally, by having motors/propellers on the wingtips, the wingtip vortices can also be controlled, and consequentially the aircraft efficiency is increased.[4]

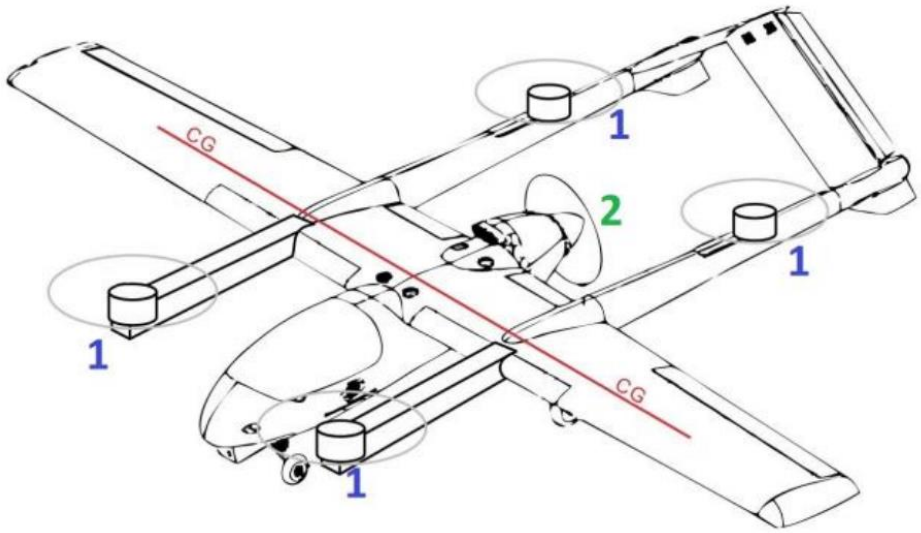

Figure 5: RMRC Anaconda VTOL hybrid with four lifting motors (1) and one forward propulsive motor (2). This illustration is from Cummings [7].

There have been many different attempts at VTOL UAVs in recent years, but most of the research has not been with distributed electric propulsion or tilting wing UAVs. The most common type of UAV researched is a hybrid between a quadcopter planform and a typical fixed wing UAV. An example of this method of VTOL can be seen in Figure 5, above. This aircraft concept uses four motors permanently mounted vertically (labeled: 1) for the vertical flight phases, and one motor that pushes the aircraft horizontally (labeled: 2). This image depicts a ReadyMadeRC (RMRC) Anaconda (the base aircraft of this study).

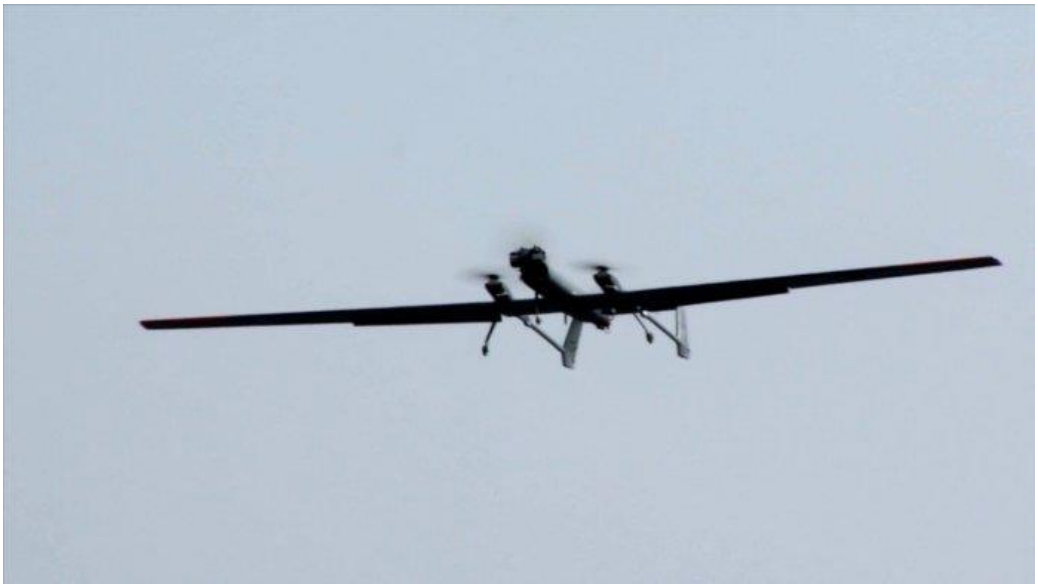

Figure 6: The Israel Aerospace Industries Panther-FE proof of concept in vertical flight. Image from Austin [8].

This attempt to VTOL has been used in various aircraft, including the Panther-FE (Figure 6, above) developed by Israel Aerospace Industries (IAI) and Hankuk Carbon (a South Korean company). This UAV is a proof of concept UAV for South Korea and uses a similar planform to that seen in Figure 5, above. The difference being that it uses three electric motors for vertical propulsion, and an internal combustion engine for horizontal flight.[8] There are no known published papers on this aircraft. Another example of a similar concept is the Quantum Tron UAV (see Figure 7, below), developed by the German based company, Quantum-Systems. This aircraft uses four electric motors that rotate vertically for VTOL. The aircraft then transitions to forward flight by rotating the front two motors forward, and the rear two motors backward. The two motors in front are the driving motors for forward flight, and the rear motors have collapsible propellers that close to become more streamline. The aircraft boasts a flight time of up to 90 minutes and a maximum take-off weight of 14 kg. The cruise speed is between 32 and 48 knots.[9, 10]

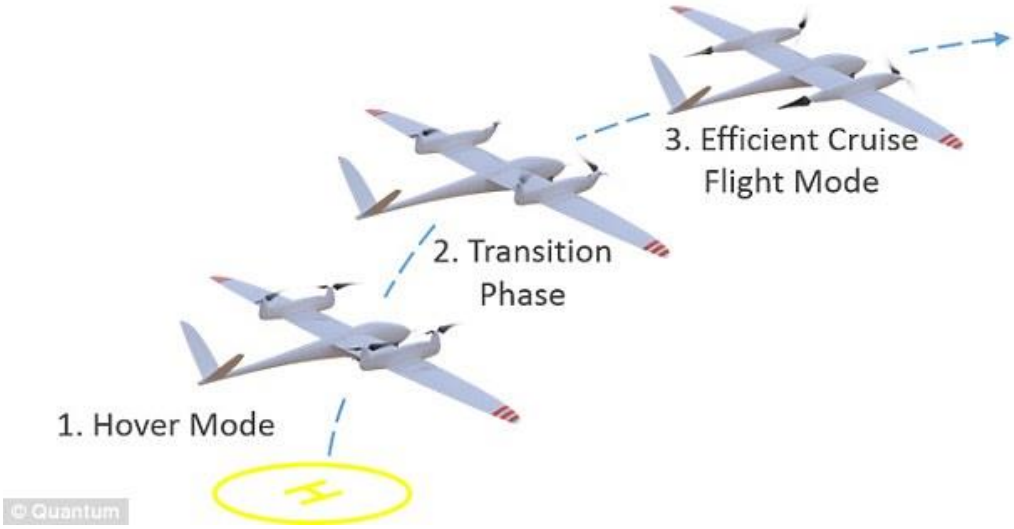

Figure 7: Quantum Tron by Quantum-Systems. The aircraft first uses all four motors for the vertical take-off and landing (1), then the motors rotate in opposite directions to transition to forward flight (2). The aircraft only uses the front two motors for forward flight (3). Image from Drew [9].

The issue with this method to fixed-wing VTOL aircraft is that some or all the motors that make the aircraft fly vertically become dead weight as well as create parasite drag for the aircraft. For such a situation, distributed electric propulsion is useful. A project to study distributed electric propulsion (DEP) was started in 2014 by researchers from NASA Langley Research Center and Armstrong. These two organizations partnered with Emperical Systems Aerospace (ESAero) and Joby Aviation. This project was named Leading Edge Asynchronous Propeller Technology (LEAPTech) and its purpose was to prove that tighter propulsion/airframe integration could improve the efficiency and safety of aircraft and have a positive environmental impact. LEAPTech was also supposed to help NASA in their goal to promote the aircraft industry to transition to electric powered aircraft within the next decade.[11] A picture of the LEAPTech concept can be seen in Figure 8, below.

Figure 8: NASA LEAPTech concept image. Picture from Ranstone & Jones[12].

Joby Aviation was responsible for the design and manufacturing of LEAPTech's electric motors, propellers, and wing.[11] According to a study published in 2014 by Alex M. Stoll and JoeBen Bevirt of Joby Aviation, DEP is capable of increasing the coefficient of lift of a wing and decreasing the drag when in the cruise condition. This is due to the induction of flow over the wing at slow speeds which increases the dynamic pressure. The baseline comparison was with the Cirrus SR22 as it is approximately the same size aircraft. Stoll and Bevirt state that LEAPTech could achieve a predicted coefficient of lift of 20 when flying at 200 mph in the cruise condition. This compares to the SR22's lift coefficient of 11 at an equal speed. They also noted that if the propellers on a given wing all rotate in the same direction, swirl is imparted into the slipstream which increases the angle of attack (AoA) on one side of the propeller and decreases it on the other, but Stoll and Bevirt also state that swirl can be overcome by counter-rotating propellers. However, counter rotating propellers would increase the complexity and noise of the system.

Although they claim to have figured out how to reduce swirl without counter-rotating propellers, they do not discuss specifically how.[13]

Figure 9: Canadair CL-84 in the transitional flight phase. Picture from Royal Aviation Museum of Western Canada [28].

Another demonstrator of how distributed electric propulsion can benefit STOL and VSTOL (very short take-off and landing) aircraft is with the Canadair CL-84 Tilt Wing Design, shown in Figure 9, above. Canadair conducted seven years of VSTOL studies before they started designing the CL-84 in 1963. This aircraft, despite only having two engines/propellers, had similar properties to DEP aircraft today. The aircraft can rotate its wing and horizontal stabilizer for VSTOL and VTOL capabilities. It also had a tail rotor for stability purposes. The two propellers (each 14 ft in diameter) completely immersed the wing in flow – Figure 10, below. This, not unlike DEP, induced a flow over the wing of the aircraft. Because of this induction of flow, when the aircraft was in the STOL/VSTOL configurations or transitional flight, the wing was prevented from stalling.[14]

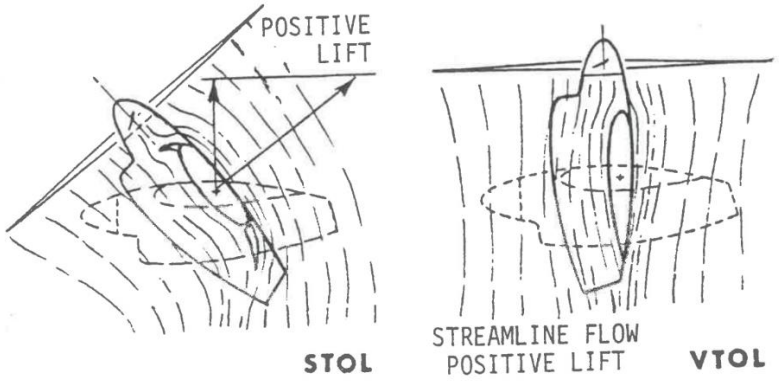

Figure 10: Illustration of the induced flow over the wing of the CL-84 in the STOL and VTOL configurations. Illustration from Stoll, Bevirt, Pei & Stilson [14].

To summarize this section, DEP offers many advantages for aircraft. These advantages range from higher efficiencies and lift coefficients in the cruise conditions to induced flows over the wing in the VSTOL and transitional flight phases. These are all reasons that DEP is being pursued in the ElectraWing concept.

2.2 VTOL CONCEPTS

In this section, a few different approaches to VTOL will be examined, but emphasis will be on the blown-wing and tilt-wing concepts.

2.2.1 LTV XC-142A

Figure 11: LTV XC-142A in VTOL configuration (left). The aircraft has a tilting wing to transition between vertical and forward flight. In the middle image, it can be seen that it has a rotor on the tail that rotates in the horizontal plane to ensure stability when in the vertical flight configuration. This rotor stops rotating when in forward flight. On the right, the aircraft can be seen in the forward flight configuration. Pictures from Ozdemir [4] and globalsecurity.org.

The LTV XC-142A, seen above in Figure 11, was first flown in 1964, and was intended to be a military troop and cargo transport aircraft that could fly long range and land nearly anywhere.[15] This aircraft was one of the earlier attempts at a tilting wing VTOL aircraft. It utilized four General Electric T64-GE-1 free turbine turboprop engines for its main propulsion system. These engines drove the four main propellers and the tail rotor. For cruise, the tail rotor was declutched and braked so it would not keep spinning. Ultimately, this aircraft was found to use more runway for take-off and landing in the STOL configuration than was initially anticipated – take-off distance over a 50 ft obstacle was 500 ft and landing over a 50 ft obstacle had a 860 ft roll. In addition to this, the thrust in the VTOL configuration was approximately 12% less than predicted.[16] It was this, combined with stability issues and a crash causing the death of three people that eventually caused an end to the XC-142 project. [15]

2.2.2 NASA Greased Lighting

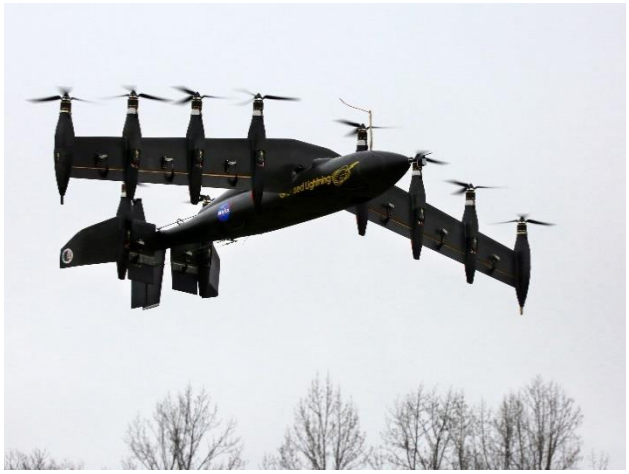

Figure 12:NASA GL-10, Greased Lightning during a flight test. Photo from NASA

NASA has been working on a distributed hybrid electric propulsion (DHEP) aircraft called GL-10, or Greased Lighting. The aircraft was named Greased Lightning for two reasons. One reason is that it utilizes a diesel engine that can run on a variety of different heavy fuels, including bio diesel which comes from fryer oil (grease). The second reason is that it utilizes electric propulsion (lightning). A picture of this aircraft flying can be seen in Figure 12, above.[17]

Greased Lightning utilizes two diesel engines onboard that rotate alternators to supply power for the battery system that powers the electric motors. This aircraft also utilizes a blown wing design to help prevent the aircraft from stalling while transitioning between vertical and forward flight modes. This was discovered by NACA/NASA in the 1950s and 1960s. In addition to this, electric motors were chosen in part for the propulsion system for their ability to be scaled easily. Additionally, while in the cruise condition, only two motors remain spinning: the two at the wingtips. These wingtip motors spin opposite the wingtip vortices which helps reduce the induced drag naturally seen by the aircraft.[17] A picture of the aircraft in the forward flight configuration

and vertical flight configuration can be seen in Figure 13, below. It should also be noted that this aircraft uses retractable rods for landing gear at the nose and also perches on its tail and wingtips. This prohibits the aircraft from landing conventionally if needed and limits it to VTOL.

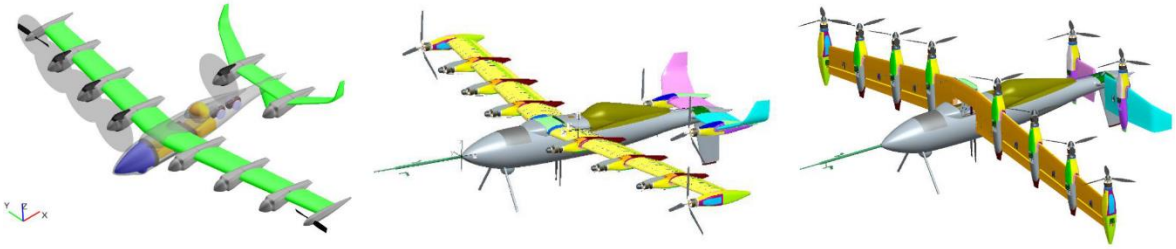

Figure 13: This image illustrates the aircraft in the forward and vertical flight configurations. In the forward flight configuration, the inboard motors stop spinning, and the propellers fold in to reduce drag, while the outside most two keep rotating and provide the thrust to sustain flight. In the vertical flight configuration, all ten motors and propellers provide thrust for the aircraft. Picture from Ozdemir [4].

2.2.3 Joby S2

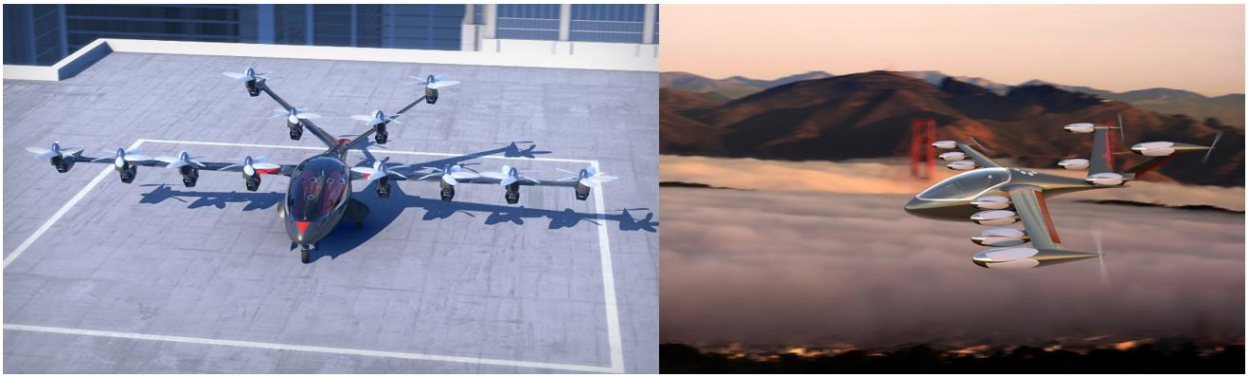

Figure 14: Joby S2 in VTOL (left) and cruise (right) configurations. Picture from Oates [18]

The company Joby Aviation is currently working on an aircraft they call the S2, as seen in Figure 14, above. This aircraft is designed to be completely electric, utilize twelve lifting motors, cruise at 200 mph, and have a range of 200 miles. Joby intends for it to be a personal manned aircraft with a capacity of two people (including the pilot).[18]

The Joby S2 uses similar concepts to NASA's Greased Lighting. The main differences being that the tail and wing do not rotate for vertical flight. Joby Aviation claims this will eliminate the threat of a single point of failure and add redundancy to the aircraft. In addition to this, the Joby S2 stops using all lifting propellers when in the cruise condition and starts using four propellers designed for cruise. These cruise propellers, like Greased Lightning, use the aircraft's wingtip vortices to help improve efficiency. The Joby S2 has yet to be built and flown and is still in the design phase.[18]

2.3 AUTOPILOT INTEGRATION FOR A TILT-WING AIRCRAFT

A tilt-wing aircraft will need to have a stabilization system onboard to ease the tasks of the pilot while in the vertical flight configuration and while transitioning to and from forward flight. There are many flight systems on the market that will stabilize a multi-rotor aircraft in a VTOL configuration, as well as other flight systems that will stabilize a fixed wing aircraft in forward flight, but the transition between vertical and horizontal flight is a more challenging task to accomplish. The autopilot/stabilization system to be used in this aircraft's proof-of-concept stage is a Pixhawk 2. This is due to a few factors: not having the time or knowledge to develop a new autopilot system, the product's price point, it being open source, and it having the capability to handle VTOL fixed wing aircraft.

2.3.1 VTOL TILT-WING CONTROLS BY MURAOKA

Figure 15: The QUX-02 airframe in transitional (top) and vertical (bottom) flight configurations. Picture from Dornheim [15].

The project by Muraoka was the design and test flight of a quad tilt wing VTOL UAV. The aircraft discussed in this paper was called the QUX-02, and is shown in Figure 15, above. This aircraft had multiple challenges. It required a Primary Flight Control System (PFCS) installed in the ground radio control (RC) system to ease the load from the pilot. This PFCS needed to be able to handle vertical flight like that of a quadcopter, horizontal flight much like a fixed wing airplane, and transitional flight which is defined as the part of the flight envelope between vertical and forward flight. See Figure 16, below, for a depiction of the flight profile for the QUX-02.15

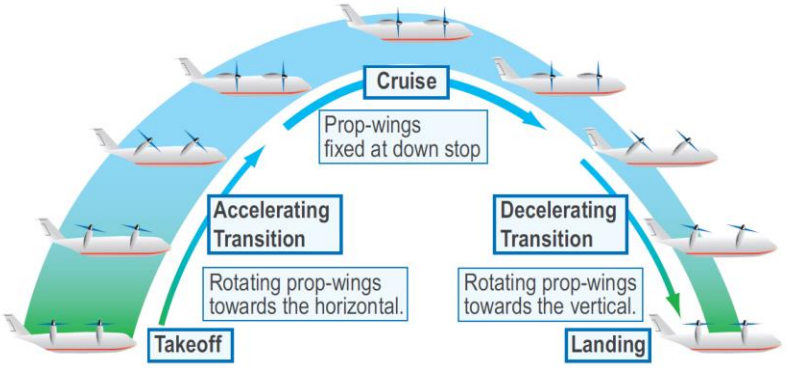

Figure 16: Flight profile for the QUX-02. Picture from Dornheim [15].

For the vertical flight component of this aircraft, the wings are rotated to 90 degrees, and the QUX-02 flies much like a quadcoper. It uses differential thrust for pitch and roll, but unlike a quadcopter, it uses the control surfaces on both sets of main wings to control the aircraft's yaw. It is claimed that in the one-engine-inoperative scenario, while in the vertical flight configuration, the thrust would be reduced in the opposite diagonal motor.[19]

For the horizontal flight configuration, the aircraft controls much like a conventional aircraft. The flaperons control both the pitch and roll of the aircraft. There is some discrepancy in the paper as to how the yaw is controlled. The paper says the yaw is controlled "by rudder or differential thrust." It seems they have the capability to control the aircraft's yaw in the horizontal flight configuration by both methods, but it is unclear which they primarily use or if they use both of these simultaneously.[19]

Both forward flight and vertical flight have well documented flight control systems, however, the problem is with the transitional stage. It is here that the aerodynamics and flight characteristics start to change significantly between flight modes. To handle this transitional phase, they use a combination of the methods for vertical and horizontal flight. While the aircraft transitions from

vertical to horizontal flight, the wings start to rotate (see Figure 16, above), and the aircraft uses a combination of differential thrust as well as aerodynamic control surfaces to maneuver. This transition is regulated by a relation with airspeed. As airspeed increases, the wings' angle of attack decreases, and the control surfaces are used more and the differential thrust is used less. This transition gradually progresses until the aircraft is flying like a conventional fixed wing aircraft. For the transition back to vertical flight, this same process is used, but in reverse.[19]

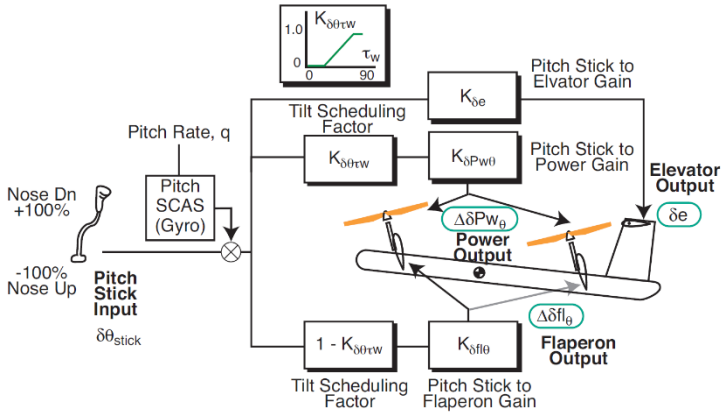

Figure 17: PFCS for the aircraft pitch. Image from Volpe [19].

The logic for the longitudinal PFCS is depicted by Muroaka in Figure 17, above. Muroaka gives very little explanation to this logic, and instead just provides the diagram. Likewise, the diagram for the overall control system can be seen in Figure 18, below. To aid in the control of the aircraft throughout its three stages of flight, a stability augmentation system was installed which utilized pitch and roll rate gyros. In addition to this, a "thrust mixing computer" is said to have been developed for the aircraft while in the vertical flight configuration.[19]

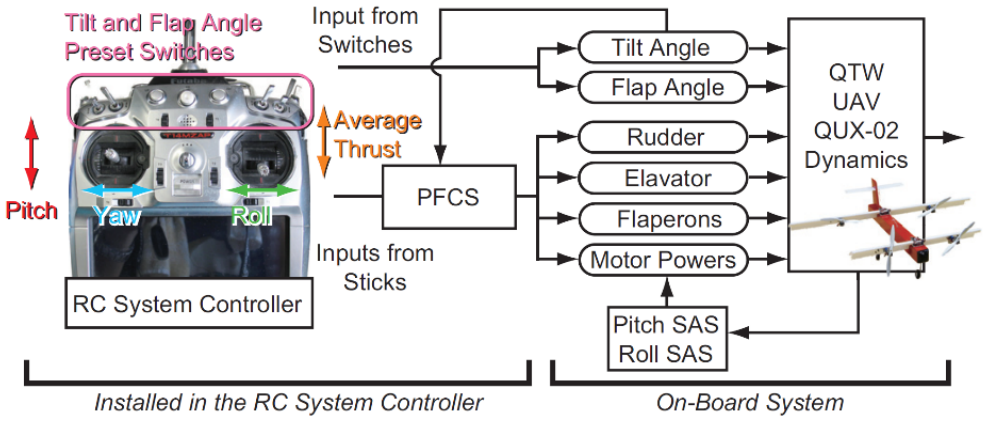

Figure 18: Overall scheme of how the QUX-02 works. Image from Dornheim [15].

2.3.2 CONTROLS OF A FLYING WING DUCTED VTOL AIRCRAFT BY BECKER

In this paper, the authors, Michael Becker and David Sheffler, developed a flying wing VTOL UAV with the University of Virginia. The goal of this project was to develop a proof of concept UAV that could meet the following requirements:

1) VTOL capability
2) Autonomous flight
3) High-speed payload delivery
4) Intelligence, surveillance, and reconnaissance mission capable
5) Improved endurance
6) Stealth capabilities

The aircraft they designed is depicted in Figure 19, below.[20]

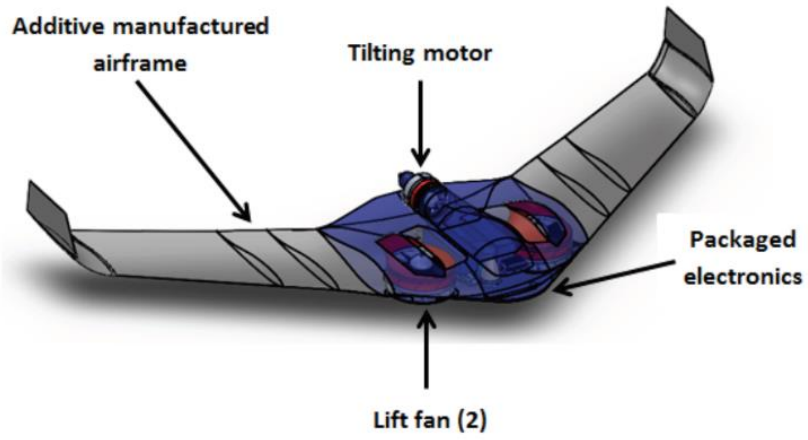

Figure 19: VTOL UAV concept designed by Becker and Sheffler. Image from Thompson [20].

This aircraft will take-off and land vertically by using two ducted fans situated vertically in the fuselage, and a rear tilting motor. When transitioning to forward flight, the fans will decrease power and eventually turn off. Simultaneously, the rear motor will tilt up and start to push the aircraft horizontally. The transition back to vertical flight will be similar, but the steps will be in reverse order. Their design is similar to the commercially available Firefly6 RC airplane.[20]

This system is said to eventually be controlled by a Samsung Galaxy S6, an IOIO board for the input/output communication for the Galaxy S6, and a Pixhawk for stability and control of the aircraft. The RC transmitter will communicate flight controls to the Pixhawk, and the Pixhawk will also be in communication with a Ground Control Station (GCS). See Figure 20, below, for a diagram of how all of these components are intended to work together.[20]

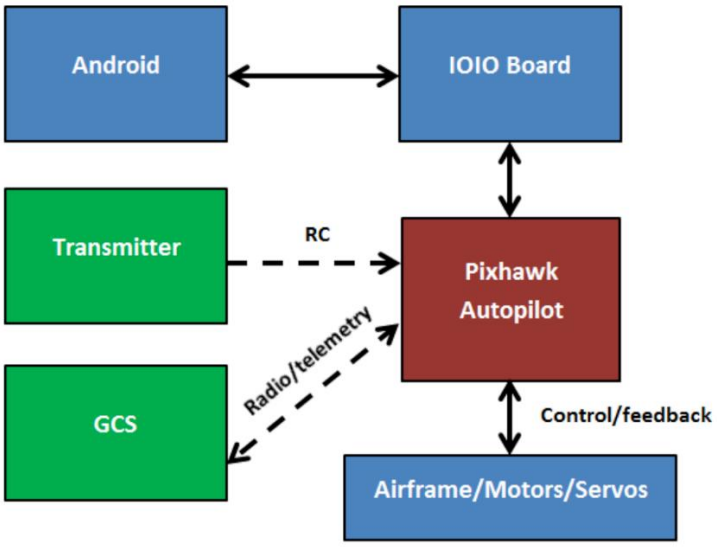

Figure 20: Schematic of components. Image from Thompson [20].

To accomplish this task, the design team will write a code for the open source Pixhawk that will contain "mixer methods," and proportional/integral/derivative (PID) gains. However, this system is said to be in development, so in order to perform preliminary testing, a different system was used. A picture of the test rig system can be seen in Figure 21, below. The system used for the test platform was a HobbyKing KK2.1.5 multi-rotor flight control board. This control board was loaded with an open-source firmware called "OpenAeroVTOL." This allowed them to test the rig in Figure 21 without needing to do any programming. The KK2.1.5 flight control board did allow for PID gain values to be tuned.[20]

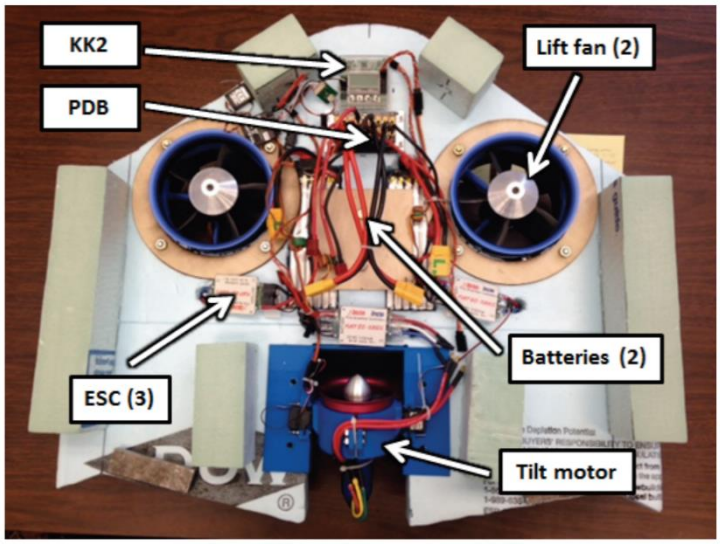

Figure 21: Test platform for the VTOL flying wing. Image from Thompson [20].

The OpenAeroVTOL firmware focused on a hovering mode and a forward flight mode. They were able to customize a sequence of events that would occur when switching between the two modes via an RC handheld unit. They used "output mixers" to regulate throttle mixture between all three motors.[20]

Very little is said about this project as a whole as it was in the early stages of development. This project definitely has aspects that could be used in the aircraft designed by Darrold Cummings. However, time will be needed to find out where the team goes with this project as this paper was published in 2016.

2.3.3 CONTROLS OF A QUADPLANE BY HADI

This paper focuses on two aspects of a fixed wing VTOL UAV: the avionics of the UAV and the control system design for vertical, transition, and horizontal flight. A 3D CAD picture of the aircraft being discussed can be seen in Figure 20, below. It is worth noting that this aircraft was in

fact constructed and flown, but images of the actual aircraft in the paper were not of high quality.[21]

Figure 22: A CAD image of the aircraft being discussed in Chapter III B. Image from Pircher, Geipel & Korsaeth [21].

This aircraft utilizes a total of five motors: one motor for horizontal flight and four motors for vertical flight. When the aircraft is taking off, the four vertical motors will be active and control the aircraft much like a quadcopter. During the transitional phase, all five motors are active: the four vertical motors for attitude adjustment and altitude, and the horizontal motor will start pushing the aircraft forward to gain airspeed and therefore lift. Once in the cruise phase, the four vertical motors will be disengaged, and the single horizontal motor will push the aircraft forward. When the aircraft is landing, the same process is accomplished, but in reverse. The only difference here is that in the transitional phase, the one horizontal motor is used for positioning and is smoothly decreases thrust. A visual description of these scenarios can be seen in Figure 23, below.[21]

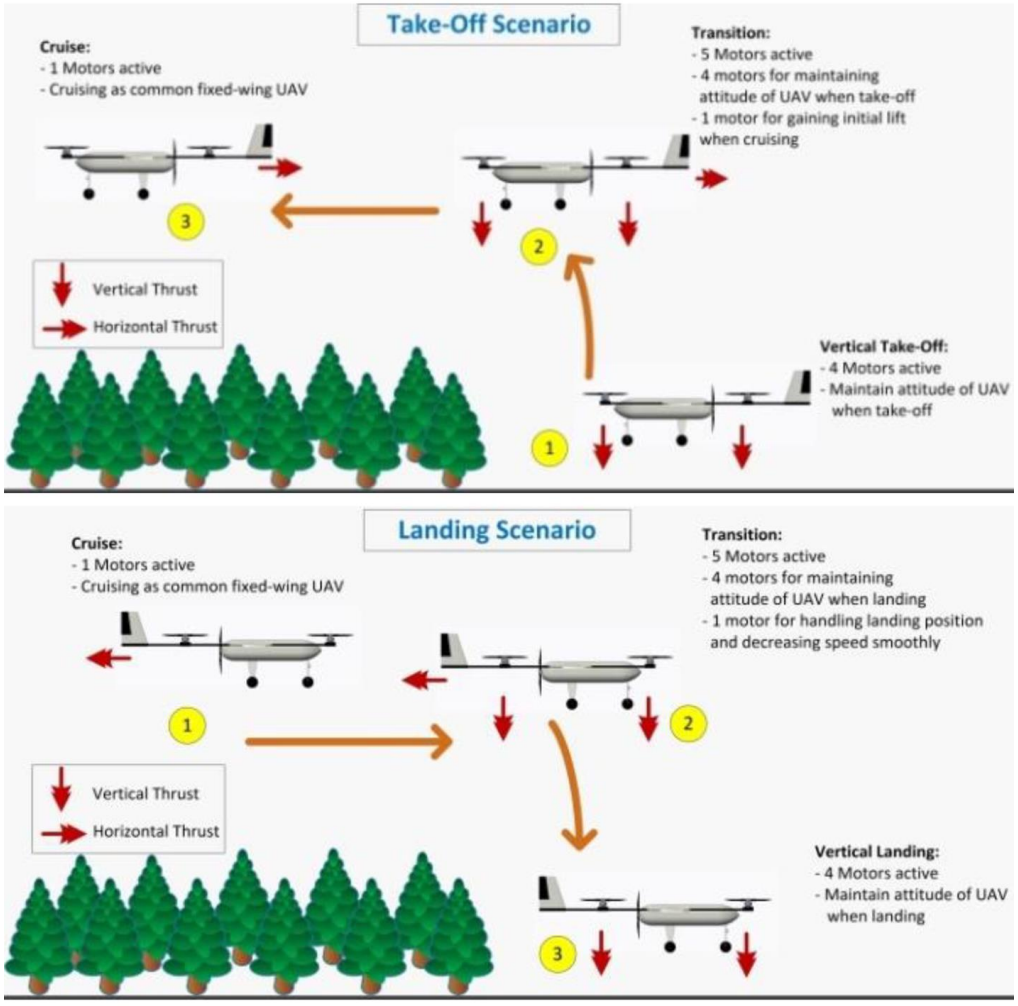

Figure 23: Take-off and landing sequences for VTOL UAV discussed in chapter IIIB. Image from Pircher, Geipel & Korsaeth [21].

To control the aircraft through all three phases of flight, an autopilot is utilized. A quote from the abstract reads: "There are two topics that will be discussed in this paper. Firstly, avionics system of the UAV including its power system and its peripherals interfacing. Secondly, control system design of the UAV including flight scenario when the UAV is on transition mode/stage." [21] It can be concluded that this paper includes a discussion of the control system design. This leads to the conclusion that this paper includes a discussion of the control system design; however, no such

discussion occurs. In lieu, a schematic (see Figure 24 below) was included from [22]. This schematic contains only very standard information which even RC hobbyists will know.

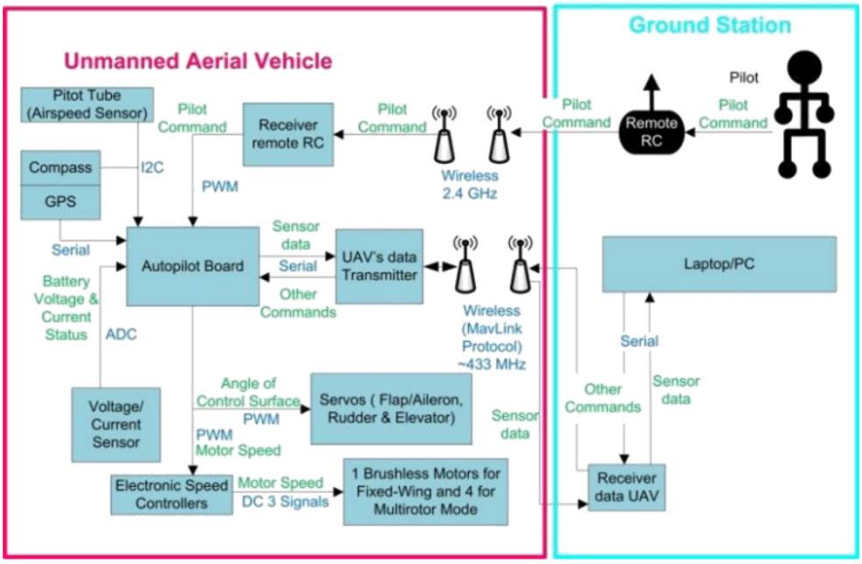

Figure 24: Schematic of avionics of aircraft and ground station. Image from Peyret & Taylor [17].

2.3.4 SUMMARY OF PIXHAWK RESEARCH

Many fixed wing VTOL projects were found, including aircraft like the U-Lion in source [23] or the Pacflyer S100 in source [24]. However, when it comes to Pixhawk implementation, very few were focused on the controls of fixed wing VTOL aircraft that take-off like those from sources [20,21] or ones that utilize tilting wings. Although the transition between vertical flight and horizontal flight for a VTOL aircraft like the U-Lion would be an interesting topic on its own, it is out of the scope of this paper, and therefore will not be discussed.

CHAPTER III

METHODOLOGY

The prototype design for ElectraWing was to be approximately 55lb and called for an aircraft with two turboshaft engines located on the forward ends of the tail booms. This aircraft was to be capable of CTOL, STOL, and VTOL. Additionally, it would have four electric motors powered by batteries: one on each wingtip, and one on each end of the horizontal stabilizer. The wings on the outside of the booms would rotate, as would the turboshaft engines and the horizontal stabilizer. In the initial proof of concept phase, the turboshaft engines would not power generators to keep the batteries charged. The electric motors on the wingtips would help with vortex control, vertical lift, and roll control in the VTOL phase of flight. The tail motors would provide lift and pitch control in the VTOL mode. They would also wash the tail to provide more elevator authority.

For the sake of cost and to avoid designing a new airframe, it was decided to start with an all-electric foam aircraft that was pre-built. A foam airframe was selected for ease of modification and durability when compared to a wood or composite airframe. The two aircraft considered for modification were a Skyhunter and a Ready Made RC (RMRC) Anaconda (see Figure 25, below).

These two airframes were looked at based on past experience working with both of them. They are both fairly sturdy and durable aircraft. ultimately, the RMRC anaconda was chosen for a couple of reasons: it had landing gear that came with it, and the empennage was thicker and sturdier than that of the Skyhunter. The sturdier empennage made it easier to change the overall design of the tail and to add two tail motors.

Figure 25: Stock RMRC Anaconda. Image from NASA [25].

The choice to add an extra electric motor between the wingtip and the boom mounted motor was also made. This was added to make the wing more "blown" to test a more DEP aircraft and to help keep the wing from stalling while in the transition between VTOL and forward flight. An image of the initial concept can be seen below in Figure 26. This initial design was made in OpenVSP.

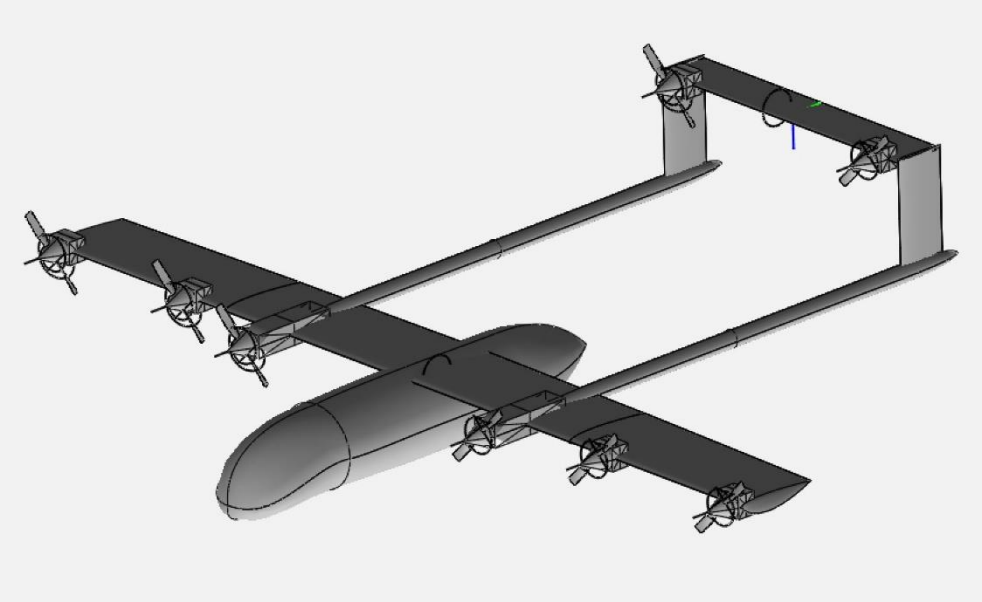

Figure 26: First design revision of ElectraWing using an RMRC anaconda

3.1 MOTOR SELECTION & PERFORMANCE ANALYSIS

3.1.1 WEIGHT ESTIMATION

The first step in selecting the motor, electronic speed control (ESC), and propeller to be use was to figure out the approximate take-off weight of the aircraft. The weights of the stock Anaconda without the stock motor/ESC combination and Pixhawk 2 with supporting equipment were all recorded. Since the Anaconda being used was a ready-to-fly platform, the servos in the aircraft were already installed, so the individual weights did not need to be estimated. ECalc was then used to size the battery, motor, and ESC. The weights of these items were also calculated in eCalc. For more details on this program, see section 3.2.2.

3.1.2 ECALC

ECalc.ch is a German website used for calculating performance characteristics of electric aircraft. The website is capable of calculating performance for fixed wing aircraft, electric ducted fan

fixed wing aircraft, helicopters, and multi-rotors. The website uses a mathematical model for propeller theory to estimate various performance parameters.[30]

The website takes into account various inputs ranging from aircraft specifications such as wing area, to which propeller you want to use. The method to selecting the appropriate propeller/motor/ESC configuration is trial and error. The inputs portion of the website can be seen in figure 27, below.

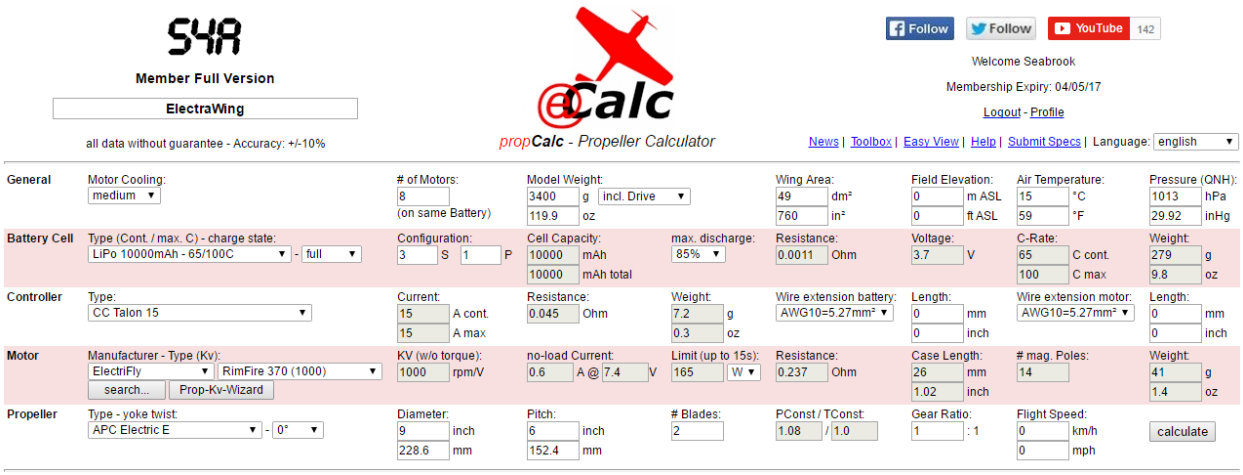

Figure 27: The general layout of the input section of eCalc.

Starting in the top left, and working right, in figure 27 above, it can be seen that inputs required are as follows:

- Motor cooling
- Number of motors on a single battery
- Model weight
- Wing area
- Field elevation
- Air temperature
- Pressure
- Battery selection
    - The user can choose a battery from the list or input the specifics for a particular battery if the chosen battery is not listed.
    - For this analysis, a LiPo battery was chosen from the list of batteries available
- Controller (ESC)
    - The website offers a large selection of ESCs to choose from, but if one is not listed, the user can elect to input specific data, as in the case of the battery

- Motor
    - The motor input is much like that of the battery and ESC
- Propeller
    - This selection process is identical to the previous three selections

To find the propeller/motor/ESC combination needed for this specific aircraft, the motor cooling was chosen to "medium" as the initial design for the motor pods did not have cooling ducts. One of these pods can be seen in Figure 28, below (they will be discussed in more detail in section 3.3.2). These motor pods were designed for two reasons: aesthetics (to be more like the design by Cummings) and to be more aerodynamic. Each of the aircraft's motors was to have one of these pods.

Figure 28: 3D printed motor pod with motor, propeller, and spinner mounted to RMRC Anaconda wing.

According to the design, the aircraft required eight motors, so that was the next input. The weight of the Anaconda was input into the model weight section of the website. Next, the field elevation, air temperature, and pressure were input. For this section, a standard condition used in the industry was assumed: standard atmosphere at sea level. The elevation was chosen to be 0 ft, air temperature set to 59^{o} F, and pressure to be 29.92 inHg.

As per discussion with Dr. Jacob and Mr. Cummings, the aircraft should have a power to weight ratio of approximately 1.2. This is to give the aircraft VTOL capabilities, but not be completely overpowered. In an attempt to account for weight not factored into the design, such as wires and miscellaneous components not considered, a 50% higher power to weight ratio was chosen. The

new power to weight ratio designed for was 1.8. To accomplish this power to weight ratio, the following components were selected: the battery chosen was a Lithium Polymer (LiPo) battery with 10,000mAh, and a continuous discharge rate of 65C and 100C burst. The cell configuration was 3S1P. This was chosen due to the size of the motor and power requirements. The motor was then selected to be an ElectriFly RimFire 370 1000kV. This motor draws a continuous 135W, and a burst of 165W. The ESC was chosen to be a Castle Creations Talon 15 as it is a reputable brand, reasonably priced, and can handle a 15A continuous output with a 3 cell LiPo, which is slightly more than needed by the motor.

The propeller chosen for this aircraft was an APC electric series (E) 9X6E. APC was the brand chosen as the propellers are relatively inexpensive when compared to other brands. Since eight propellers would be needed on the aircraft at any given time, and more propellers will be needed in the event of a prop strike, the toughness and relatively low cost of APC propellers was the propeller of choice for the first attempt at an aircraft of this type. The 9X6E propeller provided the performance required for this aircraft.

3.1.3 XROTOR

XROTOR is an open source DOS-type text console window program created by Mark Drela at Massachusetts Institute of Technology.[27] The program uses 2D blade element analysis to determine the aerodynamic calculations that are used for propellers.[28] XROTOR is capable of predicting performance of free-tip propellers, ducted propellers, and windmills.[29] It is capable of many different things, but for the scope of this project, the focus will be on thrust and efficiency.

To use XROTOR, CROTOR was downloaded from Esoteric Technology Developments (esotec.org). This version of the program enabled an easier use of XROTOR and was recommended to me by Ethan Scott and Jordan Feight of Oklahoma State University. After selecting the propeller/motor/ESC combination from eCalc and getting the outputs, the selected

propeller (APC 9X6E) was divided into 24 segments, as shown in figure 29, below. The propeller was then measured with a caliper as accurately as possible. The measurements that were taken were chord and pitch. Feight provided a propeller file in the required format for XROTOR. This propeller file was then modified with the appropriate parameters for this analysis, including the propeller characteristics at each of the 24 segments and atmospheric conditions. The file was edited using a free program called Notepad++, as per the recommendation of Feight.

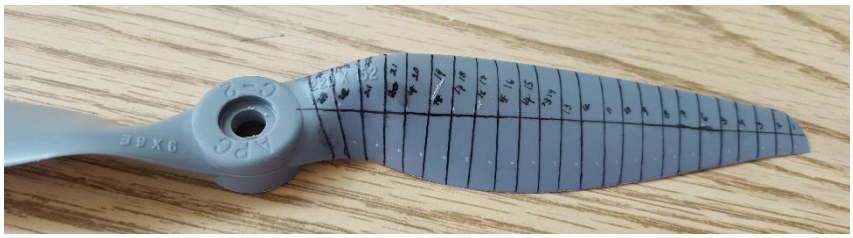

Figure 29: APC 9X6E divided into 24 segments for XROTOR analysis.

Certain aerodynamic parameters were required by XROTOR for a proper propeller analysis. These parameters included lift curve slope, maximum coefficient of lift (C_{lmax}), minimum coefficient of lift (C_{lmin}), minimum coefficient of drag (C_{dmin}), CLCDmin, and dCDdCL^2. It was unknown what the last two values were, so they were left to default. There were a couple of other unknown inputs that were left to default values. They are as follow: XI0, XIW, REexp. According to Dr. Jacob, REexp is a Reynolds number scaling exponent, and has to do with the flow region (laminar vs. turbulent). He stated that the default should be alright to use.

To determine the airfoil parameters mentioned above, a Clark-Y airfoil was used as APC uses an Eppler E63 toward the root, and a Clark-Y toward the tip.[30] However, the exact blend is proprietary. The 2D blade element analysis program for airfoils, XFOIL, was initially used to determine the airfoil properties previously mentioned. It was found that XFOIL does not work well with low Reynolds number calculations (approximately 11,000 for this propeller), so Airfoiltools.com was used to find the properties of the Clark-Y at higher Reynolds number values (Re = 50,000).

After running the program, it was found that 24 segments were not enough for XROTOR to analyze. The program required 30 segments to be input. Since the propeller is small, and not a large aviation propeller, that made it difficult to accurately measure more points. Therefore, an assumption was made: a linear interpolation was done between a few of the data points toward the root of the propeller. Since the linear assumption was close, but not perfectly accurate, this was done at the root of the propeller as the majority of the thrust is produced at approximately 75% of the propeller radius.

XROTOR was run for six different RPM and airspeed combinations. The combinations can be seen in table 1, below.

Table 1: XROTOR run combinations

RPM	V_{oo} (m/s)
6500	1.43
6500	14.75
7000	1.43
7000	16.09
7500	1.43
7500	16.99

The 6500, 7000, and 7500 RPM settings were chosen to match up with the output from eCalc. At each of these RPM settings, two airspeeds were used. The first was a nearly static condition because XROTOR is incapable of analyzing propellers in a static condition. These nearly static speeds were chosen to match the minimum speeds provided in the APC propeller data (more on that in the next section). Table 2, below, shows the following parameters seen by the propeller at 75% chord (C) for the RPM settings used: airspeed (V), Reynolds number, and Mach number. For XROTOR results, see the results section, below.

Table 2: Parameters used in XROTOR for the various RPM settings

RPM	V @ 75% C, m/s	Re	Mach
6500	9.29	10804	0.027
7000	10.00	11635	0.029
7500	10.72	12466	0.031

3.1.4 APC PROPELLER DATA

Advanced Precision Composites (APC) is a manufacturer of model aircraft propellers. They make a variety of different size propellers and different styles. They offer their classic APC injection molded propellers for both nitro/gasoline premixed charge engines and the thinner version for electric motors, like the one selected for this project.

Upon contacting APC about details on the selected propeller, Robert Holik from APC offered to run simulations on their proprietary software at whatever conditions were needed for the project. He stated that their program is a modified NASA TAIR program and that it utilizes vortex theory. He said that they use 30mph to generate the drag polars, and that the airspeed has little impact on the CL-CD data. Additionally, for each RPM setting selected, Holik provided data for an array of airspeeds. The RPM values requested were 6500, 7000, and 7500 RPM.

3.1.5 DYNAMOMETER TESTING

After the motors and ESCs were purchased, a motor mounted to a dynamometer and ran through a series of tests to ensure the accuracy of the calculated data from sections 3.2.2 through 3.2.4, above. The brand and model of the dynamometer was an RCbenchmark Series 1520 V1.0. It had 4 pulse width modulation (PWM) outputs, and a USB interface. The free open source software provided by RCbenchmark (download at https://www.rcbenchmark.com/learning-center/app-download/) was a Chrome application and was capable of automatically running the motor

through a series of step inputs for a defined period of time. It would then save a CSV file that could be imported to Microsoft Excel for further analysis. The version of the software that was used for this project was RCbenchmark GUI-1.0.8. A picture of the software can be seen in Figure 30, below.

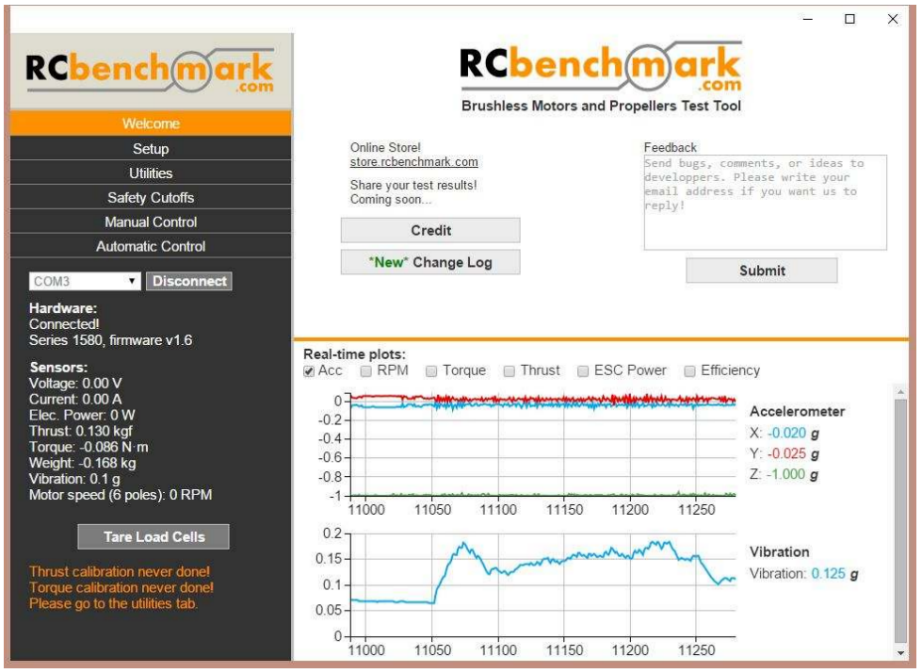

Figure 30: RCbenchmark software graphical user interface (GUI) example (not actual data from project). Image from RCbenchmark.com.

The RCbenchmark thrust stand was bolted to a heavy piece of wood so the platform would not move. The RimFire motor was attached to the thrust stand, and the CC Talon 15 ESC was attached to the motor, a 3S 5,000 mAh LiPo battery, and the PWM input was plugged into the thrust stand. The thrust stand was connected via USB to a personal computer (PC) running the RCbenchmark GUI-1.0.8 software. An image of this setup can be seen in Figure 31, below.

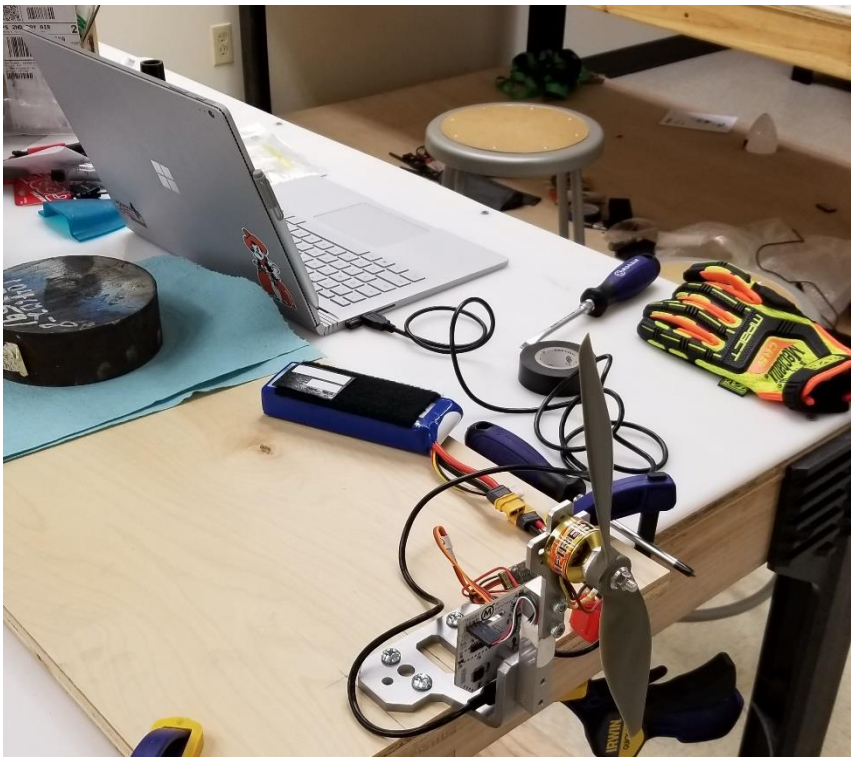

Figure 31: Setup of RCbenchmark thrust stand. The thrust stand is bolted to a piece of wood that was clamped to the table in the front, and had a heavy metal weight in the back. Various propellers were swapped out and tested with this motor/ESC/battery combination.

Using the open source RCbenchmark program with a modified example Javascript (See Appendix A for script used), a total of 11 data points was recorded for each propeller. These data points were in increments of 100 PWM starting at 1,000 PWM (motor not spinning) and run through 2,000 PWM (maximum throttle setting). The script let the motor run at each given PWM input for 3.5 seconds as to let the motor run at a steady state and the thrust to equalize.

To verify the propeller selection made by the iterative process in eCalc, a few different APC propellers were tested on the thrust stand. Each of these propellers were run using the same script. The following diameter (D) and pitch (P) combinations were used (in the format DXP): 9X6, 9X7.5, 10X7, and 11X7. These were spare propellers in the lab that were close to the propeller selected for the project.

3.2 OBJECTIVE I ANALYSIS & EXPERIMENTATION

The first of three phases of test flights were to conduct a conventional take-off and landing with the ElectraWing proof of concept vehicle. This test was to ensure the aircraft could successfully take-off, fly, and land with eight small electric motors placed around the aircraft. This was in part a manual controllability test as much as it was a test to see if it had enough thrust to fly.

3.2.1 TAIL CONSTRUCTION

To accomplish the first phase of testing, the base Anaconda had to be modified extensively. The first step was to reconstruct the empennage of the aircraft. The Anaconda's A-tail needed to be converted to a box tail. The first step in this process was to calculate the Anaconda's directional stability and increase it by approximately 15% to ensure stability of the new design. Since directional stability and the vertical stabilizer area have a linear relationship,[31] the vertical stabilizer area could simply be increased from the original A-tail's equivalent by 15%. This yielded a vertical stabilizer height of 8.3 inches, and a chord length of 6.25 inches. The horizontal stabilizer had the same equivalent A-tail dimensions as the new box tail with a span of 20.5 inches and a chord of 6.25 inches.

To show the linear relationship between the vertical stabilizer and directional stability, Equations 1 and 2 were combined to yield Equation 3, below. Where $C_{n_{\beta_v}}$ is the vertical tail contribution to directional stability, V_v is the vertical tail volume, S_v is the vertical tail area, S is the main wing area, $\Lambda_{c/4w}$ is the wing sweep at quarter chord, Z_w is the distance, parallel to the z-axis, from the wing root quarter chord point to the fuselage centerline, d is the maximum fuselage depth, and AR_w is the aspect ratio of the wing. [32]

$$C_{n_{\beta_v}} = V_v \eta_v C_{L_{\alpha_v}} \left(1 + \frac{d\sigma}{d\beta}\right) \quad (1)$$

$$\eta_v\left(1+\frac{d\sigma}{d\beta}\right)=0.724+3.06\frac{S_v/s}{1+\cos\Lambda_{c/4w}}+0.4\frac{Z_w}{d}+0.009AR_w \quad (2)$$

$$C_{n_{\beta_v}}=V_vC_{L_{\alpha_v}}\left(0.724+3.06\frac{S_v/s}{1+\cos\Lambda_{c/4w}}+0.4\frac{Z_w}{d}+0.009AR_w\right) \quad (3)$$

The vertical tail volume was found using $V_V=l_VS_V/(bS_w)$ from reference [33] where l_v is the distance from the aircraft's center of gravity to the aerodynamic chord of the vertical stabilizer. The vertical tail volume of the original A-tail was found to be 0.07 in^2 and the vertical stabilizer's contribution to directional stability was found to be 0.53. After increasing this stability value by 15%, the new value was 0.61, and the new vertical tail volume was 0.08.

The tail was constructed using two anaconda A-tails. Two foam sections were butted up against each other to make the horizontal stabilizer (each of the two pieces were too short for the new design). They were secured using two biscuit joiner type connections (made out of popsicle sticks instead of actual biscuit joiners) and glue, then two carbon fiber strips inlayed into the underside of the horizontal stabilizer: one right behind the leading edge, and one in front of the elevator hinge. The carbon fiber strips were to both help hold together the two pieces of stabilizer, strengthen it, and help minimize flex while in flight.

The vertical stabilizers were made using the existing boom clamps and inlaying the same two carbon fiber strips as the horizontal stabilizer used. The stabilizers were cut in such a way that the existing servos could be used in the new tail without having to re-mount them. This put one servo for each of the two rudders, and two servos along the elevator to minimize flex of the elevator toward the ends. The horizontal stabilizer was connected to the vertical stabilizers using the existing screw, plastic plates, and aluminum angle iron (bent to 90 degrees instead of its original angle). A picture of the assembled tail can be seen in Figure 32, below.

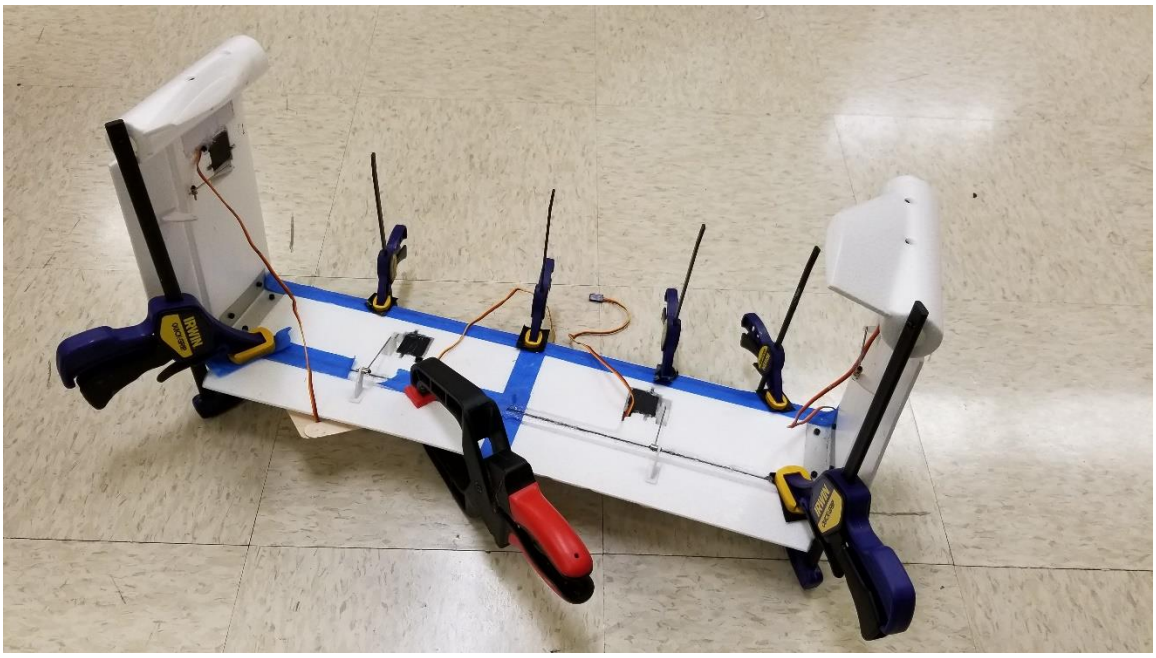

Figure 32: Box tail assembled and clamped while the glue is drying for the carbon fiber inlays. Two servos for the elevator and two servos for the rudders are pictured along with the aluminum angle iron in the corners.

3.2.2 STATIC STABILITY CALCULATIONS

To examine the center of gravity (CG) limitations for static stability of the aircraft, a spreadsheet in Microsoft Excel was created. First, the known aircraft parameters were defined. The wingspan, b_w, was 80 in, wing mean aerodynamic chord (MAC), $\bar{c}_w$, was 8.75 in, the span of the horizontal stabilizer, b_t, was 21.5 in, the horizontal stabilizer MAC, $\bar{c}_t$, was 6 in, and the distance of the aerodynamic center back from the leading edge of the wing, x_{cg}, was estimated to be 2.19 in (quarter chord). A Clark Y airfoil was assumed for the wing with a two-dimensional lift curve slope, $C_{l\_\alpha\_w}$, of 0.1 /degree with a zero lift angle of attack, $\alpha_{l=0}$, of -5 degrees. A tail two-dimensional lift curve slope, $C_{l\_\alpha\_t}$, was assumed to be 0.1 /degree, a coefficient of moment about the aerodynamic center of the wing, $C_{m\_ac\_w}$, of -0.09. A wing incidence, i_w, of 0 degrees, tail incidence, i_t, of 0 degrees, and an angle of attack, α, of 0 degrees. The airfoil information was deduced from airfoiltools.com.

After basic values were determined, the stick fixed neutral point was calculated to find the aft CG limitation using equation 4, below[32]. The assumption was made that fuselage effects were negligible.

$$\frac{x_{NP}}{\bar{c}} = \frac{x_{ac}}{\bar{c}} - \frac{C_{m_{\alpha_f}}}{C_{L_{\alpha_w}}} + \eta V_H \frac{C_{L_{\alpha_t}}}{C_{L_{\alpha_w}}}\left(1 - \frac{d\varepsilon}{d\alpha}\right) \tag{4}$$

Where,

$$C_{m_\alpha} = C_{L_{\alpha_w}}\left(\frac{x_{cg}}{\bar{c}} - \frac{x_{ac}}{\bar{c}}\right) + C_{m_{\alpha_f}} - \eta V_H C_{L_{\alpha_t}}\left(1 - \frac{d\varepsilon}{d\alpha}\right) \tag{5}$$

$$C_{m_0} = C_{m_{0_w}} + C_{m_{0_f}} - \eta V_H C_{L_{\alpha_t}}(\varepsilon_0 + i_w - i_t) \tag{6}$$

$$\frac{d\varepsilon}{d\alpha} = \frac{2C_{L_{\alpha_w}}}{\pi AR_w} \tag{7}$$

$$V_H = \frac{l_t S_t}{S\bar{c}} \tag{8}$$

$$C_{L_\alpha} = \frac{C_{l_\alpha}}{1 + C_{l_\alpha}/(\pi AR)} \tag{9}$$

$$\varepsilon_0 = \frac{2C_{L_{0_w}}}{\pi AR} \tag{10}$$

$$C_{L_{0_w}} = C_{L_{\alpha_w}}|\alpha_0| \tag{11}$$

Using the above equations, the forward CG limitation was established by changing the value for the distance from the leading edge of the wing back to the CG (xcg) and observing the values of the coefficient of moment at 0 degrees angle of attack (Cm_0). From the calculated results, a cm vs. α plot was created. Additionally, a graph of wing rotation angle vs. CG location was created. This was done using three scales (one under each wheel of the aircraft) and rotating the wing and horizontal stabilizer from 0 to 90 degrees.

3.2.3 MOTOR MOUNTING AND WIRING

The motors were mounted to the aircraft using 3D printed motor pods. These pods were designed in SolidWorks and printed using a formlabs Form 2 stereolithography (SLA) 3D printer and printed in Tough Resin. These motor mounts can be seen in Figure 33, below. The motor pods were designed to make the aircraft look more like the design by Cummings, and to make the motors easier to remove (instead of permanently mounting to the wing). To ensure a perfect contour to the wing, a wrecked Anaconda wing was cut along the chord line and a trace of the airfoil was made on a piece of paper. The trace was scanned and imported into SolidWorks for modeling.

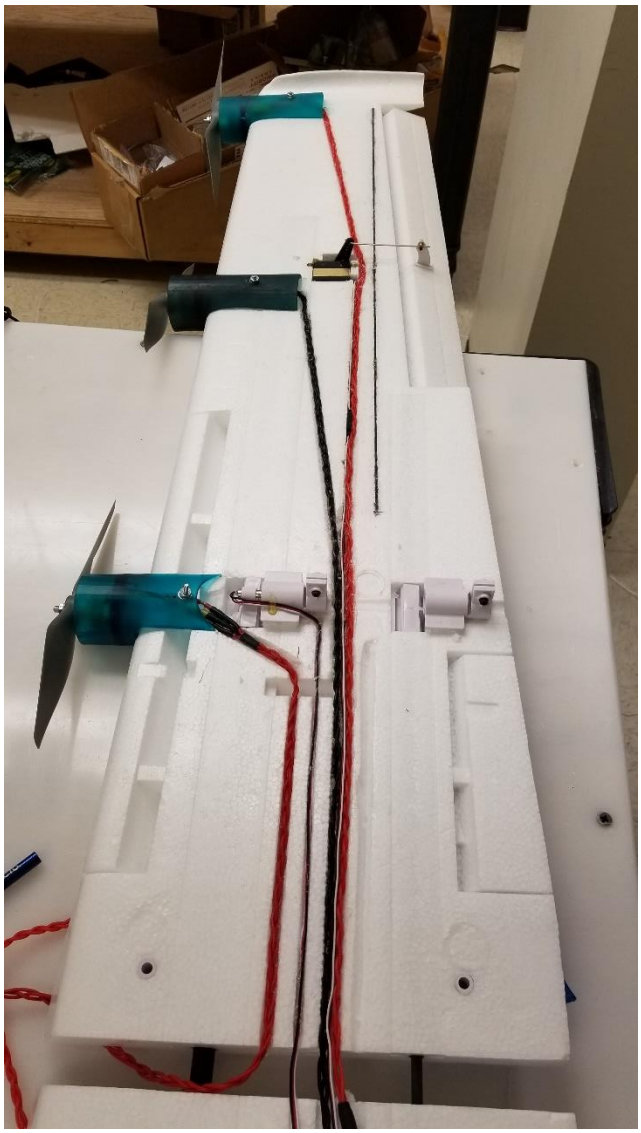

Figure 33: 3D printed motor mounts and wiring routes on the bottom of the Anaconda's wing.

After the motor pods were printed, a hole was drilled through them and the wing where a screw and nut securely fastened them to the wing. To ensure the screws would not compress the foam over time and create play between the motor mount and wing, plastic plates with holes in them were placed on the top and bottom of the wing where the screws would go through. These plates were glued in place using Foam Tac foam glue. Motor mounts for the horizontal stabilizer were also 3D printed and mounted to the tail using the same method as the wing's motor pods. However, to save weight in the tail, a different design was use. The tail motor mount design can be seen in Figure 34, below.

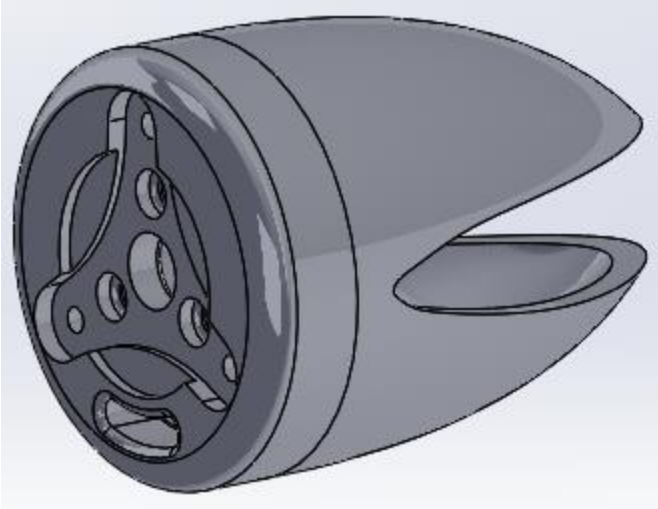

Figure 34: Horizontal stabilizer motor mount design in SolidWorks

After the motors were securely fastened on the wing, motor wire routes were determined and measured. After contacting Castle Creations directly, they said to extend the three motor leads, and not the battery lead side of the ESC. The reasoning they gave is that if the battery lead is extended, ripple current can damage the ESC, but the worst that will happen by extending the motor leads is the timing might be off and the motor will not function properly. They also said that to help prevent mistiming in the motor, the extension's three wires should be braided. 20 gauge (AWG) was used for the motor lead extensions. This size wire was chosen to match the size of the wire on both the motor and ESCs. The extensions were braided, and channels were cut in the wing, and the wires hot glued in the channels. The channels were to help the wire be even along the bottom of the wing to reduce the chances of it tripping the flow along the underside of the wing. The wiring can be seen in Figure 33, above.

3.2.4 OBJECTIVE I TEST FLIGHT

The goal of the first test flight was to determine controllability and see if the aircraft had enough power to successfully take-off and fly. This was conducted before adding the wing and horizontal tail rotational mechanisms to give it the best possible chance of success. Before the first flight, the center of gravity was measured and calculated using three scales (one under each wheel) and an

Excel spreadsheet. The desired center of gravity (CG) for the base Anaconda model was approximately 3.5 inches back from the leading edge of the wing (measured at the root of the wing). However, with the two 5,000 mAh LiPo battery packs as far forward in the nose as possible, the CG was approximately three inches behind where it was supposed to be. To get the CG to its required position, a total of five flight batteries were added to the nose of the aircraft. The aircraft was then held vertically and full throttle was applied to see if the aircraft had enough thrust to lift its own weight (for future VTOL flights), but the aircraft was unable to lift itself with the five flight batteries, and a different design approach had to be considered.

Despite not having enough power for VTOL with the five flight batteries, the CTOL flight test continued. The weight of the aircraft in this configuration was 12.31 lb, and the CG was located 3.5 inches back from the leading edge of the wing, measured at the root. The aircraft started out with slow taxing around the runway, to test ground controllability. After this was accomplished, the aircraft then performed a few high speed runs down the runway without taking off. Once the aircraft passed these tests, it then proceeded to take-off conventionally, flew a couple oval laps around the airfield, then proceeded to land conventionally.

3.4 OBJECTIVE II ANALYSIS & EXPERIMENTATION

Phase II of the project was initially meant to design and implement the wing and horizontal stabilizer rotational mechanisms to enable STOL and VTOL capabilities. However, due to the CG issue noticed at the Phase I flight test (see section 3.3.3), a partial redesign of the aircraft was needed to shift the CG forward to its required location.

3.3.1 A REDESIGN FOR WEIGHT & BALANCE

To help shift the CG forward, the motor mounts on the horizontal stabilizer were removed and the motors were then mounted to the stabilizer semi-permanently. Thin plywood motor mounts were

cut out and the motors mounted directly to them. Wood dowels were then used as pegs to go through the motor mounts and into the horizontal stabilizer; each mount got to pegs. Flat spots were cut into the leading edge of the horizontal stabilizer for the mounts to be placed. The mounts and pegs were then glued onto these flat spots using hot glue. A picture of this motor mount can be seen in Figure 35, below

Figure 35: Plywood motor mount mounted on right wingtip. The mount was hot glued and pegged.

Despite this change, the CG was still not far enough forward with the two-battery configuration, so more modifications were needed. Additionally, since the aircraft still did not have enough thrust to lift the aircraft with the five-battery configuration, another alternative to adding weight needed to be considered. One concept was to lengthen the fuselage to try to shift the batteries farther forward. After performing a moment calculation, the distance the batteries needed to be moved forward was estimated to be 27.5 inches. Since the distance from the desired CG of the aircraft to the farthest forward tip of the nose was only 19.5 inches, it was clear that extensive fuselage modifications would be needed to pursue this path. This would be possible if a second anaconda fuselage was spliced into the current fuselage. Since the fuselage is a destabilizing entity, an XPlane 10 model was made and tested to ensure the aircraft could fly and be directionally stable. An image of this aircraft can be seen in Figure 37, below.

Figure 36: XPlane 10 simulation of the extended nose concept of ElectraWing.

After this idea was considered, there were further discussions with Cummings. He stated that the two motors on the booms of the aircraft could be extended forward to help with VTOL stability and CG shift for the first attempt at the aircraft. This extended boom concept was a much simpler solution to the CG issue, plus it made for a more stable platform while hovering as it would be more like a quad+ airframe and offset the overall moment of the aircraft since it had motors on the tail.

3.3.2 MOTOR BOOM EXTENSIONS

To accomplish this modification, a carbon fiber tube was inserted into the front of the boom's carbon fiber tube and glued in place using hot glue. A picture of this boom extension can be seen in Figure 38, below. The motor was to be placed equidistant from the center of gravity as the motors on the horizontal stabilizer. The distance each are from the center of gravity is 30.5 inches. From there, a new boom motor mount was designed using SolidWorks and 3D printed with Tough Resin using the Form 2 printer previously mentioned. A picture of the STL file of the motor mount can be seen in Figure 39, below. The mount was then fastened to the end of the

boom using hot glue, and the motor fastened to the mount using screws and nuts. Unlike the original design, this new motor mount would not allow the boom mounted motors to rotate between a forward position and a vertical position. The decision to keep the two motors permanently vertical was to save weight and mechanical complexity. Although it was not an idea scenario, it would still prove the aircraft's vertical and transitional capabilities.

Figure 37: Boom extensions for placing the boom motors forward of the center of gravity.

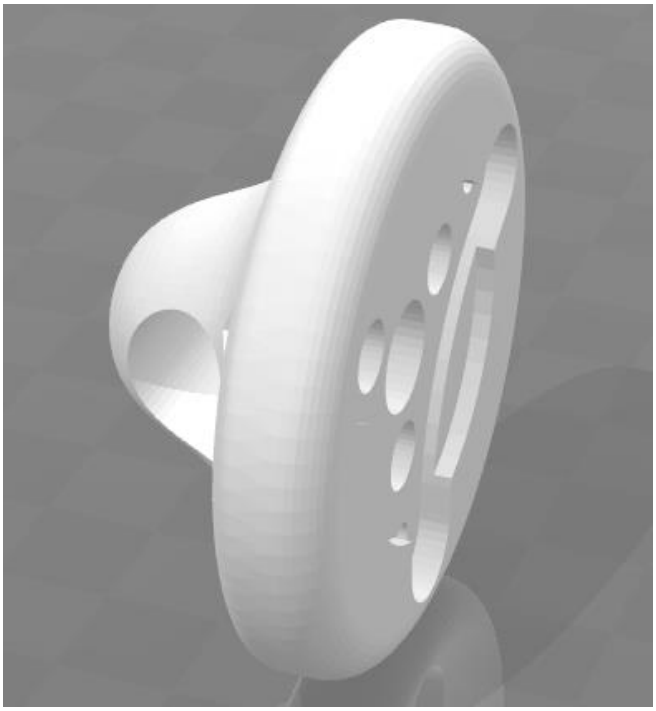

Figure 38: Computer generated image of the vertical motor mount for the boom extensions.

3.3.3 WING ROTATIONAL MECHANISM

To accomplish vertical flight, as per the design, the wing and horizontal stabilizer needed to rotate 90 degrees from horizontal to vertical and back. The first piece that was worked on was the main wing. The Anaconda already had a carbon fiber sleeve mounted inside the wing for almost the entire span. This tube is where the main wing tube would slide into place to keep the two halves from folding in the middle while flying. This tube was located at approximately quarter chord, and can be seen in Figure 33, above. Additionally, there was a smaller carbon fiber sleeve that a solid carbon fiber rod would slide into, so the wing would not twist and remain stronger in flight. This sleeve was located at approximately ¾ chord, and can also be seen in Figure 33, above.

A few different rotational mechanism design concepts were considered, but it was decided early on that the easiest method to rotating the main wings would be to use the existing hardware: the carbon fiber sleeves in the wings. The idea was to fasten the wing tube inside of the sleeves in the

wings. This way just the wing tube would be rotated from inside the fuselage, causing the wings to move in unison. Five different methods of twisting the wing tube were examined: a chain and sprocket system, worm gear, belt drive, direct gear, and linear actuator. The chain and sprocket idea would have been to put a sprocket on the wing tube, and a sprocket on a servo, then the servo would drive the wing tube via a chain. Similarly, this same mechanism could have been accomplished with a belt instead of a chain. The worm gear would be similar, but there would be a worm gear mechanism between the servo and wing tube. Direct gears could have also been used between the servo and wing tube. Finally, a linear actuator pushing a control horn attached to the wing tube was considered. Below (Table 3) is a table of pros and cons that was made while looking at all of the different systems.

Table 3: Pros and cons for rotational mechanisms considered

Chain/Sprocket		Belt Drive		Worm Gear		Direct Gears		Linear Actuator	
Pros	Cons	Pros	Cons	Pros	Cons	Pros	Cons	Pros	Cons
Strong	Needs to be tight	Light weight	Can slip	Consealed	Price	Gear reduction	Bulk	Light weight	Linkage between actuator and wing or wing tube
	Can slip			Strong	Weight	Light weight	Precision of mounting in foam plane	Strong	
	Weight						Slip or strip easily	No slip	
	Bulk							Precise	
								Compact	

After looking at the various pros and cons of the five methods considered to rotate the wings, the linear actuator method was chosen. This mechanism would have two servo horns permanently glued to the carbon fiber wing tube, and a linear actuator would be between them and attached to the inside of the fuselage. Based on a recommendation by a colleague, the brand Actuonix was looked at as they take PWM input without any programming, are light weight, run on 6V, and fairly priced. The stroke of the linear actuator needed to move was solved for using simple trigonometry and a 45/45/90 triangle where the 90-degree angle was at the wing tube. The linear

actuator used was an Actuonix L16-R and had a stroke of 100mm and a gear ratio of 63:1 for a medium speed and strength.

After the overall concept was worked out, the first step was to cut the wings off of the aircraft. To do this, a hack saw was used, and a cut was made along the chord line of the aircraft just to the outside of the booms, just as the design had called for. After this cut was made, a carbon fiber wing tube that was similar in diameter and wall thickness to the original wing tube, but longer, was purchased from Rock West Composites. This new carbon fiber tube had an inner diameter of 0.375 inches, outer diameter of 0.459 inches, and a length of 60 inches. The longer tube was purchased so that more surface area could be made in the carbon fiber sleeve inside the wing when being glued in. the wing was test fit with the new wing tube, and then it was time to narrow in on a control horn design.

A few different shapes and sizes were considered for the control horn. Given that the linear actuator selected had a travel of 100mm, or approximately 3.9 inches, in order for the control horn to move 90 degrees with full travel of the linear actuator, the control horn needed to be 2.5 inches long, from the center of the wing tube to the hole drilled in the end to attach the linear actuator. An illustration of the two primary control horn concepts are shown in Figure 40, below. The first one was just a straight control horn and fairly simple, the second one had a curve to it. The curved control horn was designed in case the straight control horn hit the structure inside the aircraft that the wings bolt down to.

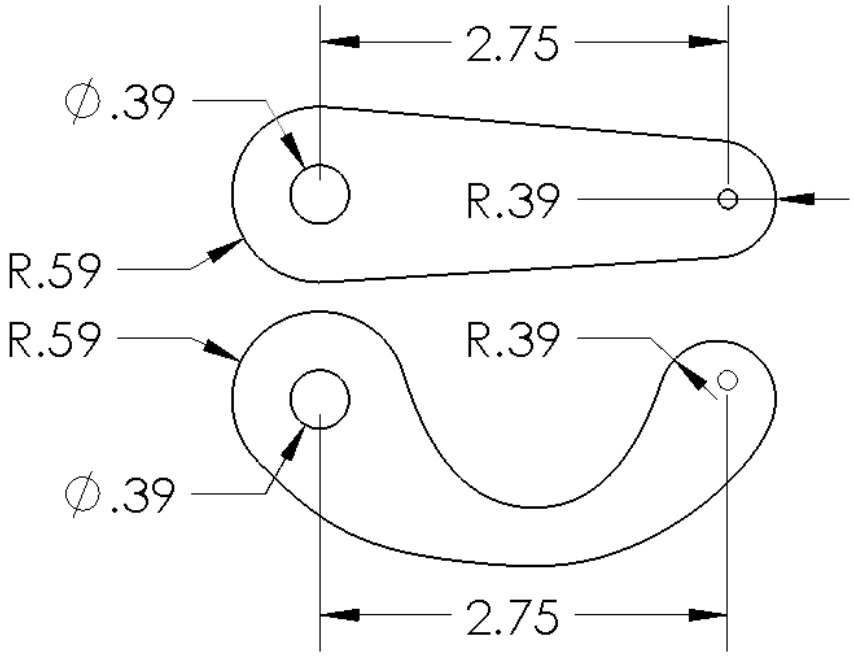

Figure 39: Two primary design concepts for the control horns on the wing rotational mechanism.

Multiple of these control horns were made using balsa wood and Gorilla tape. These weak control horn tests were purely to test the travel with the linear actuator, and not intended to be the final product. These control horns were made in pairs as the final design would utilize two of them. These prototypes can be seen in Figure 39, below. On the left, is one of the two curved variants, in the middle is the second of the curved variants, and on the right is the straight variant. After testing each of the three variants, the curved control horns on the left and the straight ones worked best and were selected to make carbon fiber variants. The carbon fiber variants were made using a small CNC machine and a 2.2mm thick carbon fiber plate. The straight carbon fiber variant can be seen in the top of Figure 41, below. After testing both the straight and curved carbon fiber variants, the curved carbon fiber control horns were selected to be implemented.

Figure 40: Carbon fiber variation

To assemble the wing rotation mechanism, the new carbon fiber wing tube was roughed up on the ends that would go into the rotating wing sections. After roughing it up with sandpaper and a razor blade knife, the tube was then cleaned off using rubbing alcohol and a rag. After drying, one end of the tube was lightly coated in 30-minute Devcon 2-ton epoxy epoxy, and more of the same epoxy was poured into the right wing tube sleeve. The wing tube was then inserted all the way into the wing section. After the glue set, a nylon washer was put on the wing tube, and put up against the wing section. This created a slight gap between the wing section and the boom as to help prevent friction and binding. The wing tube was then inserted into the center right wing section, and the two wing sections were pushed together. The center right wing section was then bolted onto the fuselage of the aircraft to help align things. Next, the carbon fiber control horns were fitted onto the carbon fiber tube with a slightly larger carbon fiber tube segment between them for added strength and spacing. These three parts were then epoxied in place using 5-minute epoxy. After the epoxy had set, fiberglass strips were soaked in a Resin Services WB-400 resin and SC-150N hardener mixture and wrapped between the two control horns for additional strength. After letting the glue cure for 24 hours, the left middle wing section was bolted onto the

fuselage as well, and the wing tube inserted into it. Next, the remaining wing section was glued onto the wing tube using the same process as described for the right section. The top of the control horns and can be seen put together in Figure 42, below.

Figure 41: Control horns attached to the wing tube after the assembly was complete. As pictured, the wings are in the horizontal configuration. A section in the middle of the wings had to be cut away as to allow room for the control horns.

After the wing was assembled, the linear actuator was installed using the included mounting hardware on the side that connected to the plane. At the wing end, a machine screw was inserted into the holes of the control horns and through the hole at the end of the linear actuator. This put the linear actuator between the two control horns. A picture of this can be seen in Figure 43, below.

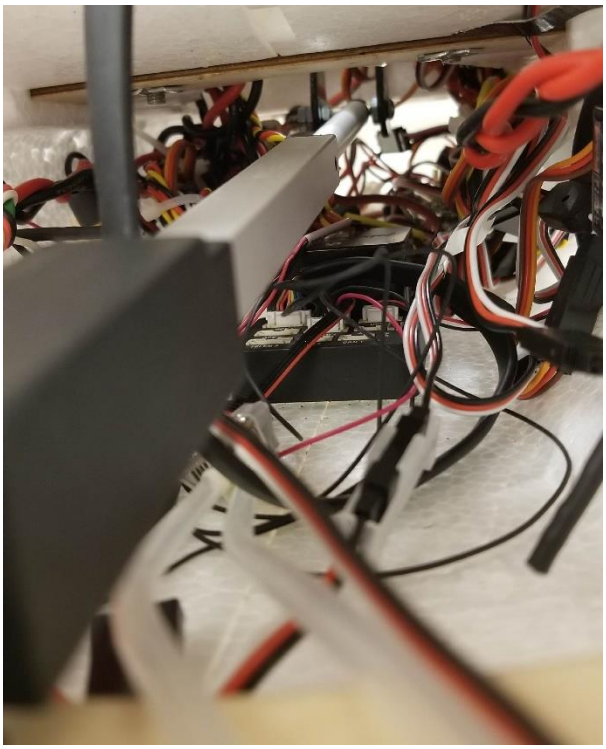

Figure 42: Image of the linear actuator extended (horizontal flight configuration) and the control horns deep in the fuselage of the aircraft.

Once this assembly was put together, the wings were put in the vertical configuration, and the small carbon fiber rod was inserted through the middle wing section. At this point, it was measured and cut so that only about an inch of the rod would extend out each side. After this, the rod was glued in place using hot glue. Hot glue was used as it was quick and did not need to be as securely fastened as the main wing tube. The sleeve that this rod normally went into was cut in half length wise the same length as the tip of the rod sticking out and was done on both sides. This created a stop for the wing while in the horizontal flight configuration, which helped prevent the wing from being over rotated and to help keep the trailing edge from flexing upward. A picture of this can be seen in Figure 44, below. Finally, after all of these modifications, the wing rotational mechanism was tested to ensure it rotated 90 degrees.

Figure 43: Wing rotation stop rod right before it locks into place. In this image, the main wing (to the left) has about a 20 degree rotation from horizontal

3.3.4 HORIZONTAL STABILIZER ROTATIONAL MECHANISM

To rotate the horizontal stabilizer, just one simple design was considered. There would be a carbon fiber tube that would go all the way through the quarter chord of the horizontal stabilizer, and at one end, it would connect to a servo which would be mounted at the top of one off the vertical stabilizers. At the other end, it would stick through a bearing which would be mounted at the top of the other vertical stabilizer. Ultimately, this design was mostly followed, but the carbon fiber tube just went through the bearing and part way into the horizontal stabilizer. This was done to save weight in the tail. A nylon washer was placed on the carbon fiber tube between the horizontal stabilizer and the vertical stabilizer to help prevent binding. Additionally, another

nylon washer was hot glued on the carbon fiber tube on the other side of the vertical stabilizer. This was done to keep the tube from slipping out of the bearing and falling apart mid-flight. Hot glue was the glue of choice here because it would stick well to the carbon fiber tube but would be easy to cut away with a knife should the tail need to be disassembled in the future, in addition to its fast-drying properties. At the servo end, a double ended servo arm was attached to the servo and fastened to the horizontal stabilizer with two pegs (one in each side) and hot glue. The carbon fiber tube used for the stabilizer had an inner diameter of 0.250 inches, and an outer diameter of 0.395 inches (10mm). The carbon fiber tube was a unidirectional torsion tube. The bearing that this tube went into was a double sealed steel needle-roller bearing (pictured in Figure 45, below) that would work with a 10mm shaft diameter and was 14mm wide.

Figure 44: Needle-roller bearing that was used in the rotating tail mechanism. Picture from McMaster.com.

The servo used to rotate the horizontal stabilizer was a Hitec HS-5685MH high torque, metal gear digital sport servo. The part number from hitecrcd.com is 35685S. This servo was chosen for its ability to be programmed, its torque, and because it had metal gears (as opposed to carbonite or nylon). The servo runs on 6.0V to 7.4V power input with a maximum torque of 157 oz-in at 6.0V. The circuit type was G1 Programmable Digital. A notch was cut out of the top of the left horizontal stabilizer for the servo to rest in. Three sides of the servo were roughed up with an Xacto blade, then hot glued into the cutout space in the horizontal stabilizer. Pictures of the finish rotational mechanism can be seen in Figure 46, below.

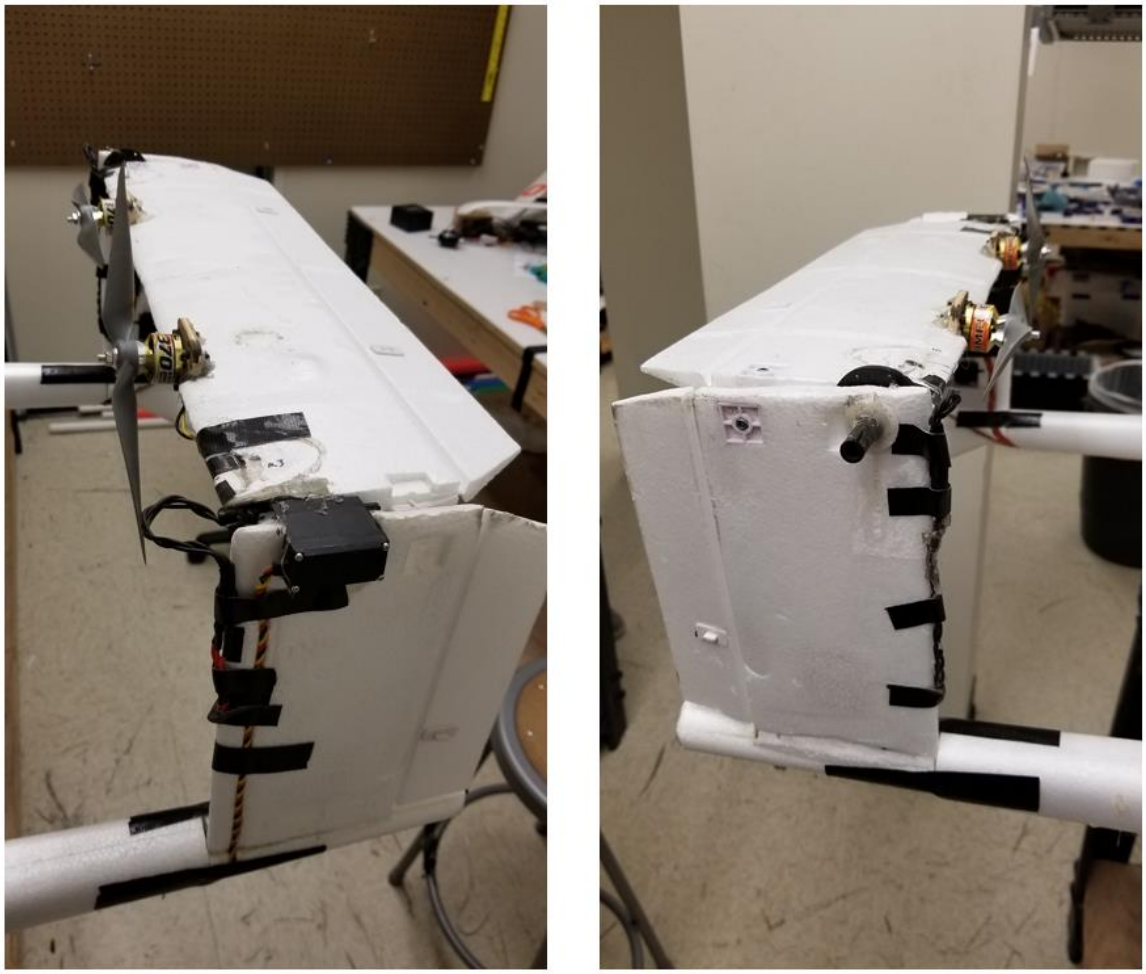

Figure 45: The completed horizontal stabilizer rotational mechanism

3.3.5 FLIGHT TEST I: CTOL

The next flight test was purely to test the aircraft in the CTOL configuration to see if both rotational mechanism held together in a normal flight. The aircraft was again using straight RC input with a 12 channel Futaba R6014HS receiver. The ailerons were connected to a Y-harness and plugged into channel 1, the elevator servos were plugged into channels 2 and 3, the rudder servos and nose gear servo were all connected via a series of Y-harnesses and plugged into channel 4. The horizontal stabilizer was plugged into channel 5, and the six forward facing throttle servos were plugged into channels 6 through 11. The front two boom motors were disabled, and the linear actuator for the wing rotational mechanism was also disabled.

The flight testing procedures were much like that of the first test flight outlined in section 3.3.3, and the wind was negligible. The aircraft was taxied around the runway slowly to ensure nothing was going to go wrong immediately. Next, the aircraft performed a few high speed runs down the runway, but did not become airborne. Finally, the aircraft lined up on the runway into the wind and took off. A couple oval patterns around the field were made, but the aircraft remained in direct line of sight. A picture of the flight can be seen in Figure 47, below.

Figure 46: ElectraWing phase II flight test I. in this picture, the aircraft was landing in the CTOL configuration. Image by Antonio Valencia.

3.3.6 CONFIGURATION CHANGES

Since the Futaba 14SG only had 12 usable channels available, and 14 channels would have been needed once the wing rotation mechanism and two boom motors were added. To lower the number of channels required, the rudder channels were disabled, and the rudders were locked out with gorilla tape. Additionally, one of the elevator servos needed to be physically turned 180 degrees to allow for a Y-harness to be added to reduce the number of elevator channels to one. To

still allow for yaw control in the aircraft, a thrust differential mixing was done in the Futaba radio. This would allow the two motors on the left wing to go to a higher throttle setting, and the motors on the right wing to go to a lower throttle setting when a right yaw input was made. This would effectively give the aircraft an overall directional moment to the right.

3.3.7 FLIGHT TEST II: CTOL

Given this new yaw differential setting, and to double check all systems were still in working order, the aircraft performed identical ground testing as the previous two flights: first a slow taxi test, then high speed runs down the runway, and finally take-off in the CTOL configuration. However, this time, shortly after take-off, the aircraft crashed. Luckily there was only minor damage. For a detailed report of this incident, refer to Chapter 4, and possible causes of the crash will be discussed in Chapter 5. Wind data for this flight was not recorded but was estimated to be 10-15mph and gusting.

3.3.8 INCIDENT DAMAGE & REPAIRS

STOL flight testing was conducted to test the rotating wing mechanism in higher stress environments before testing VTOL. After the incident outlined in section 3.3.7, the aircraft needed a few minor repairs. The old pegs for the motor mounts needed to be removed, the motor mounts also needed to be glued back on. This was done using hot glue. Next, all of the motor mounts on the wing and horizontal stabilizer (even the ones that did not come off in the crash) were re-drilled, and larger carbon fiber pegs were hot glued in. The pegs were two inches long and were made out of the same carbon fiber as the wing rotation mechanism forward stop depicted in Figure 44, above. The crushed part of the nose of the fuselage was then glued back in place using hot glue.

3.3.9 TEST III: CTOL & STOL

Before this flight was conducted, there were only a couple configuration changes. To help prevent the incident in section 3.3.7 from happening again, the thrust differential was disabled, the rudder servos were enabled, the elevator servos were disabled, and the elevator was locked out. To compensate for this, the horizontal stabilizer rotation servo was used to move the stabilizer to become an all moving stabiliator (the combination of a stabilizer and an elevator, like with supersonic aircraft). This was to allow the stabilizer to be constantly adjusted in flight, should there be any flex in the system. After this modification, a CTOL flight was conducted to ensure the stabiliator would work. After the initial CTOL flight, the aircraft was put through a series of CTOL and STOL tests.

Figure 47: ElectraWing lined up on the runway against the north end of the run-up area

Before each test, the aircraft was lined up to the north edge of the run-up area at the runway, and nose pointed down the runway into the wind. A picture of this can be seen in Figure 48, above. Each of the following tests were run three times: CTOL, STOL with a wing rotation of

approximately 10 degrees, 20 degrees, 30 degrees, and 45 degrees. More wing rotation angles would have been measured, but all wing angles were measured by measurements taken on the wing in pictures after the flights were conducted. Additionally, with the flex of the wings and wing tube, precision was not possible. An image of the rotated wing can be seen in Figure 49, below. For each of the tests, the throttle was immediately put to 100%, and the wings were slowly put back to zero degrees angle of attack after the aircraft achieved a positive rate of climb. The point of take-off was noted, and the roll distance was recorded. To remain conservative with the testing, a short landing was not attempted until after all of the test points were achieved. All of the landings were conventional with no wing rotation. For the final landing of the day, the wings were rotated slightly (no way to measure the exact amount of wing rotation in flight), but the landing was very unstable and resulted in two broken propellers. The exact result of the landing will be discussed in Chapters IV and V.

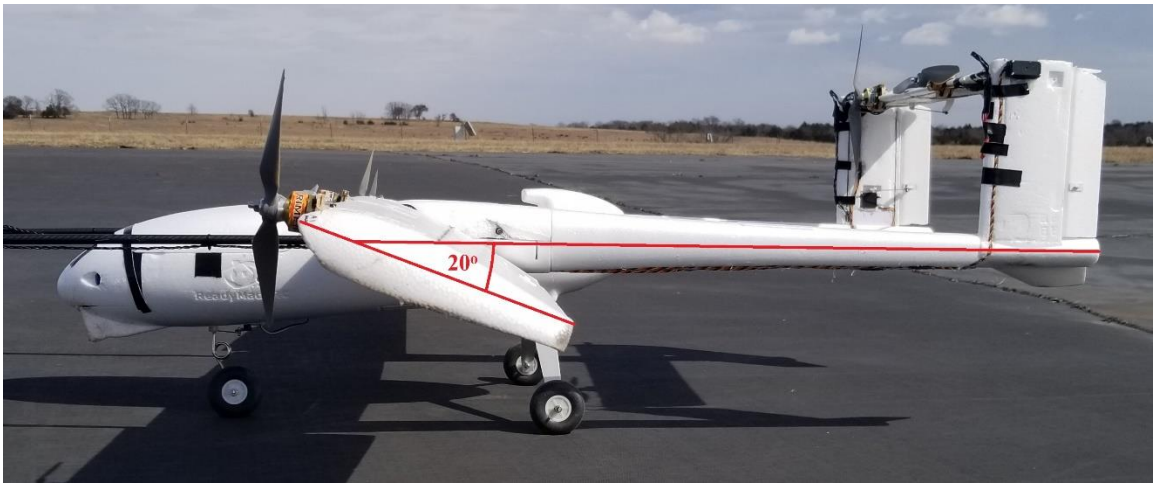

Figure 48: Wing rotated 20 degrees for STOL testing

3.4 VTOL ANALYSIS, AUTOPILOT CONFIGURATION & TESTING

3.4.1 VTOL TRAJECTORY PREDICTION

To observe how much wind affects the aircraft in a vertical take-off, a VBA program was written in Microsoft Excel. The code can be seen in Appendix B. For this analysis, it was assumed the

autopilot would not attempt to negate the effects of wind with a GPS hold. Only flat plate drag for the rotating wing sections and horizontal stabilizer were considered. Flat plate drag was also applied to the transitional phase of flight. The equation for flat plate drag can be seen in Equation 12, below [34].

$$C_d = \frac{D}{\rho V^2 A/_2} \tag{12}$$

Drag force, D, was calculated iteratively as the relative airspeed, V, changed based on the velocity of the aircraft. Standard sea level conditions and flat plate coefficient of drag, C_d, value of 1.28, were used [34]. The drag was input to the kinematic equation of motion as the acting force in the x direction as the aircraft ascended. The kinematic equations of motion were used. Equation 13, below, was used for the trajectory in the x-direction on the ascent and transitional phases of flight. Equation 14 [35], below, was used for the trajectory in the y-direction for the transitional phase of flight only. A constant vertical climb speed of 1ft/s was assumed for the purely vertical phase of flight and wing rotation started once the aircraft climbed to an altitude of 30 feet above ground level (AGL).

$$\Delta x = v_i t + \frac{1}{2} a_x t^2 \tag{13}$$

$$\Delta y = v_i t + \frac{1}{2} a_y t^2 \tag{14}$$

For the calculations, a weight of 12 lbf was used, and the thrust was estimated to be 15.13 lbf. This figure was calculated using the thrust stand for the RimFire motors, and eCalc for the SunnySky motors. A percentage limitation on thrust was assumed on the Pixhawk for control purposes. Based on previous test flights and calculated thrust to weight ratios, it was estimated to reduce the maximum allowed thrust by approximately 15%. Using the specifications of the linear actuator, the wing was calculated to rotate at a speed of 18 degrees per second, and three different

wind conditions were defined: 0 mph, 5 mph, and 11 mph. The 11 mph wind was used to match the conditions at the airfield when the final VTOL test flight was conducted, the 5 mph condition was a mid-way point used, and the no wind condition was used to demonstrate the ideal take-off path of the aircraft.

3.4.2 THE EFFECT OF VTOL ON WING STRUCTURE

To determine the effect of VTOL on the rotating wing's structure, moment and shear stress was calculated. A free body diagram of the forces acting on the rotating wing section can be seen in Figure 50, below. For the scenario evaluated, the thrust was the maximum allowed physically with no Pixhawk limitations considered and the aircraft fixed in space. This was to represent the worst scenario the aircraft should ever experience

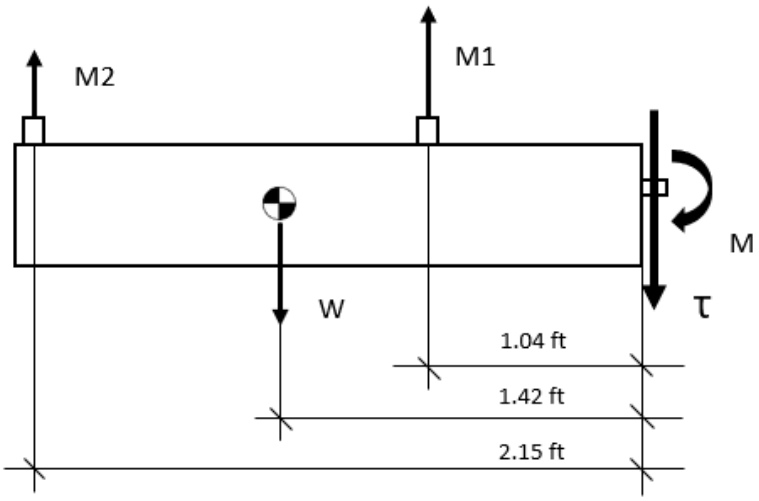

Figure 49: Free body diagram of rotating wing section in vertical configuration.

In this diagram, M1 was a SunnySky motor and M2 was a RimFire motor. The center of gravity of the wing section was approximated to be at 1.42 feet from the point of rotation. M1 was located 1.04 feet from the point of rotation, and M2 was located 2.1 feet from the point of rotation. The moment at the point of rotation was calculated using equation 15, below.

$$\sum M_{point\ of\ rotation} = 0 = 1.42W - 1.04T_{M1} - 2.15T_{M2} \quad (15)$$

Where W is the weight of the section, and T represents thrust. After this was completed, the transverse shear stress was calculated for the carbon fiber tube. The shear stress, τ, was found using equation 16, below. Where V was the force being applied to the joint, Q was the moment of the area about the neutral axis (Equation 17, below), I was the moment of inertia (Equation 18, below), t was the width of the cross-sectional area, c_i was the inner radius, and c_o was the outer radius [36].

$$\tau = \frac{VQ}{It} \quad (16)$$

$$Q = \frac{4c_o}{3\pi}\left(\frac{\pi c_o^2}{2}\right) - \frac{4c_i}{3\pi}\left(\frac{\pi c_i^2}{2}\right) \quad (17)$$

$$I = \frac{1}{4}\pi\left(c_o^4 - c_i^4\right) \quad (18)$$

3.4.3 AUTOPILOT CONFIGURATION

Figure 50: A typical quad-plane setup. The electric motors spin up for vertical take-off, and slowly turn off as the forward flight propulsion system slowly turns on. This process happens in reverse for landing. Image from Advanced Precision Composites [38].

The Pixhawk 2 was the platform decided upon as it has a lot of documentation online on how to configure it for various vehicles and its VTOL capabilities. These fixed wing VTOL capabilities were added to the Pixhawk in APM:Plane firmware 3.5.0 and later.[37] A comprehensive guide on how to setup the Pixhawk using the MissionPlanner software can be found at ardupilot.org. This same guide was used extensively for the setup of this aircraft. Despite this comprehensive guide, a few challenges still existed in the setup. This was mostly due to the fact that most aircraft that use the Pixhawk for VTOL are quadplanes (pictured in Figure 51, above) and tilt-rotor aircraft. A popular tilt-rotor aircraft that utilizes the Pixhawk is the BirdsEyeView FireFly (pictured in Figure 52, below). Both of these types of aircraft have similarities to ElectraWing, but a direct comparison cannot be made.

Figure 51: BirdsEyeView FireFly platform. When this aircraft takes off vertically, all three sets of motors are vertical facing to provide lift, as the aircraft transitions, the front two sets of motors rotate to a horizontal configuration while the rear motors to a horizontal configuration while the rear motors turn off. The reverse happens for vertical landing. Image from ArduPilot.

For this phase, a Pixhawk 2 autopilot was added to the aircraft. The Pixhawk was fastened to the inside of the aircraft on the belly using the included double sided 3M double sided foam tape. The following equipment was attached to the Pixhawk:

- 2x 5,000 mAh 3S LiPo batteries
- 1x HS-200-LV Mauch Power module
- Buzzer
- Airspeed sensor: Holybro PX4 Airspeed V1.2
- RFD900 Ultra Long Range Radio Modem for telemetry
- Proficnc Here GNSS M8N GPS Unit
- 8x servos
- 1x linear actuator
- 8x ESCs/motors
- Futaba R6203SB receiver

To start, the main power from the two LiPo batteries used were plugged into custom made squid connectors that divided the power from each battery to four motors. One battery supplied power to all of the motors on the left side of the aircraft and the other battery powered all of the motors on the right side of the aircraft. Between one of the batteries and squid connectors, the Mauch power module tapped into the positive connection of the battery to monitor the current flow to the motors. Also coming from one of the battery leads was a small separate wire going to a Castle

Creations CCBEC 10A Peak 25V Max input SBEC. This BEC (battery eliminator circuit) reduced the voltage from the batteries down to 5.1V and was input to the Mauch power module which then transferred a signal from the current sensor and the 5.1V power to the POWER1 port of the Pixhawk. The GPS module/arming button combination was connected to the GPS 1 port, the airspeed sensor was connected to the I2C2 port, the telemetry radio was connected to the TELEM 1 port, the Futaba receiver was connected to the RCIN port, and the buzzer was connected to the USB port on the top of the Pixhawk.

The Pixhawk only has eight MAIN OUT ports and six AUX OUT ports that can be used for servos, motors, or any other function that could be needed. The aircraft had a total of seven servos for basic flight control: two aileron servos, two elevator servos, two rudder servos, and one nose wheel servo. Additionally, it had eight motors and ESCs, one servo for the horizontal stabilizer rotational mechanism, and one linear actuator for the wing rotational mechanism. This totaled to needing 17 outputs from the Pixhawk. To reduce the number of output channels needed from the Pixhawk, the two aileron servos were connected via a Y-harness, the two elevators were connected via a Y-harness, and the two rudder servos and the nose wheel servo were also connected via a series of Y-harnesses. The elevators needed to be enabled again since the Pixhawk was not capable of using the horizontal stabilizer's rotation servo as both a stabiliator and a rotation mechanism. After searching for a solution, it was decided to condense the signals for eight motors into four channels. Schematic of the propulsion of this aircraft that was used to figure out a layout can be seen in Figure 53, below. After combining the two motors on the left wing to effectively control as one motor, the two on the right wing as one motor, the two in the front as one motor, and the two on the tail as one motor, the aircraft when in the VTOL configuration resembled a quadcopter plus (quad+) airframe. All the motors on ElectraWing are numbered the same as those of the quad+ configuration that Pixhawk uses (Figure 54, below). For

this specific configuration, the following channels and Pixhawk outputs were used (a schematic of the servo channels can be seen in Figure 55, below):

Channel 1: MAIN OUT 1: Aileron

Channel 2: MAIN OUT 2: Elevator

Channel 3: MAIN OUT 3: - -

Channel 4: MAIN OUT 4: Rudder

Channel 5: MAIN OUT 5: Motor 1

Channel 6: MAIN OUT 6: Motor 2

Channel 7: MAIN OUT 7: Motor 3

Channel 8: MAIN OUT 8: Motor 4

Channel 9: AUX OUT 1: Horizontal stabilizer rotational mechanism

Channel 10: AUX OUT 2: Wing rotational mechanism

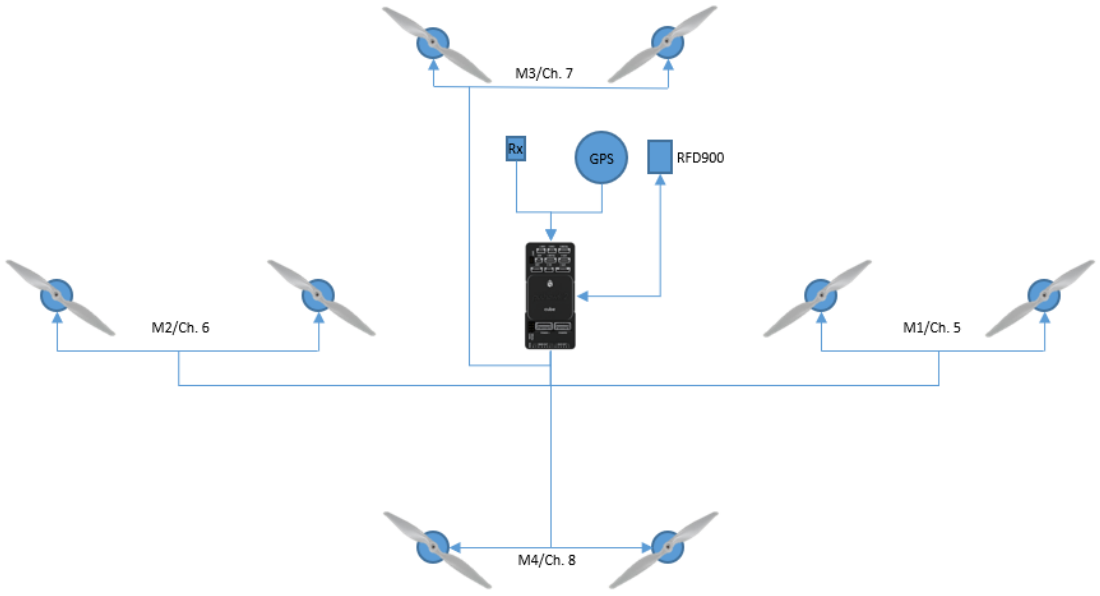

Figure 52: Schematic of ElectraWing motor signal wires. The two motors on the right wing function as "motor 1," the motors on the left wing as "motor 2," the front two motors as "motor 3," and the two motors on the tail as "motor 4." Image of propellers from Advance Precision Composites [38].

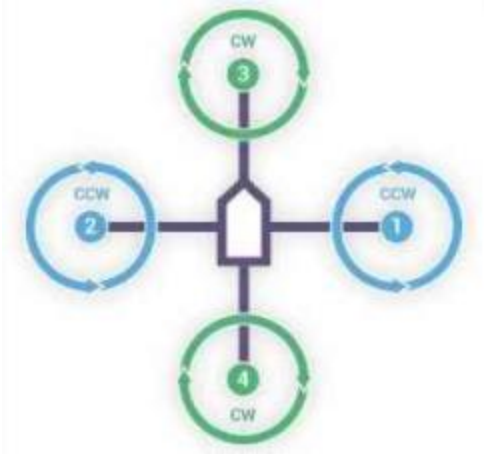

Figure 53: Quad+ frame pattern with motors labeled 1 through 4. Picture from adg.standford.edu [40].

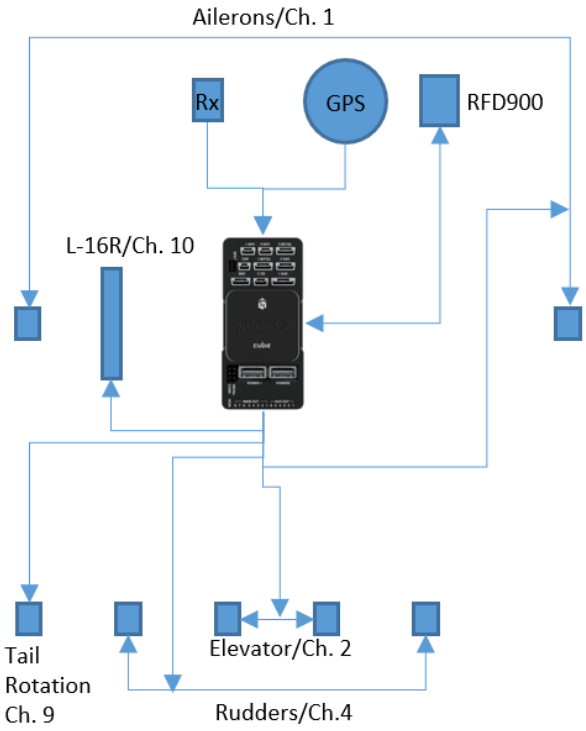

Figure 54: Schematic of Pixhawk and servo setup. Image of Pixhawk 2 from SpektreWorks.

After researching how to setup a quadplane on ardupilot.org, the following steps were used for setting up the parameters to allow for and configure the ElectraWing specific VTOL:

1. Q_ENABLE = 1
    a. This enables the quadplane and VTOL functionality in the Pixhawk and allows access to all of the VTOL parameters.
2. Refresh the parameter list.

    a. Doing this will repopulate the parameter list with the "Q_" parameters.
3. Q_FRAME_CLASS = 1
    a. This set the motor configuration to a quadcopter. If this would have been set to 4, it would have been an octaquad. Other configurations were possible.
4. Q_FRAME_TYPE = 0
    a. This set the frame type to a quad+ layout.
5. REBOOT THE PIXHAWK!
    a. This step is important. This needs to be done in order to continue changing other parameters.
6. Assigned the output channels their motor numbers, where "n" in "SERVOn" represents the channel number. Motor 1 = 33, motor 2 = 34, motor 3 = 35, motor 4 = 36.
    a. SERVO5_FUNCTION = 33
    b. SERVO6_FUNCTION = 34
    c. SERVO7_FUNCTION = 35
    d. SERVO8_FUNCTION = 36
7. ARMING_RUDDER = 2
    a. This will allow the pilot to manually arm and disarm the motors (not the entire system) with the Futaba transmitter. To do this, if the throttle is at zero, the pilot can put a full right yaw input and hold it for approximately three seconds for the motors to arm. Likewise, the same process can be used to disarm the motors, except with a left yaw input.
8. Q_THR_MD = 500
    a. This is to set the throttle setting that the aircraft will hover at to 50%.
9. Q_RTL_MODE = 1
    a. This parameter allows one to change how the aircraft will return home (RTH) in the event of a failsafe activation or the RTH command is given. Setting the parameter to "1" makes the aircraft fly to its point of launch as a fixed wing aircraft, and land in the VTOL configuration. Other available options are to return and loiter overhead in either the fixed wing or VTOL configurations, or to fly home and land all in the VTOL configuration.
10. TILT_TYPE = 0
    a. This sets the tilt type to continuous. That is, instead of the rotating motors or tilting wings only having two positions and quickly changing between them, it allows for a smooth transition.
11. Assign channels 9 and 10 (AUX OUT 1 and AUX OUT 2 on the Pixhawk) to be the tilting servos.
    a. SERVO9_FUNCTION = 41
    b. SERVO10_FUNCTION = 41
12. Q_TILT_MASK = 11
    a. The tilt mask is the most important parameter in a tilt-wing or tilt-rotor aircraft. It is a bitmask of the motors that rotate. This tells the autopilot which motors are rotating so the aircraft knows how to handle it.]
    b. It is calculated as follows
        i. Assign each motor a value: motor 1 = 1, motor 2 = 2, motor 3 = 4, motor 4 = 8, motor 5 = 16, motor 6 = 32, etc…
        ii. Add up the values for all of the motors that are rotating
        iii. In the case of ElectraWing, motors 1, 2, and 4 are rotating, but motor 3 is permanently vertical. Therefore, ElectraWing's would be 1+2+8 = 11.

The firmware used for this setup was Arduplane 3.9.0. It should be noted that all parameters starting with "Q_" relate to VTOL capabilities. It should be noted that all the instructions above were found from [38], but the Q_TILT_MASK parameter was not explained very well on the instructions on ardupilot.org, so after posting to a forum at discuss.ardupilot.org, two users, Nathan Eick and Greg Covey, were able to help explain the parameter.

Additionally, the flight modes channel was assigned to channel 11, which was a three-position switch on the Futaba transmitter. The three modes selected for the first test flight were as follows: QSTABILIZE, FWBA (fly by wire A), and MANUAL. The QSTABILIZE mode allowed for the aircraft to automatically transition to vertical flight by rotating the wings and horizontal stabilizer to the vertical position and spin up the two front motors. In this mode, the aircraft was to hover and control like a quadcopter. The FWBA mode would be the middle mode that would transition the aircraft out of the vertical flight mode. When the aircraft was converted to a fixed wing mode, this mode would stabilize the aircraft and automatically bring it back to a wings level attitude after any input or disruption in flight. Finally, the MANUAL flight mode would be a straight RC input where the pilot would have complete control of the aircraft in forward flight.

3.4.4 INDOOR FLIGHT TESTING AND GAIN TUNING

For the first few flights, ElectraWing was flown indoors at the Richmond Hills facility at Oklahoma State University. A picture of the aircraft at the indoor facility can be seen in Figure 56, below. These tests were only test the vertical flight capability in zero wind conditions. The disadvantage of testing indoors was the lack of GPS signal for position lock. However, this environment still provided the most ideal one for initial testing. The aircraft was put into the QSTABILIZE mode, and then armed. Gradually, throttle was applied until the throttle was at 100%. At this point, the aircraft was still not taking off despite all eight motors running. After turning to the forums and discussing with colleagues, it was decided that a 1.2 thrust to weight

ratio was not enough to lift the aircraft off the ground. More about this will be discussed in Chapter 5. Since this was the case, another design iteration was needed.

Figure 55: ElectraWing being tested indoors for VTOL capability

To increase the amount of thrust needed, the only possible solution was to put larger motors on the aircraft. This could have been done by replacing either all of the motors or just a couple of them. To avoid the cost of replacing all eight of the motors and ESCs, plus avoid the time it would take to order them and replace them, two motors and ESCs from the lab were used instead. The inboard two motors and motor mounts on the wings were taken off and replaced with new carbon fiber motor mounts and a SunnySky X2820–6 920kV motor. An image of the SunnySky motor mounted on the wing can be seen in Figure 57, below. The new ESCs were Hobbywing ESCs. The motor mounts were mounted exactly the same as the smaller ones were as described in section 3.4.3. The propellers for the new motors were APC 12x6E and 12x6EP. Similarly, to the RimFire motors, the three motor leads were braided, but the wires used were 16 AWG.

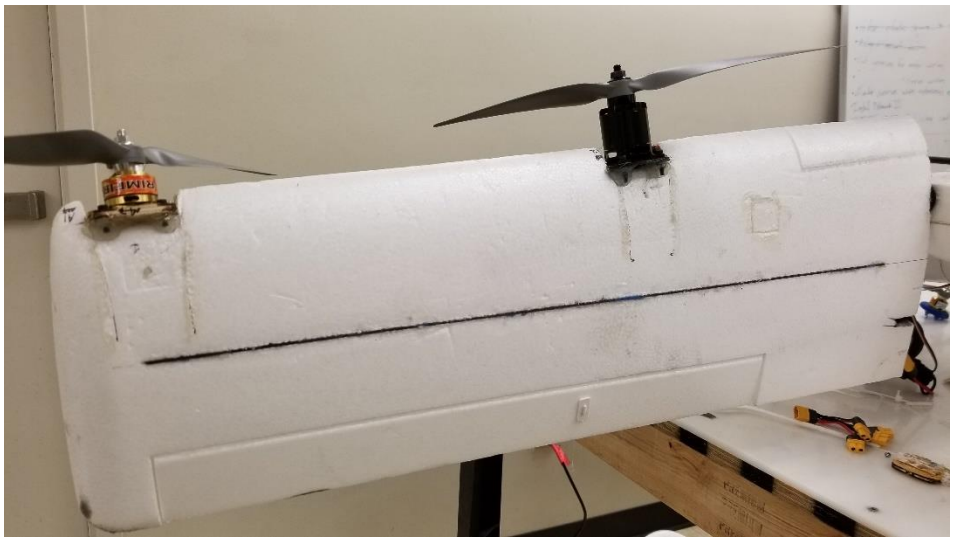

Figure 56: Larger motor on inboard of wing with original RimFire motor on wingtip

After this modification was made, another hover test was conducted indoors. The aircraft was able to lift off the ground, but it was not stable, and fairly uncontrollable. The next step was to tune the gains in the hover configuration. To do this, the proportional (P), integral (I), and derivative (D) gains were all set to the lowest values possible. The P gain was then increased after each hover test in very small increments. This was repeated until the aircraft started oscillating while in a hover. At this point, the P gain was cut in half, and the I gain was then increased using the same method until the aircraft started to oscillate, and any offset is corrected. Finally, the D gain was increased to smooth it out. This method was recommended by Dane Johnson of the Unmanned Systems Research Institute (USRI).[41] After this method failed to produce good results (the aircraft remained unstable while in the hover configuration), Fred Keating of the USRI was brought in for his knowledge of tuning gains with Pixhawk. He tweaked the gains and increased the Q_AZ parameter, which had the greatest impact on the aircraft's stability. This parameter controlled the vertical acceleration of the aircraft.

3.4.5 OUTDOOR FLIGHT TESTING

After the aircraft was hovering relatively reliably indoors, it was taken out to Oklahoma State University's UAS field. At this time, another hover test was conducted. The 10-minute average wind speed was 11 mph, but hover was only attempted when the wind dropped. After this hover test proved to be a little unstable, the I gain was lowered slightly. This same process was repeated two more times until a stable hover was established. A high-speed taxi test was conducted with the aircraft yet again. This time, the aircraft was allowed to lift off the ground, and was immediately landed. This test was conducted three times to test that the elevators were working properly after the previous incident. The aircraft was also armed in QSTABILIZE mode while on the ground and switched to FWBA. Throttle was slowly increased, and the aircraft started to lift off and slowly transition to forward flight approximately 1ft off the ground. As soon as the aircraft started to move forward, the take-off was aborted, and the aircraft was returned to QSTABILIZE mode.

For the last test, the aircraft took off vertically approximately 6 feet off the ground. A low altitude was used to hopefully minimize damage should the aircraft lose control. The aircraft was then switched to FWBA. The aircraft then started to slowly move forward and transition to forward flight. However, before the aircraft could fully transition to forward flight, it gave a sharp pitch up, and immediately nosed down about 90 degrees into the ground. For a breakdown of this incident, refer to chapters 4 and 5.

CHAPTER IV

RESULTS

4.1 PROPELLER PREDICTIONS AND TESTING

4.1.1 ECALC RESULTS

eCalc outputs data in a few different ways: first, it shows little gauges for a quick data reference. This output can be seen in Figure 58, below.

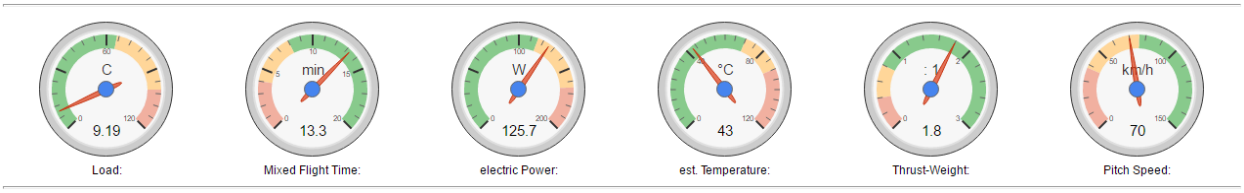

Figure 57: Quick visual outputs for eCalc [46].

At the bottom of the page, eCalc outputs data to a graph. Unfortunately, this graph is just a picture on the website, and cannot be interacted with. It is for the ease of comparison that this graph will not be used in the analysis of this propeller/motor/ESC combination. Figure 59, below, shows the graphical output of eCalc.

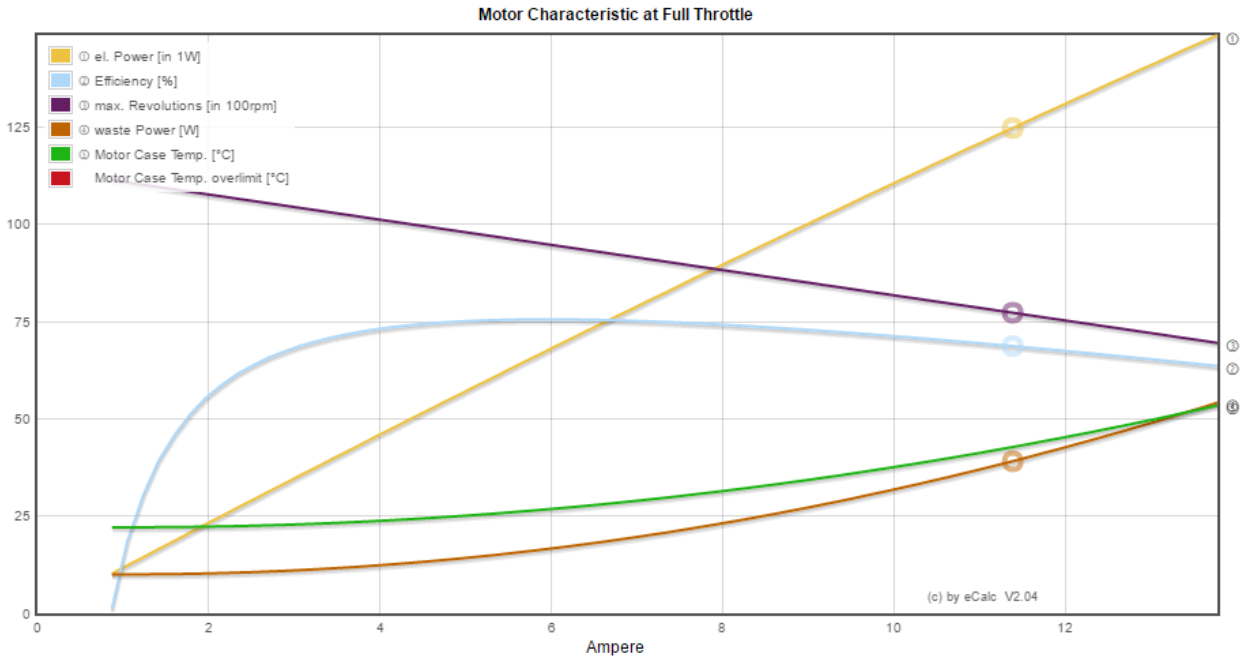

Figure 58: Graphical output from eCalc. Pictured here are plots for power, efficiency, maximum revolutions, waste power, motor case temperature, and motor case temperature "overlimit" vs. Amperes. The results of this graph will not be discussed as the numerical data is what is of interest for this analysis. This graph was provided to show all the outputs from eCalc.

Lastly, a Microsoft Excel file can be downloaded from the website with the data. However, the data present in the Excel file is very limited and is not in a very user-friendly format as data is separated by semicolons instead of in separate cells. It was found to be easier to just transpose the data from the website to a blank Excel file.

4.1.2 VERIFICATION OF eCalc

As mentioned previously, this aircraft is intended to have VTOL capabilities, and requires a power to weight ratio of approximately 1.2. However, in an attempt to plan for unaccounted weight, a designed power to weight ratio of 1.8 was used. To help validate eCalc, the static thrust output was used compared to the nearly static case of XROTOR and the nearly static case of APC

data. For the nearly static cases with XROTOR and APC data, the 7500 RPM was used for a maximum possible value for thrust. Table 4, below, shows the static thrust and power to weight ratios for all three methods. The accuracy of the APC data is unknown, as is the accuracy of XROTOR given the unknown parameters entered and the exact blend of airfoils for APC propellers being proprietary.

Table 4: Comparison of static thrust at 7500 RPM for all three methods discussed. The freestream velocity (V) is given in both knots and feet per second, separated by a forward slash respectively

Static Thrust Comparison	eCalc	XROTOR	APC Data
V (knots/ft/s)	0	2.6/4.4	2.8/4.7
Thrust for single motor (lbf)	1.66	1.43	1.61
Thrust for 8 motors (lbf)	13.28	11.44	12.88
Power to weight ratio	1.77	1.53	1.72

XROTOR yields a total thrust (8 motors) of 1.84 lbf lower than eCalc's prediction, and 1.44 lbf lower than the APC prediction. Meanwhile, eCalc only predicts 0.4 lbf higher than the APC prediction. This difference in thrust may sound small, but 1.44 lbf is approximately 20% the overall weight of the aircraft.

For the flight condition, only three data points were able to be used since this is all eCalc displayed in initial runs. In later runs, only one extra data point was usable for the 6000 RPM point. The following graphs are comparisons between eCalc, XROTOR, and APC data for the flight condition in Figures 60 and 61, below. These airspeeds range between 48 ft/s and 56 ft/s. Specifics on this data can be seen in Table 5, below.

Table 5: Data comparison for the flight condition

		XROTOR		eCalc		APC	
RPM	V_{oo} (ft/s)	Thrust (lbf)	Efficiency	Thrust (lbf)	Efficiency	Thrust (lbf)	Efficiency
6500	48.4	0.596	0.753	1.16	0.714	0.281	0.638
7000	52.8	0.677	0.757	1.34	0.709	0.324	0.644
7500	55.7	0.798	0.755	1.54	0.702	0.419	0.664

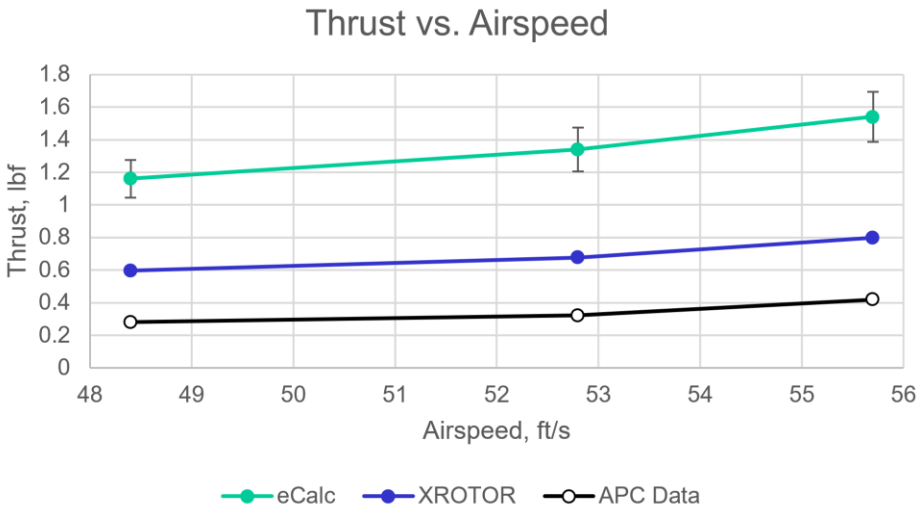

Figure 59: This graph shows the data presented in table 5, above. The error bands in the eCalc data represent a 10% error, which is eCalc's disclaimer. The error bands are depicted in this graph to show how far off eCalc is from the other two methods.

Figure 60, above, shows that when the aircraft is flying, eCalc's prediction for thrust is much higher than the predictions from XROTOR and the APC data. The maximum difference between XROTOR and APC is 0.379 lbf, at 7500 RPM and 55.7 ft/s airspeed. While at the same data point, eCalc predicts 0.742 lbf higher than XROTOR and 1.121 lbf higher than the APC data prediction. It is possible that the XROTOR prediction may be off due to inaccuracies in the measurements of the propellers or due to the unknown inputs discussed in Chapter 3.2.3. As for

the eCalc prediction, it is uncertain due to possible input inaccuracies with the aircraft weight. Also, it is possible that the data on file for the APC propeller could be inaccurate. This is a possibility since the data posted on their website is out of date and not as accurate as the data Holik provided. The reasoning for this is because, according to Holik, they have not updated their website since they modified their prediction software. Therefore, since eCalc leaves it up to companies to submit data to them, the most current data may not be in their database.[42]

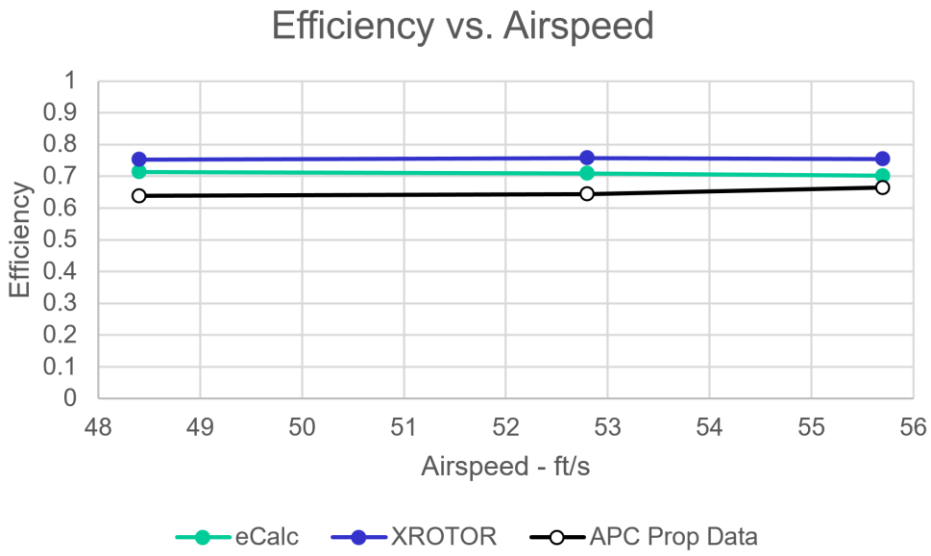

Figure 60: This graph shows the efficiency in the flight conditions of all three methods. eCalc is relatively close to the other two methods.

When looking at the efficiency data seen in figure 61, above, it can be seen that all three methods yield similar results. ECalc shows up in the middle of the two other methods and is within 10% accuracy from the other two methods. These results, however, have questionable accuracy due to the reasons listed above.

Since the results of the three methods differed from each other, an iteration using XROTOR was produced to compare with the APC data. This iteration was run at 7000 RPM for the same array of airspeeds provided by APC. The iteration was done with the "VSEQ" command under the .OPER menu in XROTOR. This was done in an attempt to verify XROTOR over a variety of data points when compared to the APC data, which is speculated to be the most accurate considering it

comes directly from the manufacturer. This would hopefully clear up some of the gap between the three methods shown above. The results of this analysis can be seen in Figures 62 and 63, below.

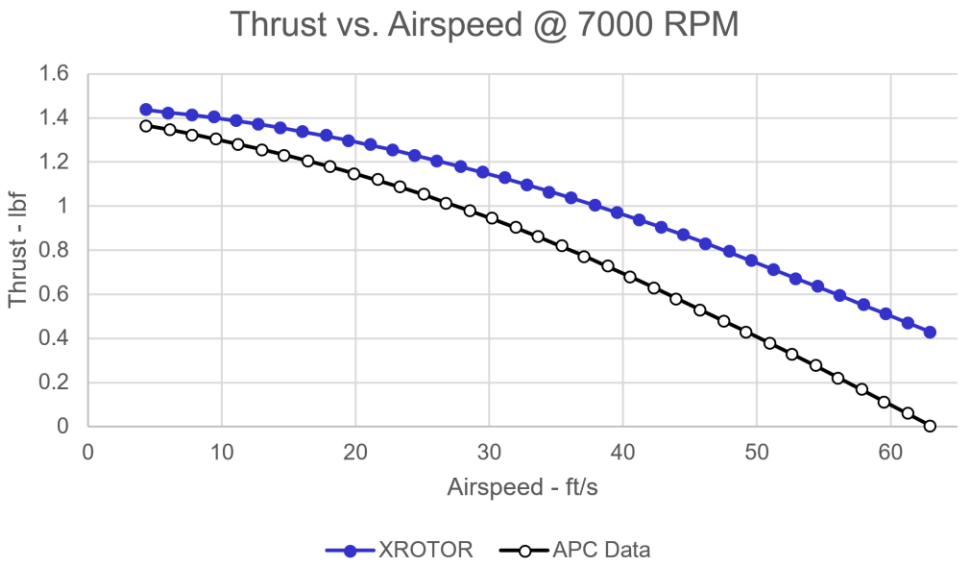

Figure 61: Comparison between XROTOR and APC. Note that the data diverges as the airspeed increases. Potential reasons for this will be discussed below.

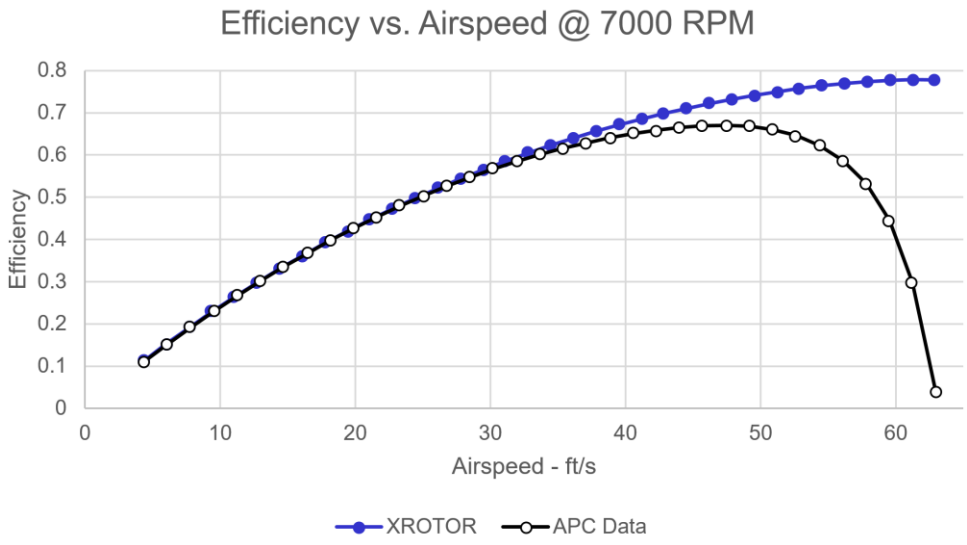

Figure 62: A comparison between the efficiency prediction of XROTOR and the APC data. The two predictions diverge at higher airspeeds, but agree at lower airspeeds. Potential reasons for this will be discussed below.

When the arrays of data for XROTOR and APC were compared (see Figures 62 and 63, above), it was noticed that at higher airspeeds, the data diverged, but at lower airspeeds, the data was very

similar. This observation was the same with both the thrust prediction and the efficiency prediction. Since the airspeeds being compared with eCalc are at 48.4 ft/s, 52.8 ft/s, and 55.7 ft/s, it can be seen that this is in the range of efficiencies that XROTOR starts to separate at and thrust is pretty well separated at. The potential reason for this divergence of data is due to the potential inaccuracies in propeller measurements put into XROTOR, the incorrect aerodynamic data inputs from airfoiltools.com (taken from wrong Reynolds number value as discussed above), the unknown inputs for XROTOR, and the unknown blend of Eppler E63 and Clark-Y airfoils used in the APC 9X6E propeller. This assumption definitely makes sense, especially with the aerodynamic data being off due to having to get it from a higher Reynolds number. The reasoning is that with a higher Reynolds number, it implies a higher velocity, and as seen in Figure 63, the XROTOR prediction keeps getting higher until it reaches a peak of about 80% at a freestream velocity of about 65 ft/s before it starts coming back down.

4.1.3 THRUST STAND RESULTS

As previously mentioned, the RCbenchmark stand was used to analyze four different propellers over a series of throttle settings. The propellers used were APC 9x6E, 9x7.5E, 9x10E, and 11x7E. each of these propellers were run at each throttle setting for 3.5 seconds, and the average thrust was recorded. The throttle PWM settings were: 1000, 1100, 1200, 1300, 1400, 1500, 1600, 1700, 1800, 1900, and 2000. Where at 1000 PWM the motor is not spinning, and 2000 PWM is full throttle. The results of these tests can be seen in Figure 64, below. The tolerances of thrust measurements for the RCbenchmark 1520 V1.0 are not available online. The author reached out to the company, but RCbenchmark has not responded. However, the datasheet from V1.2 of the thrust stand is currently available. For this version of the stand, the tolerance is 0.5%.[43]

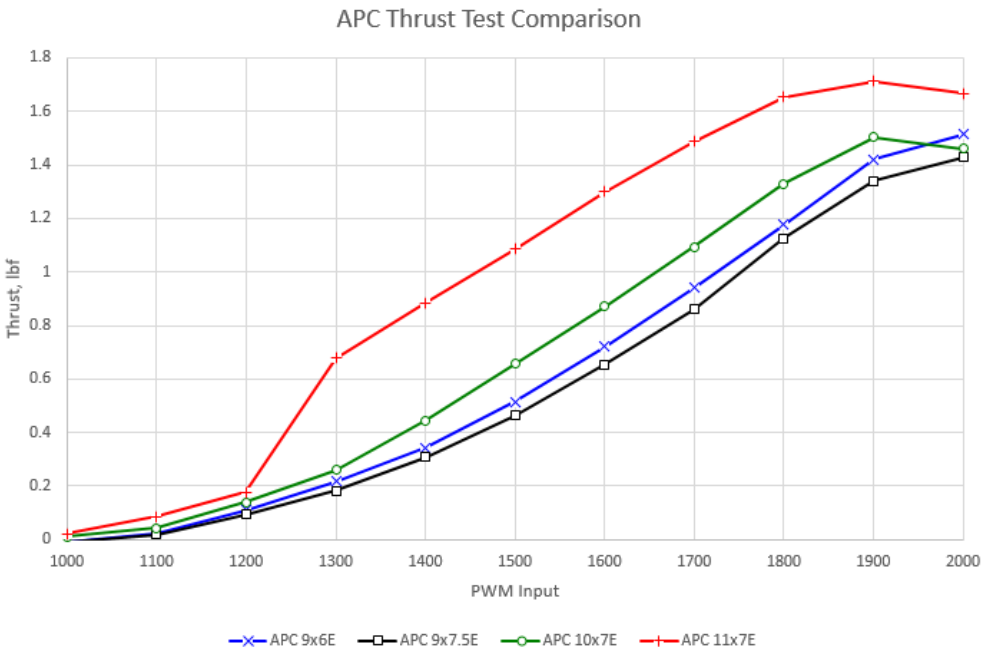

Figure 63: RCbenchmark thrust stand test results using four different APC propellers. It is worth noting, that the error bars for this data are too small to be seen

4.1.4 COMPARISON OF DATA

As previously mentioned, this aircraft is intended to have VTOL capabilities, and requires a power to weight ratio of approximately 1.2. However, to plan for unaccounted weight, a designed power to weight ratio of 1.8 was used. To help validate eCalc, the static thrust output was used compared to the nearly static case of XROTOR and the nearly static case of APC data. For the nearly static cases with XROTOR and APC data, the 7500 RPM was used for a maximum possible value for thrust. Additionally, these computational thrusts were compared to the RCbenchmark thrust stand tests. Table 6, below, shows the static thrust and power to weight ratios for all four methods.

Table 6: Comparison of static (or near static) thrust of eCalc, XROTOR, and APC data with the RCbenchmark thrust stand. The first three computer methods for determining the data were using 7500 RPM

Static Thrust for APC 9x6E	eCalc	XROTOR	APC	Thrust Stand
V (ft/s)	0	4.4	4.7	0
Thrust for single motor (lbf)	1.66	1.43	1.61	1.51
thrust for 8 motors (lbf)	13.28	11.44	12.88	12.08
T:W	1.23	1.06	1.19	1.12

4.2 OBJECTIVE I ANALYSIS & EXPERIMENTATION

4.2.1 OBJECTIVE I STATIC STABILITY RESULTS

Using the equations in section 3.2.2, a graph of the pitching moment about the center of gravity versus the angle of attack was constructed and can be seen in Figure 65, below. The data stops at 15 degrees angle of attack due to the stalling limitations of the assumed Clark Y airfoil. The aft CG limitation was found to be 50% of the MAC, at which point the aircraft would become neutrally stable (represented by "x" in the graph). If the center of gravity were to travel behind this point, the aircraft would become statically unstable (represented by "+"). RMRC recommends the CG be placed 3.5 inches behind the root leading edge which is 32% MAC (represented by squares). However, from theoretical calculations, the desired trim point for this aircraft was found to be at approximately 4 degrees angle of attack (represented by triangles). This was based on a 12-pound take-off weight, standard sea level conditions, and an airspeed of 50 feet per second. This discrepancy is possibly due to the airfoil selection used for the estimates. These were the most restrictive limitations of the aircraft out of all phases of flight. It was also found that CG travel needed to be kept behind 29% MAC (represented by circles). This limitation

is due to the trim angle of attack. If the CG is moved in front of this limit, the trim point would be at a negative angle of attack which would result in a descent.

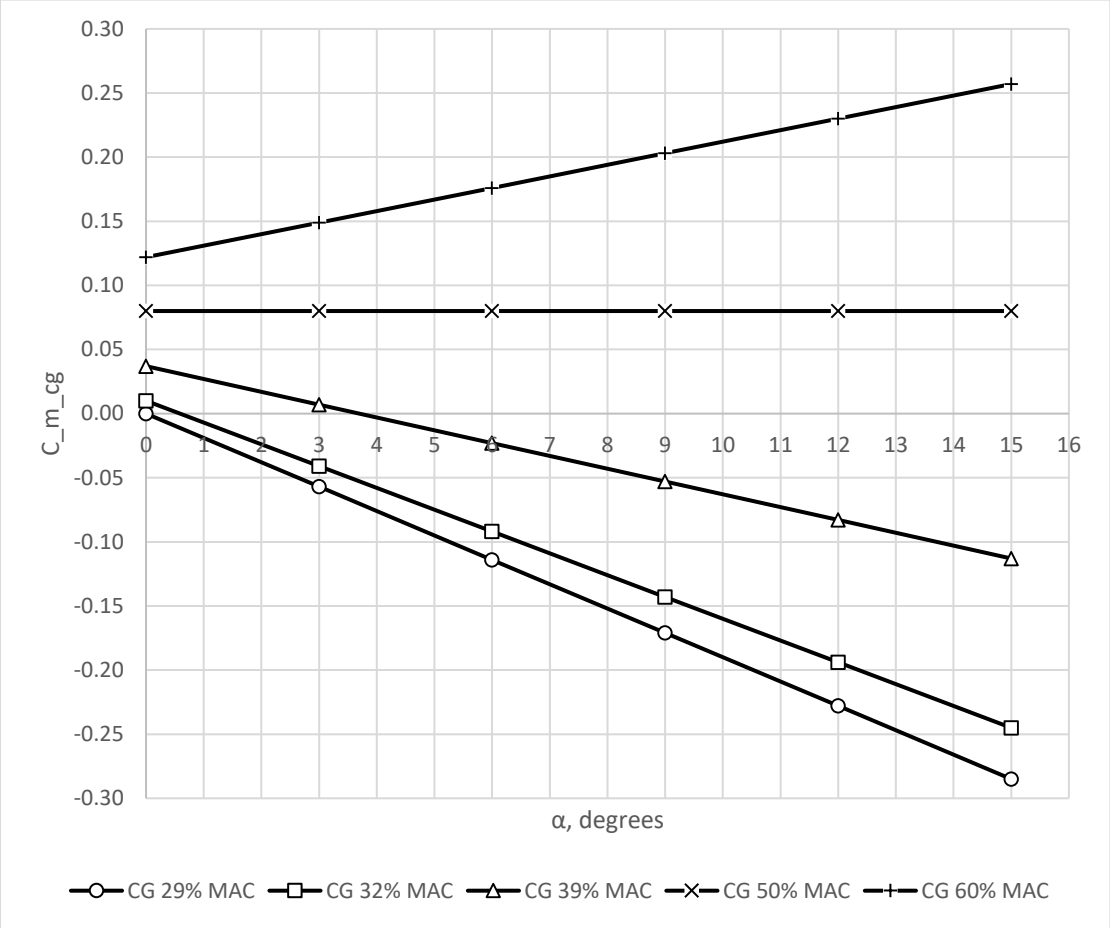

Figure 64: Coefficient of moment vs. angle of attack graph for ElectraWing.

Using a static moment equation, it was found that in the hover configuration, the center of gravity could be as far forward as 4.1 inches ahead of the root leading edge. A CG vs. wing rotation angle graph can be seen in Figure 66, below. The data depicted by circles represent the wing rotation only, while the data depicted by triangles represent both the wing and tail rotating. From this, the maximum CG travel remains within 37% MAC and 40.5% MAC. Both points are within the limits depicted by Figure 65, above.

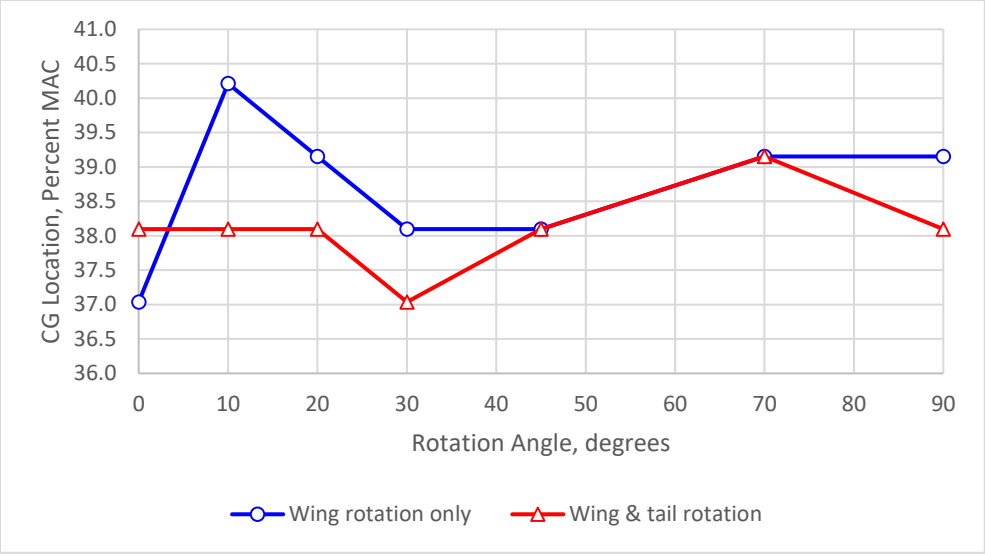

Figure 65: CG shift between horizontal (left) and vertical flight modes (right).

4.2.2 OBJECTIVE I FLIGHT TESTING

Since the first flight test was just to test whether the aircraft could fly manually, it did not have an autopilot onboard, and therefore was not recording data. For the purposes of this flight, the Cooper–Harper Handling Qualities Rating Scale was used. This scale was introduced in 1969 at NASA as a method to measure the quality of an aircraft's handling capabilities for a specified task.[44] Figure 67, below is the flow chart from the paper *Handling Qualities and Pilot Evaluation* by Robert P. Harper Jr. and George E. Cooper in 1984. Flight qualities of an aircraft are completely subjective and make it hard to reliably rate on the Cooper–Harper scale. However, the Cooper–Harper scale attempts to take as much of the human element out of the equation as possible, but it is still very possible to have point differences from pilot to pilot. Ideally, multiple pilots would fly the aircraft and perform the same tasks, and the average rating from each of them would be used.

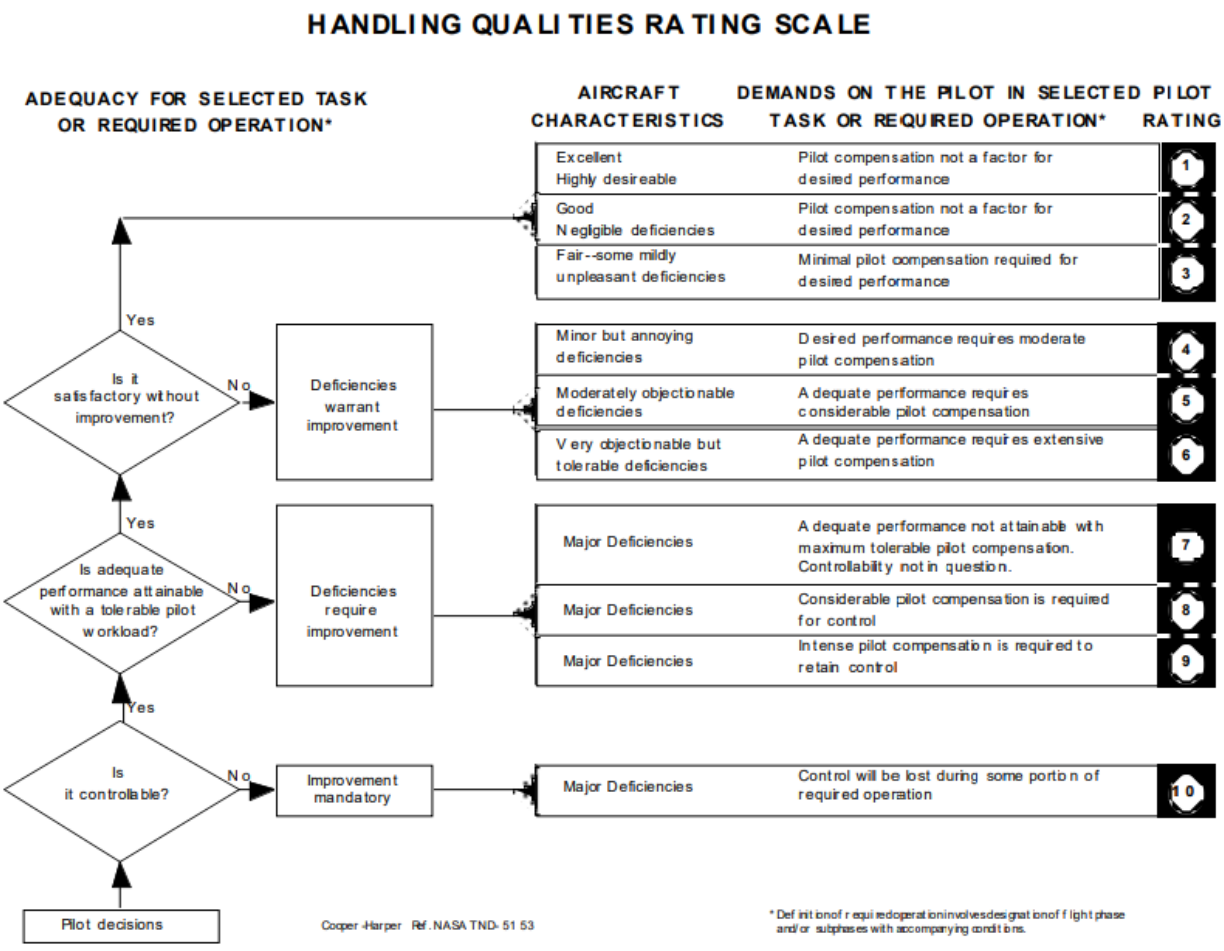

Figure 66: Cooper–Harper Handling Qualities Rating Scale flowchart. Image retrieved from aopa.org

Once the aircraft's mission has been defined and the pilot tries to execute that mission, the pilot then goes through the flowchart shown in Figure 67, above. For the first flight of the ElectraWing concept, the mission was to perform a conventional take-off, fly one lap around the airfield, and land conventionally. For this test, ElectraWing received a score of 2 on the Cooper–Harper scale. This rating means that ElectraWing had good flight characteristic and negligible deficiencies. The pilot did not have to input any compensation to get the aircraft to complete its mission. The wind on this day was negligible. Table 7, below is a flight test card with objectives and results of the flight test.

Table 7: Flight test card for first test flight. This card was modeled after the test cards in Zach Barbeau's Thesis, Oklahoma State University.

Test Sortie:	Conventional Takeoff and Landing Test w/o Rotational Mechanisms		
Aircraft: ElectraWing	Date/Location: 16-Oct-17	Supervising Test Engineer SRW	
Test Objectives: To test the flight characteristics of the modified Anaconda	Weather: Wind: 0 knots Temperature: N/A Barometric Pressure: N/A		Limits: 1. < 10 minutes 2. < 400 ft AGL 4. < 17 knots wind
Configuration: 1. Direct RC input 2. Wings fixed 3. Horizontal stabilizer fixed	Notes: After aircraft is airborne, it will fly one lap in the traffic pattern for trimming and flight control testing.		
Frequencies: 2.4GHz	Weight & Balance: CG Measured (est.): 30% CG Calculated: 35%	TOW lbs: 12.3	
PROCEDURE			
Start Time: 5:15pm		End Time: 5:17pm	
1	Perform slow taxi tests on the ground & trim rudder		
2	Perform high speed runs down the runway without taking off & trim rudder		
3	Take off CTOL		
4	Fly 1 lap in traffic left-hand traffic pattern & trim aircraft		
5	Land aircraft & finish		
# Takeoff/Landing	Comments		Issues
1	Aircraft performed as expected. No issues with controls. Aircraft had a lot of authority and was able to sustain a high angle of attack on landing without stalling.		N/A

4.3 OBJECTIVE II ANALYSIS & EXPERIMENTATION

In this section, the CTOL flight characteristics will be looked at using the Cooper–Harper scale. The aircraft did not have a Pixhawk onboard as the manual flight characteristics and structural integrity of the new rotating wing and horizontal stabilizer mechanisms was being examined.

4.3.1 FLIGHT TEST I: CTOL

On this flight, the mission was to perform a conventional take-off, fly a lap around the airfield, then land conventionally. The aircraft performed this task without any issues. The Cooper–Harper scale rating for this flight was 2. It had negligible deficiencies and performed its task with ease. The wind on this test was negligible. The flight test card for this flight can be seen in Table 8, below.

Table 8: Flight test card outlining the first CTOL flight test with the wing and horizontal stabilizer rotational mechanisms in place. Test card modeled after those in Zach Barbeau's thesis, Oklahoma State University

Test Sortie:	Conventional Takeoff and Landing Test w/ Rotational Mechanisms		
Aircraft: ElectraWing	Date/Location: 16-Oct-17	Supervising Test Engineer SRW	
Test Objectives: To test the flight characteristics of the modified Anaconda	Weather: Wind: 10 knots Temperature: 48 F Barometric Pressure: 30.264 inHg		Limits: 1. < 10 minutes 2. < 400 ft AGL 4. < 17 knots wind
Configuration: 1. Direct RC input/no Pixhawk 2. Wing rotational mechanism in place 3. Horizontal stab. mechanism in place	Notes: After aircraft is airborne, it will fly one lap in the traffic pattern for trimming and flight control testing.		
Frequencies: 2.4GHz	Weight & Balance: CG Measured (est.): 30% CG Calculated: 32%		TOW lbs: 10.9
PROCEDURE			
Start Time: 4:48pm		End Time: 5:52pm	
1	Perform slow taxi tests on the ground & trim rudder		
2	Perform high speed runs down the runway without taking off & trim rudder		
3	Take off CTOL		
4	Fly 1 lap in traffic left-hand traffic pattern & trim aircraft		
5	Land aircraft & finish		
# Takeoff/Landing	Comments		Issues
1	Aircraft performed well with the new rotational mechanisms. The wing rotational mechanism did not seem to flex mid flight, nor did the horizontal stabilizer.		N/A

4.3.2 FLIGHT TEST II: CTOL

On the first flight, once the aircraft left the ground in the CTOL configuration (to ensure the aircraft was still trimmed properly), it attained a positive rate of climb. However, shortly into the climb, the aircraft pitched down and descended uncontrolled until it hit the ground. Although there was minimal damage, the pilot was unable to stop the aircraft's descent. From this, the aircraft started out as a 1 or 2 on the Cooper–Harper scale, but quickly it became a 10 on the scale, as it was uncontrollable. For a discussion of the possible causes of this incident, see Chapter 5. The average wind speed for this test was South at 11 mph gusting to 18 mph. The test card outlining this flight can be seen in Table 9, below.

Table 9: Flight test card for Phase III flight Test I. The aircraft was performing a CTOL mission to check all control surfaces were trimmed before STOL testing. Test card modeled after those in Zach Barbeau's thesis, Oklahoma State University

Test Sortie:	Conventional Takeoff and Landing Test w/ Rotational Mechanisms		
Aircraft: ElectraWing	Date/Location: 26-Feb-18	Supervising Test Engineer SRW	
Test Objectives: To test the flight characteristics of the modified Anaconda	Weather: Wind: 10 knots Temperature: 64 F Barometric Pressure: 30.155 inHg		Limits: 1. < 10 minutes 2. < 400 ft AGL 4. < 17 knots wind
Configuration: 1. Direct RC input/no Pixhawk 2. Wing rotational mechanism in place 3. Horizontal stab. mechanism in place	Notes: This test is just to ensure aircraft is flying properly before conducting STOL tests.		
Frequencies: 2.4GHz	Weight & Balance: CG Measured (est.): 30% CG Calculated: 32%		TOW lbs: 10.9
PROCEDURE			
Start Time: 2:21pm		End Time: 2:22pm	
1	Take off CTOL		
2	Trim aircraft in flight		
3	Land aircraft CTOL		
4	Set up for takeoff distance tests		
# Takeoff/Landing	Comments		Issues
1	Aircraft took off and immediately established a positive rate of climb. Soon after, the aircraft pitched down and crashed. Damage was minimul, but could not be fixed at the field.		Shortly after take-off, aircraft pitched down and became unresponsive to pitch inputs causing the aircraft to crash.

4.3.3 FLIGHT TEST III: STOL

For the second set of flights, the whole moving stabilator had been implemented, so the first flight was purely to take-off conventionally, fly one lap around the airfield, and land conventionally.

For this flight, the aircraft performed well and received a score of 1 on the Cooper–Harper scale. This score meant that the aircraft had no deficiencies in flight. Likewise, on all of the STOL flights, the aircraft performed with minimal deficiencies.

After the first test flight of the day, it was time to start with STOL testing. The approximate take-off roll distance was taken for each of the wing positions was recorded along with the wind speed and direction. This data can be seen in Table 10, below. Few data points were recorded to be conservative with the aircraft since the VTOL phase still needed to be tested. This test was to be revisited on a calmer day with the Pixhawk installed.

Table 10: Table of take-off distance vs. wing angle and wind speed/direction. The average wind speed along the bottom of the table has been corrected for wind direction. There are inaccuracies in these assumptions as the UAS field weather data only outputs wind direction in letter form. The assumptions were made that SE = 45 degrees from the runway, SSE = 20 degrees, and ESE = 70 degrees.

Wing Rotation (degrees)	0	Wind (MPH)	10	Wind (MPH)	20	Wind (MPH)	30	Wind (MPH)	45	Wind (MPH)
Takeoff Distance (ft)	106	7/SE	63	11/S	91	6/SE	77	10/SSE	No takeoff	8/ESE
	91	12/S	63	12/S	91	8/ESE	85	7/SSE	No takeoff	11/SSE
Average:	98.5	8.5/S	63	11.5/S	91	3.5/S	81	8.0/S	--	6.5/S

The data in Table 10 shows that the take-off distance for the 10 degrees of wing rotation yields the shortest take-off distance, while the CTOL condition yields the longest. However, at 45 degrees of wing rotation, the aircraft was unable to become airborne. For the 30-degree scenario, the aircraft was able to become airborne, but could not establish a positive rate of climb. Instead, the aircraft remained in ground effect 1 to 2 feet above the surface of the runway until the take-off was aborted. It should also be noted that as the wing rotation angle increased, so did the instability of the take-off. At 20 degrees of wing rotation, it became difficult to maintain wings level until the aircraft established a positive rate of climb.

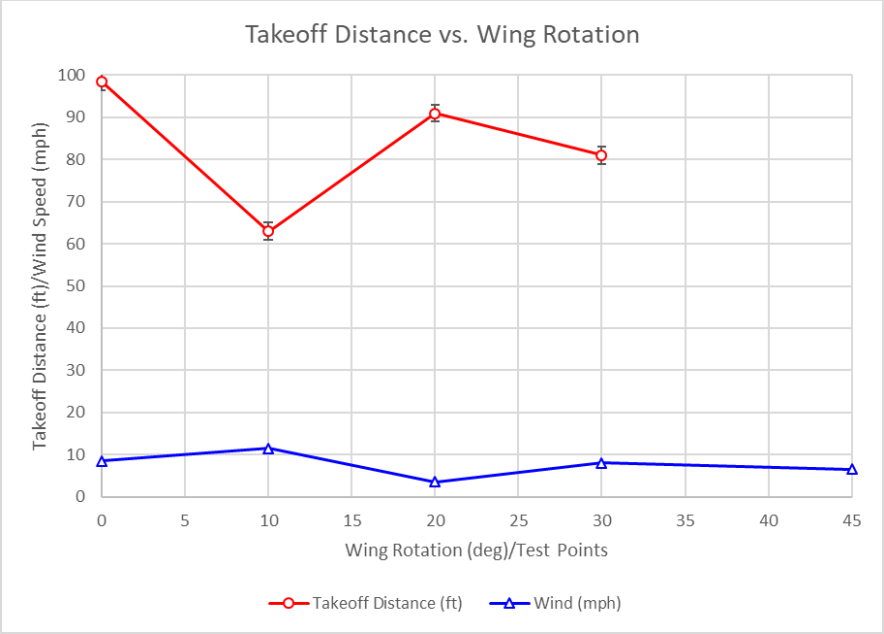

Figure 67: Graph of the take-off distance vs. wing rotation angle. Also depicted in this graph was the average wind for each of the average wing rotation angles.

Figure 68, above, is a visualization of the data in Table 10. It shows the roll distance for take-off against the wing angle. Also pictured in the graph is the average wind speed at each of the wing rotations. This helps determine how much wind was a factor for the take-off distances. The take-off distances were visually detected, therefore there is a possibility for error in the data. However, the point the aircraft left the ground was recorded via video and pinpointed on playback. Therefore, the distances shouldn't be off more than +/- 2ft. This is depicted by the error bands in Figure 68. The flight test card for the 10 degrees of wing rotation can be seen in Table 11, below. The rest of the test cards for the short take-off testing can be seen in Appendix C. They are being excluded from this chapter because they are all similar.

Table 11: This test card discusses the short take-off test with 10 degrees of wing rotation

Test Sortie:	Short Takeoff Test w/ Rotational Mechanisms		
Aircraft: ElectraWing	Date/Location: 10-Mar-18	Supervising Test Engineer SRW	
Test Objectives: To test the flight characteristics of the modified Anaconda	Weather: Wind (knots): 12/S Temperature: 70 F Barometric Pressure: 29.702 inHg		Limits: 1. < 10 minutes 2. < 400 ft AGL 4. < 17 knots wind
Configuration: 1. Direct RC input/no Pixhawk 2. Wing rotational mechanism in place 3. Horizontal stab. mechanism in place 4. Elevators locked out - using stabilator	Notes: This test is to determine takeoff roll distance with 10 degrees of wing rotation.		
Frequencies: 2.4GHz	Weight & Balance: CG Measured (est.): 30% CG Calculated: 32%		TOW lbs: 10.9

PROCEDURE

Start Time:	3:19pm	End Time:	3:21pm
1	Takeoff with full throttle and 10 degrees of wing rotation		
2	Once positive rate of climb is estabilished, slowly rotate wings back to 0 degrees		
3	Immediately land aircraft CTOL		
4	Line up on the takeoff mark and repeat steps 1 through 3		
5			
6			
7			
8			
9			

# Takeoff/Landing	Comments	Issues
2	The aircraft took off approximately 43 feet before the CTOL test. There were no stability issues on takeoff in this configuration. Aircraft did descend slightly if wings were rotated back to 0 degrees too soon.	N/A

On the last flight, a landing was attempted while slowly rotating the wings. The aircraft did complete a shorter landing, but it was very unstable and resulted in two broken propellers as the aircraft had multiple wingtip strikes. Despite the instability, this test resulted in the aircraft having a much shorter roll distance on landing. Further testing with the Pixhawk for onboard stabilization would be needed to test the short landing capabilities.

4.4 VTOL ANALYSIS, AUTOPILOT CONFIGURATION & TESTING

4.4.1 VTOL TRAJECTORY PREDICTION

Figure 69 below, depicts the calculated trajectory plot of the aircraft taking off vertically without any position holding assistance from the autopilot. The aircraft was predicted to take-off at the origin of the graph, and climb at 1 ft/s until it reached 30 feet AGL, at which time it would start transitioning to forward flight while continuing the 1 ft/s rate of climb. It was assumed that the aircraft would be pointed into the wind, and the wind would be going in the negative direction on the graph.

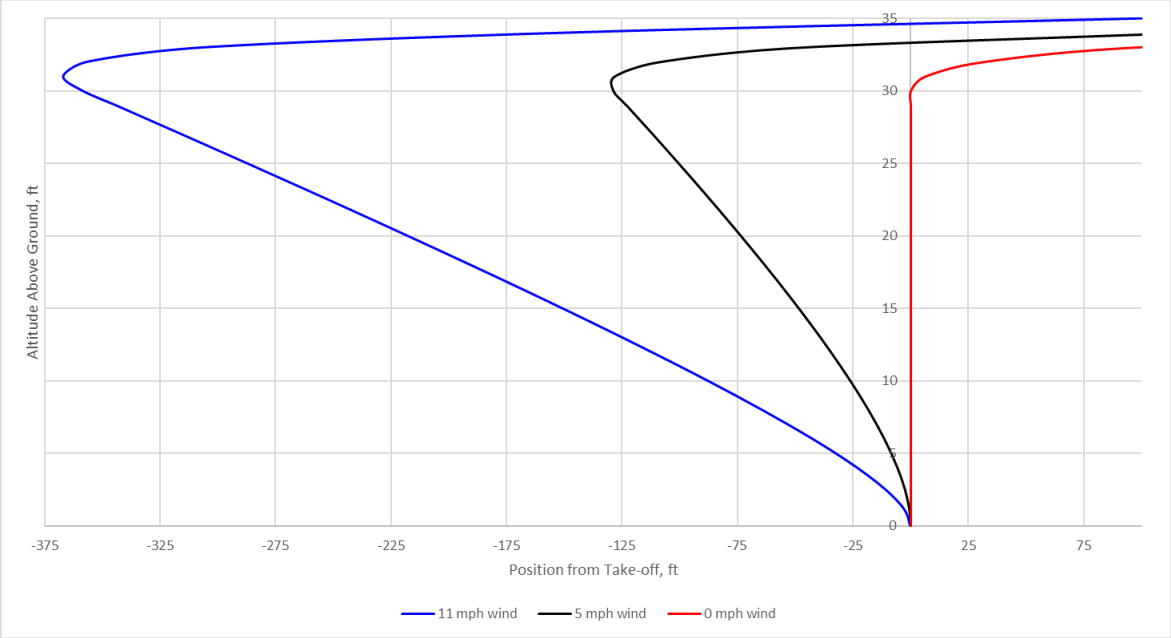

Figure 68: VTOL trajectory prediction plots. Left is with an 11 mph headwind wind, middle is a 5 mph headwind, and right is with no headwind.

The graph shows the aircraft flying vertically before the transition starts in the 0 mph wind condition (right). This compares to the 5 mph wind condition (middle), where the aircraft was predicted to traverse a maximum of 128 feet, and the 11 mph wind condition (left) where the aircraft was predicted to traverse a maximum of 366 feet before transitioning. The initial drag force on the aircraft (stationary) with the 11 mph wind was 1.54 lbf, and 0.32 lbf for the 5 mph wind.

4.4.2 EFFECT OF VTOL ON WING STRUCTURE

The thrust for M2 was the previously measured 1.5 pound-force and the thrust for M1 was approximated with eCalc to be 4 pound-force. The weight of the wing section with all motors, propellers, and wiring was measured to be 1.41 pound-force. The moment calculated at the point of rotation was 5.4 pound-feet, and the shear stress applied to the wing-tube was calculated to be approximately 9200 pounds per square foot, or 64 pounds per square inch. These relatively large

forces are due to having all the forces on the wing acting on this one point and the wing-tube having a small cross-sectional area.

4.4.1 VTOL TESTING

After the SunnySky motors were installed, the indoor flight tests and gain tuning started out as a 10 on the Cooper–Harper scale, and gradually increased. The highest score achieved for the indoor flight testing was 4 on the scale. Despite countless attempts at tuning the gains, the aircraft could not achieve 3 or above. Once the aircraft was taken outside, the Cooper–Harper score regressed to approximately 6 for the first couple of VTOL attempts. The few tests that were run in CTOL mode were approximately 3 on the Cooper–Harper scale. The first VTOL attempt at approximately one foot scored 2 on the scale. however, on the final attempt at VTOL with an altitude of about 5ft above the ground, the aircraft started out with a score of 3, but very quickly went to 10. The 10-minute average wind was SE at 10 mph. A graph of the short flight can be seen in Figure 70, below.

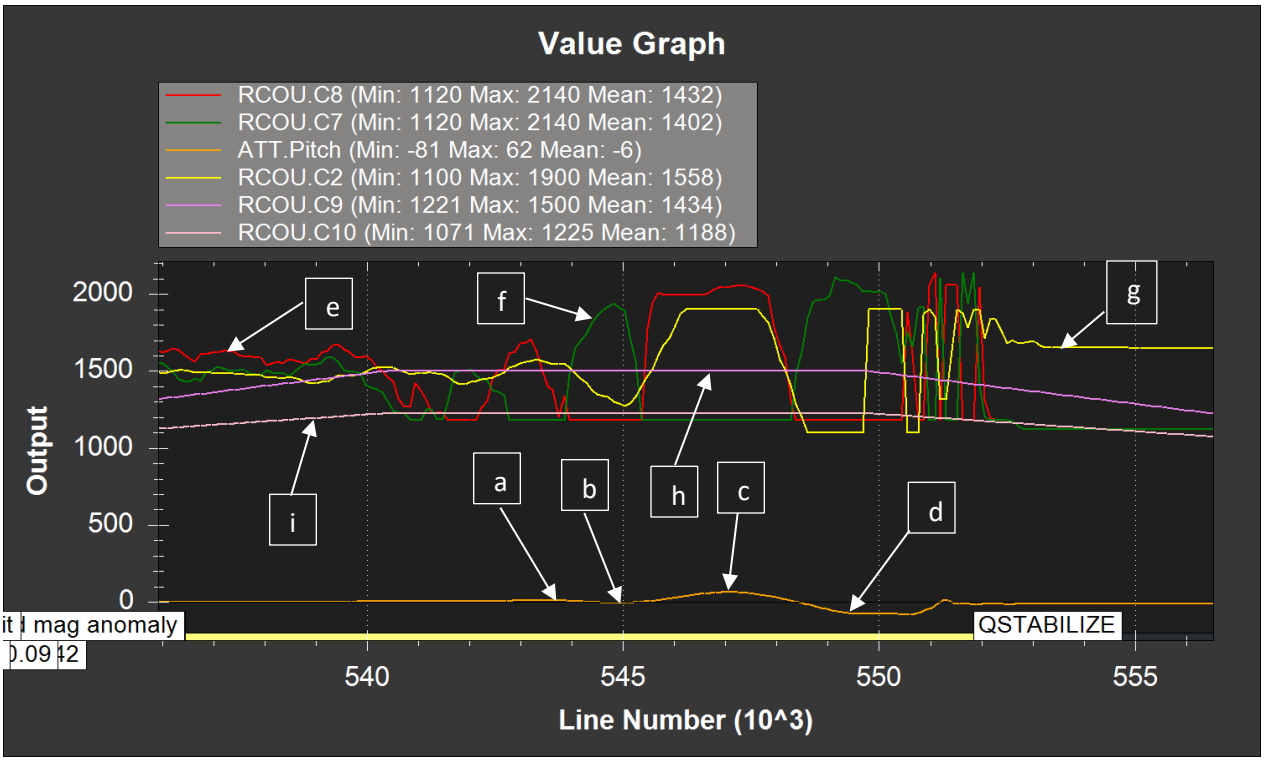

Figure 69: Pixhawk recording the pitch of the aircraft in degrees (a, b, c, d), the PWM outputs to the tail motors (e), front motors (f), elevator (g), wing rotational mechanism (h), and horizontal stabilizer rotational mechanism (i). This image was taken off of MissionPlanner.

Once the aircraft took off in the vertical configuration, it was blown backwards by the wind by about 15ft but recovered. Once the aircraft stopped, the transitional phase was initiated by switching from QSTABILIZE to FBWA. At this time, the aircraft proceeded to smoothly start the transition to forward flight. Once the aircraft's wings and horizontal stabilizer rotated to 45 degrees, the oscillation of the aircraft started with a pitch up of 10 degrees at point "a" in Figure 70, above. It then proceeded to pitch down to -7 degrees at point "b," pitch up to 61 degrees at point "c," and pitch down to -80 degrees at point "d." It can be seen at point "d" that the aircraft stayed pitched down at this -80 degrees until impact with the ground, at which point the pith immediately increases as the aircraft ended up laying upside-down. Images of the aircraft at points "c" and "d" can be seen in Figures 71 and 72, below. The accuracy of the data recorded by the Pixhawk is unknown. However, the pitch angles represented in the graph are likely to be up to 5 degrees off due to the calibration procedure required by the Pixhawk. This is due to having to

manually hold the aircraft level, as you think it would fly, while the accelerometer calibration is completed.

From Figure 71, it can also be seen that the wing rotational mechanism (h) and horizontal stabilizer rotational mechanisms (i) are both at 45 degrees at the time of oscillation and crash. This is known by the PWM value of each of them. This can also be visually confirmed in Figures 71 and 72, below. Additionally, since the aircraft is in the transitional phase, it was observed that the elevator (g) was also trying to counteract the aircraft's oscillations.

Figure 70: Image of aircraft pitched up 61 degrees as seen at point "c" in Figure 70, above

Figure 71: Image of aircraft pitched down 80 degrees as seen at point "d" in Figure 70, above.

It can be seen in Figure 72, above, that the wing and horizontal stabilizer are both rotated approximately 45 degrees. This validates the 1500 PWM output seen in this stage of flight.

CHAPTER V

DISUCSSION OF RESULTS

5.1 THRUST PREDICTION CALCULATIONS

From the results shown in section 4.1.4, XROTOR's near static thrust prediction was 13.9% lower than that of eCalc, APC's was 3% lower than eCalc, and the actual thrust test was 9% less. Given the eCalc prediction for static thrust was 9% higher than the thrust stand testing yielded, the disclaimer on eCalc.ch of data being within 10% of actual values is true. Because of this, it can be determined that eCalc is a suitable method for initial motor/ESC/propeller sizing for fixed wing aircraft. However, this comes with the assumption that manufacturers of the available motors, ESCs, and propellers have submitted reliable and up to date data to eCalc. Additionally, if the initial analysis requires more precision than +/- 10%, eCalc would not be the method of choice. If too much thrust is not an issue, a useful assumption could be to assume eCalc's thrust prediction will be 10% higher than what it actually is. And for small, lightweight aircraft, this could be an important assumption to make.

Additionally, it is likely that XROTOR's prediction is 11.2% lower than APC's prediction in part because of the unknown parameters that were most likely not filled out correctly, in addition to

the proprietary airfoil blend along the blades of the propeller. However, out of all three methods used to predict the thrust of the motors, XROTOR was the closest to the actual thrust stand as it undercut the actual value by 5.6%. Likewise, APC overshot the actual value by 6.2%, showing that eCalc was tentatively the least accurate method to predicting thrust. Another possible reason for these differences is the RPM differences from actual vs. predicted. These differences are not known as there was no way to monitor the RPM on the thrust stand tests at the time the tests were conducted. Therefore, all prediction methods used an estimate of the maximum RPM the motor/ESC/battery combination used in the thrust stand tests could produce.

5.2 OBJECTIVE I ANALYSIS & EXPERIMENTATION

Based on the placement of CG in each of the test flights and the CG limits determined for the aircraft, it can be determined that ElectraWing was statically stable throughout the project. Additionally, the wing and horizontal stabilizer rotation mechanism had little effect on the stability of the aircraft as the CG never approached the end limits for CG travel in any configuration or intermediate positions.

For the first test flight, the aircraft was relatively stable in flight. The roll erred on the side of neutrally stale, but this is a characteristic of the base RMRC Anaconda as well. While trying to flare the aircraft on landing, it was found to be capable of maintaining a high angle of attack without stalling while in ground effect. This was not an issue, but rather an aircraft characteristic noticed. This is likely due to the propellers washing the wing and horizontal stabilizer, preventing the flow from separating.

The two deficiencies this aircraft had was the excess weight in the tail causing the need for extra weight in the nose than was designed for. This negatively affected the thrust to weight ratio of the

aircraft and prohibited it from being able to take-off vertically in future flights. This problem was solved by changing out the 3D printed motor pods for basic plywood motor mounts and partially extending the booms forward for permanently mounted vertical motors. Although the motor mounts were the change made, alternatively capacitors could have been added to the battery side of the ESCs to prevent ripple current, and the two battery leads extended to reduce the weight of a single wire for each motor. This presented the issue of mounting the ESCs efficiently by each motor instead of inside the fuselage.

5.3 OBJECTIVE II FLIGHT TEST I: CTOL

After the rotational mechanisms for the wing and tail had been added as well as the booms extended forward with motors mounted permanently vertical, the flight characteristics did not change much. The only noticeable difference was the aircraft was significantly slower at full throttle, level flight. This was likely due to the extra drag added by two motors mounted vertically, two propellers causing parasitic drag, and the two boom extensions causing drag in addition to having two less motors/propellers providing forward thrust. Otherwise, the aircraft still maintained the same flight characteristics as it did in Phase I flight testing. Additionally, the wing rotation mechanism appeared to keep the wings from rotating and causing in-flight deficiencies. The tail rotation mechanism maintained a rigid position for the duration of the flight and did not cause any control issues.

5.4 OBJECTIVE II FLIGHT TEST II: STOL

Before the first STOL testing commenced, a second CTOL flight test was conducted to ensure the aircraft still performed the way it was supposed to and to ensure it could handle the windy conditions. For this test flight, the aircraft took off as expected, started with a positive rate of climb, but part way into the climb, the aircraft started descending uncontrollably at a relatively slow rate. Since the previous test flight, there were no configuration changes. After the crash, the

voltage of the two flight batteries was checked, but they were fully charged. The only theory as to why the aircraft started pitching down was that the horizontal stabilizer rotational mechanism could not handle the gusty wind conditions it was experiencing. The gusts of wind could have caused the horizontal stabilizer to increase the angle of attack (AoA) just enough to not allow the elevator to have enough control authority to keep the aircraft from descending. This potential shift of angle of attack of the horizontal stabilizer would have been likely due to the flexible nature of the aircraft. This is one reason a better test platform could be chosen in future iterations.

After the repairs had been made to the aircraft, the elevators were locked out, and the horizontal stabilizer rotation mechanism had been double purposed to be a rotational mechanism and a whole moving stabilator, another CTOL test was conducted. This time, the aircraft performed as expected, and the pitch control was even better than it had been in previous tests. Again, the aircraft was capable of high angles of attack and floating in ground effect while landing. The stabilator made it even easier to induce and maintain the higher angle of attack.

Once STOL testing was conducted, it was found that 10 degrees of wing rotation produced an average of approximately 36% decrease in runway needed for take-off. At 20 degrees of wing rotation, the runway used for take-off was an average of approximately 15% shorter than the CTOL configuration. It can also be seen that the 20 degrees of wing rotation produced an approximated average take-off distance of 33% longer than the 10 degrees of wing rotation. Finally, the 45 degrees of wing rotation did not allow for the aircraft to perform a take-off. It is likely the aircraft was too underpowered to take-off with the 45 degrees of wing rotation. Additionally, with the gap between the two propellers on each of the rotating wing sections, it is likely there was stalling occurring in that section beyond 10 degrees of wing rotation. This could account for the prolonged take-off distance from the 10-degree case. However, since parts of the wing were still washed, the 20-degree case still provided a shorter take-off distance than the CTOL configuration but did not require the amount of thrust to lift off as the 45-degree case. A

future test that would be useful would be to keep the aircraft in the CTOL configuration and apply flaps and/or slats to the aircraft and see if it produces similar results to that of the 10-degree wing rotation test. This is because for a short-field take-off in a full-scale aircraft, 10 degrees of flap input is used. It seems like the 10 degree of wing rotation is accomplishing a similar task but cannot be concluded how much of the shorter take-off distance is due to an induction of flow over the wings. However, it can be concluded that this aircraft is capable of STOL.

5.5 OBJECTIVE II & III ANALYSIS & EXPERIMENTATION

5.5.1 FIRST VTOL TEST

With the original motor configuration, when a vertical take-off was attempted, the aircraft almost became airborne, but would not completely lift off the ground despite the aircraft having a final calculated thrust to weight ratio of 1.12. This calculation was using the RCbenchmark thrust stand data previously discussed. It was clear that an eCalc initial estimate of 1.8 thrust to weight ratio to account for unknown weights was not enough to achieve the desired thrust to weight of 1.2. Regardless, it is unlikely the 1.2 thrust to weight ratio that was desired would have been enough. This is due to the Pixhawk limiting the maximum throttle output to maintain stability in the vertical configuration. If all motors were outputting 100%, it would be impossible for a few motors to output more thrust to achieve a strafing maneuver or other type of maneuver. Additionally, it is likely voltage sags from all motors applying a high throttle setting is lowering the thrust output. For this reason, hobbyists designing fixed wing VTOL systems typically design for a thrust to weight ratio of 1.5.[45]

5.5.2 INDOOR VTOL GAIN TUNING AND TESTING

After the addition of the SunnySky motors, the aircraft had sufficient thrust to take-off vertically. At this point, the process to tune the gains was conducted. The initial test before the gains were

tuned resulted in the aircraft initially taking off vertically, but almost immediately rolling and pitching in various directions without control. After the gains were tuned, the aircraft was capable of hovering indoors. However, the aircraft did not have any yaw control while in the VTOL configuration as all the motors were counter rotating to help stabilize the aircraft due to its asymmetry. Another potential cause of instability with this aircraft is that the Pixhawk seems to have difficulty with asymmetric multi-rotor frames. This was discovered by previous tests on a past project. From searching forums on hobby websites, it appears most people essentially mount a symmetric quadcopter frame to a fixed wing aircraft to accomplish VTOL. This may be to help combat stability issues with the Pixhawk's firmware for VTOL. This, however, was not able to be confirmed and is just a theory.

5.5.3 TRANSITIONAL FLIGHT TEST

When the aircraft was taken outside for a transitional flight test, a series of hover tests were conducted first. These resulted in the gains needing to be tweaked just a little. This is likely because of the introduction of wind to the system. After the gains were tuned, the transitional flight test was conducted at about 6ft above the ground as to minimize damage in the event something go wrong. There are a few potential causes to the aircraft's oscillation. As the aircraft was transitioning to forward flight, it is unknown what exactly is happening with the control loop at this point. It may be that the Pixhawk does not know how to handle the transition with this aircraft configuration. It can be seen from the data that front boom mounted motors (M3) and the tail mounted motors (M4) started oscillating with an increasing amplitude. However, the motors did appear to counteract the aircraft's pitching. That is, when the nose of the aircraft pitched up, the Pixhawk lowered the PWM signal to M3 and increased it to M4 and the exact opposite happened when the nose pitched down.

Another possible explanation is that the horizontal stabilizer, while at 45 degrees of rotation, acted like a stabiliator that was being washed by the two tail motors. Having two propellers that wash close to the entire tail could prevent stalling of the horizontal stabilizer while at 45 degrees of rotation, which would make it much more effective. As the aircraft gained forward speed, the horizontal stabilizer would have created a moment pitching the nose of the aircraft down. The autopilot would have then tried to compensate, but if a gust of wind occurred at the time of the incident, the autopilot could have tried to compensate too much, and when the wind slowed a little, the aircraft pitched up, and as the aircraft sped up, the front motors may not have had enough thrust to counteract the moment imposed by the horizontal stabilizer rotated to 45 degrees.

The less likely explanation to this incident is an aerodynamic one. When helicopters are flying straight and level, they see an increase in lift on the right side of the aircraft as the rotor moves forward into the freestream velocity depicted in Figure 73 below. Since both of the vertically mounted boom motors were counter rotating, this uneven moment that helicopters have would have been cancelled out. However, as the aircraft was transitioning forward, this could have potentially created an increase in lift, which may have started the oscillation. This explanation does not account for the oscillation, but rather what initiated it.

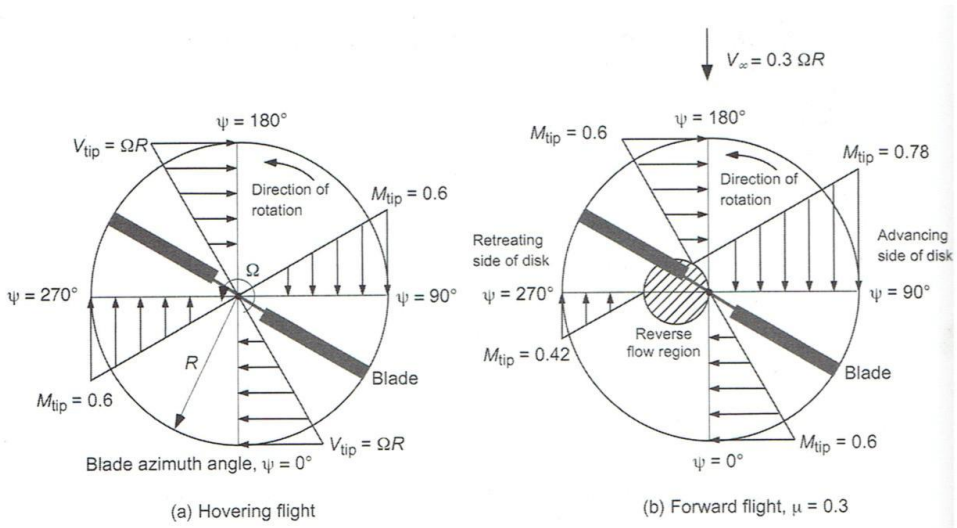

Figure 2.1 Distribution of incident velocity normal to the leading edge of the rotor blade. (a) Hovering flight. (b) Forward flight at $\mu = 0.3$.

Figure 72: Uneven lift distribution of helicopter rotors. As the helicopter flies straight and level into the wind, blades see a higher relative airspeed as they rotate into the wind than when the downwind portion. With this comes an increased lift force, creating an uneven lift distribution around the rotation. Image from Müller [46].

5.6 OVERALL DESIGN CONCLUSIONS

Over the process of building and testing the aircraft, a few design flaws were noticed. One of the issues with this design is when the wing is rotated vertically, it had a high relative surface areas while in the VTOL configuration. This is problematic in windy conditions, and was evident in theory and in flight testing. There are two possible ways to compensate for the wind. The first would be to enable GPS and tune the PIDs so the aircraft could angle down like a multirotor to compensate for wind. If the aircraft were to be scaled up to a passenger aircraft, it is unlikely people would feel comfortable in this maneuver. Likewise, for cargo aircraft, this would put excess stress on the fastening system used. To compensate for the wind and allow for a level take-off, the wings could be rotated forward to reduce the drag seen by the rotating portion of the wings and to provide enough forward thrust to counteract the drag. This too provides its own set of stability issues that would require more investigation.

Additionally, the wing had a weak point at the point of rotation. At this point, there was just a single carbon fiber tube holding the whole wing together. It was proven in the aircraft's transitional crash that this was the point of failure. Other incidents of similar sized foam aircraft striking the ground at similar speeds and angles that have been observed by the author did not result in broken wing tubes. This point of failure could be avoided by using a solid carbon fiber section at the weak spots, or a metal reinforcement, but these options would add excessive weight. Another option would be to completely redesign the aircraft and make the entire wing rotate instead of just the outboard segments. This, however, would mean the aircraft could not be a twin-boom design, but a conventional fuselage type aircraft. Such a design would prohibit some of the benefits of the twin-boom design previously discussed. Given the high forces seen at the wing joint on the small scale, this would likely cause difficulties if the aircraft were scaled up. For this aircraft to safely operate, counter measures would need to be taken to strengthen this joint as it is a single point of catastrophic failure. The issue with strengthening the joint would be the additional weight inherent with heavier structures.

Finally, a major flaw in this ElectraWing prototype was using a foam aircraft instead of an airframe with less elasticity. Even after the carbon fiber was used to stiffen the wings, vertical stabilizer, and horizontal stabilizer, it was not enough to keep the aircraft from flexing a lot. This flexibility likely caused some of the aircraft's instability in vertical flight which caused the autopilot to not be able to respond correctly. An easy solution to this would be to use a different platform made of either composites or wood. The negative aspects of this would be that the aircraft would be more expensive and more difficult to safely modify.

This aircraft design can fly and perform to the design specifications, but a different overall design should be investigated. To achieve the desired design goals, a few different avionics designs should be investigated. Larger motors should be selected, and further tuning of the autopilot should be conducted. Another potential point of failure of this aircraft could have rested in the

ESC selection. The ESCs used were fixed wing ESCs, not multi-rotor ESCs. Multi-rotor ESCs have a faster reaction time than fixed wing ESCs, which could help with some of the vertical stability issues. It has not been concluded that this was the issue with the aircraft but is another possibility. The choice to use fixed wing ESCs was made because this aircraft was initially thought of as a fixed wing that could fly vertically, not a multi-rotor that could fly like a fixed wing. This fundamental design philosophy was an error made in the engineering process.

Despite the issues inherent with this design, it has aspects that could be useful in future design iterations. The blown wing design has previously been determined to improve performance and efficiency of aircraft and by the wing, take-off distances can be significantly reduced in a STOL configuration. The rotating wing should be investigated further for aircraft STOL capabilities and compared to other commonly used high lift devices such as flaps and slats.

5.7 FUTURE WORK

For future tests of this aircraft, the airplane would first need to be repaired. After the necessary repairs, more gain tuning in the vertical configuration needs to be conducted. To accomplish this, it might be possible to load a multi-rotor firmware to the Pixhawk, so it thinks it's a quadcopter, have it tune the gains with the auto-tune function, and finally copy the resulting gains over to the fixed wing firmware in the "Q_" parameter list. This method may or may not be possible as the author was not able to find a documented instance of someone doing this. However, it could potentially be a workaround to the VTOL flight mode not having an auto-tune function.

After further testing has been completed with this aircraft, new motors and ESCs need to be selected for the aircraft and the front booms shortened and eventually removed completely. After they are removed completely, those two motors need to be able to rotate vertically. Once this has been proven to work, a different airframe needs to be selected, and an entirely different power system as well. The new aircraft platform would tentatively have a maximum take-off weight of

55lb, and have either gasoline engines or turbomachinery powering generators to aid in the life of the battery. This would effectively make the aircraft a hybrid electric system like NASA's GL-10 Greased lightning. Furthermore, in the future testing, different flight controllers should also be investigated. NASA's greased lightning utilizes a “kk” flight controller which is highly capable of handling unique VTOL aircraft designs.[47,48]

REFERENCES

1. Moore, M. D., and Fredericks, B. "Misconceptions of Electric Propulsion Aircraft and their Emergent Aviation Markets," AIAA Aerospace Sciences Meeting; 52nd. National Harbor, MD, 2014.

2. Benefits of Hybrid-Electric Propulsion to Achieve 4x Increase in Cruise Efficiency for a VTOL Aircraft

3. Fletcher, S., Flynn, M.-C., Jones, C. E., and Norman, P. J. "Hybrid Electric Aircraft: State of the Art and Key Electrical System Challenges," IEEE Transportation Electrification Community. Vol. 2017, 2016.

4. Ozdemir, U. (2014, April). Design of a Commercial Hybrid VTOL UAV System. *Journal of Intelligent & Robotic Systems*, *74*(1-2), 371-393. Retrieved April 17, 2018.

5. Nietz, T., and Baber, S. "An Innovative UAV Design," AIAA 3rd Unmanned Unlimited Technical Conference. Chicago, 2004.

6. Stoll, A. M., Bevirt, J., Moore, M. D., Fredericks, W. J., and Border, N. K. "Drag Reduction Through Distributed Electric Propulsion," Aviation Technology, Integration, and Operations Conference. Atlanta, 2014.

7. Cummings, D. B. (2014). ElectraWing Modular Air Vehicle Concept.

8. Austin, R. (2010). *Unmanned aircraft systems: UAVs design, development and deployment*. Reston, VA: American Institute of Aeronautics and Astronautics.

9. Drew, J. (2016, January 21). New search for VTOL UAVs may resurrect Bell tiltrotor. Retrieved April 17, 2018, from https://www.flightglobal.com/news/articles/new-search-for-vtol-uavs-may-resurrect-bell-tiltroto-421075/

10. Gohardani, A. S. (2011). Challenges of future aircraft propulsion: A review of distributed propulsion technology and its potential application for the all-electric commercial aircraft. *Progress in Aerospace Sciences, 47*(5), 369-391. Retrieved April 16, 2018, from https://www.sciencedirect.com/science/article/pii/S0376042110000497

11. Writer, S. (2017, March 30). *LTV XC-142 Vertical/Short Take-Off and Landing (V/STOL) Experimental Aircraft*. Retrieved from Military Factory: Military Factory

12. Ransone, R. K., & Jones, G. E. (1966, January). *XC-142A V/STOL Transport Tri-Service Limited Category 1 Evaluation.* Retrieved from Defense Technical Information Center: http://oai.dtic.mil/oai/oai?verb=getRecord&metadataPrefix=html&identifier=AD0477084

13. Fredericks, W. J., Moore, M. D., & Busan, R. C. (2013, August 12). *Benefits of Hybrid-Electric Propulsion to Achieve 4x Increase in Cruise Efficiency for a VTOL Aircraft.* Retrieved from NASA Technical Reports Server: https://ntrs.nasa.gov/search.jsp?R=20140001088

14. Stoll, A. M., Bevirt, J., Pei, P. P., & Stilson, E. V. (2014). Conceptual Design of the Joby S2 Electric VTOL PAV. *14th AIAA Aviation Technology, Integration, and Operations Conference.* Atlanta: AIAA.

15. Dornheim, M. A., "Planetary Flight Surge Faces Budget Realities," *Aviation Week and Space Technology*, Vol. 145, No. 24, 9 Dec. 1996, pp. 44-46.

16. Terster, W., "NASA Considers Switch to Delta 2," *Space News*, Vol. 8, No. 2, 13-19 Jan. 1997, pp., 1, 18.

17. Peyret, R., and Taylor, T. D., *Computational Methods in Fluid Flow*, 2nd ed., Springer-Verlag, New York, 1983, Chaps. 7, 14.

18. Oates, G. C. (ed.), *Aerothermodynamics of Gas Turbine and Rocket Propulsion*, AIAA Education Series, AIAA, New York, 1984, pp. 19, 136.

19. Volpe, R., "Techniques for Collision Prevention, Impact Stability, and Force Control by Space Manipulators," *Teleoperation and Robotics in Space*, edited by S. B. Skaar and C. F. Ruoff, Progress in Astronautics and Aeronautics, AIAA, Washington, DC, 1994, pp. 175-212.

20. Thompson, C. M., "Spacecraft Thermal Control, Design, and Operation," *AIAA Guidance, Navigation, and Control Conference*, CP849, Vol. 1, AIAA, Washington, DC, 1989, pp. 103-115

21. Pircher, Geipel, & Korsaeth. (2017). Development of a hybrid UAV sensor platform suitable for farm-scale applications in precision agriculture. *International Archives of the Photogrammetry, Remote Sensing and Spatial Information Sciences, 42*(2), 297-302. doi:10.5194

22. Defense Update News Desk. (2017, January 23). Panther-FE Fixed Wing VTOL Drone Demonstrated in Flight. Retrieved April 17, 2018, from http://defense-update.com/20170123_panther-fe.html

23. Dailymail.com, M. P. (2016, September 06). Who needs a runway! Watch the incredible triple transformer drone that takes off like a quadcopter and flies like a plane or a glider. Retrieved April 17, 2018, from http://www.dailymail.co.uk/sciencetech/article-3776766/Who-needs-runway-Watch-incredible-transformer-drone-takes-like-quadcopter-flies-like-plane.html?ITO=1490&ns_mchannel=rss&ns_campaign=1490

24. Quantum-Systems Tron. (n.d.). Quantum-Systems Tron - Heavy payload UAV for professionals. Retrieved April 17, 2018, from https://www.quantum-systems.com/tron/

25. NASA. (2015, March 16). LEAPTech to Demonstrate Electric Propulsion Technologies [Digital image]. Retrieved April 16, 2018, from https://www.nasa.gov/centers/armstrong/Features/leaptech.html

26. Sivani, S. (2015, March 28). NASA Using Distributed Propulsion for Electric Airplane. Retrieved April 17, 2018, from https://www.greenoptimistic.com/nasa-electric-airplane/#.WtV13kxFzZs

27. Moore, A., Fredericks, W., & Borer, N. (2014). Drag Reduction Through Distributed Electric Propulsion. In *Aviation Technology, Integration, and Operations Conference*. Atlanta, GA: AIAA. doi:20140011507

28. Royal Aviation Museum of Western Canada. (n.d.). Article: Canada Successful in Building Tilt-wing Aircraft. Retrieved April 17, 2018, from http://www.royalaviationmuseum.com/3388/canada-successful-in-building-tilt-wing-aircraft/

29. RMRC Anaconda - KIT [Digital image]. (n.d.). Retrieved April 16, 2018, from https://www.readymaderc.com/products/details/rmrc-anaconda-kit

30. Müller, M. (2009). Know-how - Elektrische Modelle optimal auslegen (I). Retrieved from eCalc: https://ecalc.ch/

31. Drela, M., & Youngren, H. (2011, February 10). *XROTOR Download Page*. Retrieved from http://web.mit.edu/drela/Public/web/xrotor/

32. Nelson, R. C. (1998). *Flight stability and automatic control*(2nd ed.). Boston, MA: McGraw-Hill.

33. Scott, E. (2016). *Numerical Analysis on Propeller noise for Fixed Wing UAVs.* Stillwater: Oklahoma State University.

34. Hall, N. (2015, May). Shape Effects on Drag. Retrieved May 4, 2018, from https://www.grc.nasa.gov/www/k-12/airplane/shaped.html

35. Motion in two dimensions. (1999, September). Retrieved May 4, 2018, from http://physics.bu.edu/~duffy/py105/Motion2D.html

36. Hibbeler, R. C. (2011). *Mechanics of materials*(8th ed.). Boston: Prentice Hall.

37. Drela, M., & Youngren, H. (2003, November 13). *XROTOR User Guide.* Retrieved from XROTOR Download Page: http://web.mit.edu/drela/Public/web/xrotor/xrotor_doc.txt

38. Advanced Precision Composites. (n.d.). *Engineering Design Process Used to Develop APC Propellers.* Retrieved from https://www.apcprop.com/Articles.asp?ID=262#airfoil

39. Nelson, flight stability and automatic control 2nd edition

40. Tail Design Stability. (n.d.). Retrieved September, 2018, from http://adg.stanford.edu/aa241/stability/taildesign.html

41. Needle-Roller Bearing [Digital image]. (n.d.). Retrieved April 16, 2018, from https://www.mcmaster.com/#catalog/124/1245/=1cctzia

42. ArduPilot. (n.d.). QuadPlane Support. Retrieved April 17, 2018, from http://ardupilot.org/plane/docs/quadplane-support.html

43. Pixhawk. (n.d.). Firefly 6 [Digital image]. Retrieved April 16, 2018, from https://pixhawk.org/_detail/platforms/vtol/firefly6.png?id=platforms:vtol:start

44. ArduPilot. (2016). Frame Class and Type Configuration [Digital image]. Retrieved April 16, 2018, from http://ardupilot.org/copter/docs/frame-type-configuration.html?highlight=frame

45. PID controller. (2018, March 31). Retrieved April 17, 2018, from https://en.wikipedia.org/wiki/PID_controller#Manual_tuning

46. Müller, M. (n.d.). eCalc - the most reliable RC Calculator on the Web. Retrieved from https://ecalc.ch/RC Benchmark. (2016, April 07). Series 1520 thrust stand datasheet. Retrieved April 17, 2018, from https://www.rcbenchmark.com/wp-content/uploads/2016/04/RCbenchmark-1520-datasheet.pdf

47. Harper, R., & Cooper, G. (1986). Handling Qualities and Pilot Evaluation. *Journal of Guidance, Control, and Dynamics*, *9*(5), 515. Retrieved April 17, 2018, from https://engineering.purdue.edu/~andrisan/Courses/AAE490A_S2010/Buffer/HCooper.pdf.

48. E., N., & Covey, G. (2018, March 29). Q_TILT_MASK & Misc. VTOL Questions. Retrieved April 17, 2018, from https://discuss.ardupilot.org/t/q-tilt-mask-misc-vtol-questions/27430

49. Figure 2.1. Graph of velocity distribution over helicopter blades in hover. From *Principles of Helicopter Aerodynamics*, by J.G. Leishman, 2000 Cambridge: Cambridge University Press.

50. Hahn, A., & Chaput, A. (2015). *Develop Rapid Structural Analysis Methods from Open VSP Geometry (*Rep. No. NNL13AA08). Austin, TX: National Institute of Aerospace.

51. Fredericks, McSwain, Beaton, Klassman, & Theodore. (2017). *Greased Lightning (GL-10) Flight Testing Campaign* (pp. 1-25, Tech. No. NASA-TM-2017-219643). MJoffett Field, CA: NASA.

APPENDICES

APPENDIX A – THRUST STAND JAVA SCRIPT

```
/* ///////////////// Sweep characterization /////////////////
 The script will sweep between the input values "minVal" and "maxVal". The sweep will be made in discrete "stepsQty" steps. Each step will consist of a settling time "settlingTime" after which a new log entry will be recorded. To reduce noise, "samplesAvg" will be averaged and recorded.
////////////// User defined variables ////////////// */
var minVal = 1000;       // Min. input value [700us, 2300us]
var maxVal = 1400;       // Max. input value [700us, 2300us]
var stepsQty = 4;        // Number of steps
var settlingTime = 3;    // Settling time before measurement input change [s]
var samplesAvg = 20;     // Number of samples to average
var stepsGoDown = false;  // If true, the test will step down, if false, the steps will only go up.
var repeat = 3;          // Number of times to repeat the same sequence
var filePrefix = "StepsTest";
///////////////// Beginning of the script //////////////////

//Starting new file
rcb.files.newLogFile({prefix: filePrefix});

//ESC initialization
rcb.console.print("Initializing ESC...");
rcb.output.pwm("esc",1000);
rcb.wait(startSteps, 4);

//Start steps
function startSteps(){
   rcb.console.print("Starting Steps Up...");
   rcb.console.setVerbose(true);
   rcb.output.steps("esc", minVal, maxVal, stepsQty, stepFct);
}

// The following function will be executed at each step.
var goingUp = true;
function stepFct(isLastStep, nextStepFct){
   rcb.console.setVerbose(false);

   //Settling time, then read sensors
   rcb.wait(function(){
      rcb.sensors.read(readDone, samplesAvg);
   }, settlingTime);

   //Function called when read completed
```

```
    function readDone(result){

        // Write the results and proceed to next step
        rcb.files.newLogEntry(result,function(){
            if(isLastStep){ // If it is the last step
                if (goingUp && stepsGoDown){
                    goingUp = false;
                    rcb.console.print("Starting Steps Down...");
                    rcb.console.setVerbose(true);
                    rcb.output.steps("esc", maxVal, minVal, stepsQty, stepFct);
                }else{
                    if(repeat>1){
                        repeat --;
                        rcb.console.print("Repeating script " + repeat + " more times.");
                        goingUp = true;
                        startSteps();
                    }else{
                        rcb.endScript(); // End script
                    }
                }
            }else
                nextStepFct();
        });
    }
}
```

APPENDIX B – TRAJECTORY PLOT CODE

```
Sub Trajectory_WS_11()

'define variables
Dim Fx As Double 'force in the x
Dim Fy As Double 'force in the y
Dim Ax As Double 'acceleration in x
Dim Ay As Double 'acceleration in y
Dim Thrust As Double 'thrust
Dim W As Double 'ElectraWing weight
Dim m As Double 'ElectraWing mass
Dim Dx As Double 'change in distance in x
Dim Dy As Double 'change in distance in y
Dim X As Double 'cumulative distance traveled by aircraft in X
Dim Y As Double 'cumulative distance traveled by aircraft in Y
Dim Vix As Double 'initial velocity in x
Dim Vx As Double 'new velocity in x
Dim Viy As Double 'initial velocity in y
Dim Vy As Double 'new velocity in y
Dim AGL As Double 'altitude above ground level
Dim Rho As Double 'air density
Dim Cd As Double 'coefficient of drag
Dim D As Double 'drag force
Dim Cl As Double 'coefficient of lift
Dim L As Double 'lift force
Dim Wind As Double 'speed of wind
Dim relWindX As Double 'relative wind speed seen by aircraft in x
Dim fpAREA As Double 'flat plate area
Dim g As Double 'gravitational acceleration
Dim t As Double 'time between data points
Dim Alfa As Double 'wing rotation angle
Dim Span As Double 'span of rotational section (total)
Dim Chord As Double 'average chord length of wing
Dim ChordX As Double 'horizontal componento of chord
Dim ChordY As Double 'vertical component of chord
Dim i As Integer 'counter variable for loops
Dim k As Integer 'counter variable for loops


'inputs
W = Sheet1.Cells(26, 10).Value
Thrust = Sheet1.Cells(27, 10).Value
g = Sheet1.Cells(28, 10).Value
Wind = -1 * Sheet1.Cells(29, 10).Value
t = 1 'seconds
Vx = 0 'initiate Vx
Vy = 0 'initiate Vy
Viy = 1
Alfa = 90 'set initial wing angle
```

```
Span = 4.67 'total span of rotating portions of wing in ft
Chord = 10 / 12 'chord in ft

Cd = 1.28

Rho = 0.002377

fpAREA = 3.89

'convert wind speed to ft/s
Wind = Wind * 5280 / 3600

'calculate mass of aircraft
m = W / g

'calculate drag
'D = Cd * Rho * ((Wind) ^ (2)) * A / 2
'Fx = D
'Ax = Fx / m

'calculate vertical force
Fy = Thrust - W
'Ay = Fy / m
Ay = 0 'assuming constant acceleration in Y

'output initial aircraft position
Sheet1.Cells(32, 10).Value = X
Sheet1.Cells(32, 11).Value = Y
Sheet1.Cells(32, 12).Value = Vx
Sheet1.Cells(32, 13).Value = Vy

'trajectory calculations
For i = 0 To 1000

   If Y < 30 Then

      'calculate drag
      relWindX = Vx - Wind
      D = Cd * Rho * ((relWindX) ^ (2)) * fpAREA / 2
      Fx = Thrust * Cos(Alfa * WorksheetFunction.Pi() / 180) - D
      Ax = Fx / m

      'calculate position in x & y
      Dx = Vix * t + 0.5 * Ax * (t) ^ (2)
      Dy = Viy * t + 0.5 * Ay * (t) ^ (2)

      'update aircraft position from start
      X = X + Dx
      Y = Y + Dy

      'calculate velocity after iteration
```

```
        Vx = Vix + Ax * t
        'Vy = Viy + Ay * t
        Vy = 1 'setting climb to constant 1 ft/s

        'update starting velocities for next iteration
        Vix = Vx
        Viy = Vy

        'output results to spreadsheet
        Sheet1.Cells(33 + i, 10).Value = X
        Sheet1.Cells(33 + i, 11).Value = Y
        Sheet1.Cells(33 + i, 12).Value = Vx
        Sheet1.Cells(33 + i, 13).Value = Vy

    Else 'change from "exit for" to the equations for transitional flight

        Exit For

    End If

Next i


'wing transition
'--------------------------------------------------------------------------

'loop to start iteration for wing rotation

For k = i To 1000

    'NOTE: actuator full travel time is 5 seconds
    'NOTE: actuator travels 20mm/s
    'NOTE: wing rotation is 18deg/s

    If X < 100 Then
        'calculate new angle based on time increment
        Alfa = Alfa - 18 * t '(deg/s)*s

        'calculate flat plate area
        fpAREA = Span * Chord * Sin(Alfa)

        'calculate flat plate drag
        relWindX = Vx - Wind
        D = Cd * Rho * ((relWindX) ^ (2)) * fpAREA / 2

        'sum of forces in X
        Fx = Thrust * Cos(Alfa * WorksheetFunction.Pi() / 180) - D
        Ax = Fx / m

        'sum of forces in Y
        Fy = Thrust * Sin(Alfa * WorksheetFunction.Pi() / 180) - W
```

```
        'check to see if lift is less than weight
        If Fy < 0 Then

            Fy = 0 'set to level, unaccelerated flight in the Y

        End If

        'calculate acceleration in Y
        'Ay = Fy / m

        'calculate position in x & y
        Dx = Vix * t + 0.5 * Ax * (t) ^ (2)
        Dy = Viy * t + 0.5 * Ay * (t) ^ (2)

        'update aircraft position from start
        X = X + Dx
        Y = Y + Dy

        'calculate velocity after iteration
        Vx = Vix + Ax * t
        'Vy = Viy + Ay * t
        Vy = 1 'setting climb to constant 1 ft/s

        'update starting velocities for next iteration
        Vix = Vx
        Viy = Vy

        'output results to spreadsheet
        Sheet1.Cells(33 + k, 10).Value = X
        Sheet1.Cells(33 + k, 11).Value = Y
        Sheet1.Cells(33 + k, 12).Value = Vx
        Sheet1.Cells(33 + k, 13).Value = Vy

    Else

        Exit For

    End If

Next k


End Sub
```

APPENDIX C – FLIGHT TEST CARDS

Test Sortie:	Short Takeoff Test w/ Rotational Mechanisms		
Aircraft: ElectraWing	Date/Location: 10-Mar-18	Supervising Test Engineer SRW	
Test Objectives: To test the flight characteristics of the modified Anaconda	Weather: Wind (knots): 7/SE Temperature: 70 F Barometric Pressure: 29.702 inHg	Limits: 1. < 10 minutes 2. < 400 ft AGL 4. < 17 knots wind	
Configuration: 1. Direct RC input/no Pixhawk 2. Wing rotational mechanism in place 3. Horizontal stab. mechanism in place 4. Elevators locked out - using stabilator	Notes: This test is to determine takeoff roll distance with 0 degrees of wing rotation.		
Frequencies: 2.4GHz	Weight & Balance: CG Measured (est.): 30% CG Calculated: 32%	TOW lbs: 10.9	

PROCEDURE

Start Time:	2:18pm	End Time: 2:19pm
1	Takeoff with full throttle and 0 degrees of wing rotation	
2	Once positive rate of climb is estabilished, slowly rotate wings back to 0 degrees	
3	Immediately land aircraft CTOL	
4	Line up on the takeoff mark and repeat steps 1 through 3	
5		
6		
7		
8		
9		

# Takeoff/Landing	Comments	Issues
2	The aircraft took off in approximately 106ft. It was stable throught the entire flight. No adverse reactions with the wing or horizontal stabilizer rotational mechanisms	N/A

Test Sortie:	Short Takeoff Test w/ Rotational Mechanisms		
Aircraft: ElectraWing	Date/Location: 10-Mar-18	Supervising Test Engineer SRW	
Test Objectives: To test the flight characteristics of the modified Anaconda	Weather: Wind (knots): 12/S Temperature: 70 F Barometric Pressure: 29.702 inHg	Limits: 1. < 10 minutes 2. < 400 ft AGL 4. < 17 knots wind	
Configuration: 1. Direct RC input/no Pixhawk 2. Wing rotational mechanism in place 3. Horizontal stab. mechanism in place 4. Elevators locked out - using stabilator	Notes: This test is to determine takeoff roll distance with 0 degrees of wing rotation.		
Frequencies: 2.4GHz	Weight & Balance: CG Measured (est.): 30% CG Calculated: 32%	TOW lbs: 10.9	

PROCEDURE

Start Time:	3:21pm	End Time:	3:22pm
1	Takeoff with full throttle and 0 degrees of wing rotation		
2	Once positive rate of climb is estabilished, slowly rotate wings back to 0 degrees		
3	Immediately land aircraft CTOL		
4	Line up on the takeoff mark and repeat steps 1 through 3		
5			
6			
7			
8			
9			

# Takeoff/Landing	Comments	Issues
2	The aircraft took off in approximately 91ft. It was stable throught the entire flight. No adverse reactions with the wing or horizontal stabilizer rotational mechanisms	N/A

Test Sortie:	Short Takeoff Test w/ Rotational Mechanisms	
Aircraft: ElectraWing	Date/Location: 10-Mar-18	Supervising Test Engineer SRW

Test Objectives:	Weather:		Limits:
To test the flight characteristics of the modified Anaconda	Wind (knots): Temperature: Barometric Pressure:	6/SE & 8/ESE 70 F 29.702 inHg	1. < 10 minutes 2. < 400 ft AGL 4. < 17 knots wind

Configuration:	Notes:
1. Direct RC input/no Pixhawk 2. Wing rotational mechanism in place 3. Horizontal stab. mechanism in place 4. Elevators locked out - using stabilator	This test is to determine takeoff roll distance with 20 degrees of wing rotation.

Frequencies:	Weight & Balance:		TOW lbs:
2.4GHz	CG Measured (est.):	30%	10.9
	CG Calculated:	32%	

PROCEDURE

Start Time:	2:21pm	End Time:	2:25pm

1	Takeoff with full throttle and 20 degrees of wing rotation
2	Once positive rate of climb is estabilished, slowly rotate wings back to 0 degrees
3	Immediately land aircraft CTOL
4	Line up on the takeoff mark and repeat steps 1 through 3
5	
6	
7	
8	
9	

# Takeoff/Landing	Comments	Issues
2	At 20 degrees of wing rotation, the aircraft took off only slightly shorter than the CTOL configuration. However, the headwind component for this flight was much less than it was for the other configurations.	The aircraft became somewhat unstable in the roll while departing the ground. This instability started to go away as the aircraft gained airspeed and a positive rate of climb.

Test Sortie:	Short Takeoff & Landing Test w/ Rotational Mechanisms	
Aircraft: ElectraWing	Date/Location: 10-Mar-18	Supervising Test Engineer SRW

Test Objectives:	Weather:		Limits:
To test the flight characteristics of the modified Anaconda	Wind (knots): Temperature: Barometric Pressure:	10/SSE & 7/SS 70 F 29.702 inHg	1. < 10 minutes 2. < 400 ft AGL 4. < 17 knots wind

Configuration:	Notes:
1. Direct RC input/no Pixhawk 2. Wing rotational mechanism in place 3. Horizontal stab. mechanism in place 4. Elevators locked out - using stabilator	This test is to determine takeoff roll distance with 30 degrees of wing rotation.

Frequencies:	Weight & Balance:		TOW lbs:
2.4GHz	CG Measured (est.):	30%	10.9
	CG Calculated:	32%	

PROCEDURE

Start Time:	2:25pm	End Time:	3:27pm
1	Takeoff with full throttle and 30 degrees of wing rotation		
2	Once positive rate of climb is estabilished, slowly rotate wings back to 0 degrees		
3	Immediately land aircraft CTOL		
4	Line up on the takeoff mark and repeat steps 1 and 2, and skip to step 5		
5	Slowly rotate the wings on final as the aircraft gets close to the runway		
6			
7			
8			
9			

# Takeoff/Landing	Comments	Issues
2	For the 30-degree wing rotation case, the aircraft left the ground after a significantly shorter takeoff roll than the conventional takeoff. The aircraft stopped significantly shorter on the runway when the short landing was attempted. This was probably due to both the wing rotatio and the multiple wingtip strikes.	1. The aircraft was fairly difficult to control (in roll) as it became unstable. 2. The aircraft was unable to leave ground effect on takeoff. 3. the aircraft immediately became unstable while rotating the wings during landing.

Test Sortie:	Indoor VTOL Flight Testing & Gain Tuning	
Aircraft: ElectraWing	Date/Location: 4-Apr-18 & 5-Apr-18 Richmond Hills Facility	Supervising Test Engineer SRW

Test Objectives:	Weather:		Limits:
To test the flight characteristics of the modified Anaconda	Wind (knots): Temperature: Barometric Pressure:	0 N/A N/A	1. < 10 minutes 2. < 400 ft AGL 4. < 17 knots wind

Configuration:	Notes:
1. Arduplane 3.9.0 firmware 2. Pixhawk 3. GPS 4. Airspeed sensor 5. Wing rotation mechanism 6. Horizontal stab. Rotation mechanism	This session is to tune the gains indoors before taking the aircraft outside where it will face wind.

Frequencies:	Weight & Balance:		TOW lbs:
2.4GHz	CG Measured (est.):	25%	11.6
900Mhz	CG Calculated:	28%	

PROCEDURE

Start Time:	N/A	End Time:	N/A

1	Take off vertically and observe hovering qualities
2	Try giving minor inputs to controls
3	Land
4	Tune gains
5	Repeat steps 1 through 4 as needed
6	
7	
8	
9	

# Takeoff/Landing	Comments	Issues
3	The gains proved difficult to tune manually. Q_AZ parameter had a significant effect on the stability. The aircraft was finally able to maintain a hover.	No yaw control due to all motors counter rotating. This was done because of the asymmetry of the aiframe in the vertical configuration.

Test Sortie:	Outdoor VTOL Flight Testing & Gain Tuning	
Aircraft: ElectraWing	Date/Location: 5-Apr-18 OSU UAS Flight Field	Supervising Test Engineer SRW

Test Objectives:	Weather:		Limits:
To test the flight characteristics of the modified Anaconda	Wind (knots): Temperature: Barometric Pressure:	9/SE 67 F 29.892 inHg	1. < 10 minutes 2. < 400 ft AGL 4. Unknown wind limit

Configuration:	Notes:
1. Arduplane 3.9.0 firmware 2. Pixhawk 3. GPS 4. Airspeed sensor 5. Wing rotation mechanism 6. Horizontal stab. Rotation mechanism	These tests were to determine the stability of the aircraft in outdoor conditions and tune the gains if need be.

Frequencies:	Weight & Balance:		TOW lbs:
2.4GHz	CG Measured (est.):	25%	11.6
900Mhz	CG Calculated:	28%	

PROCEDURE

Start Time:	5:00pm	End Time:	5:15pm
1	Take off vertically and observe hovering qualities		
2	Try giving minor inputs to controls		
3	Land		
4	Tune gains		
5	Repeat steps 1 through 4 as needed		
6			
7			
8			
9			

# Takeoff/Landing	Comments	Issues
Lost track.	The "I" gain was lowered which seemed to make the aircraft hover reliably in the wind.	Even a slight wind significantly blew the aircraft backwards (nose pionted into the wind) while on the ground. After takeoff, the aircraft would get blown back a little before recovering.

Test Sortie:	Outdoor VTOL Flight & Transition to Forward Flight		
Aircraft: ElectraWing	Date/Location: 5-Apr-18 OSU UAS Flight Field	Supervising Test Engineer SRW	
Test Objectives: To test the flight characteristics of the modified Anaconda	Weather: Wind (knots): 9/SE Temperature: 67 F Barometric Pressure: 29.892 inHg	Limits: 1. < 10 minutes 2. < 400 ft AGL 4. Unknown wind limit	
Configuration: 1. Arduplane 3.9.0 firmware 2. Pixhawk 3. GPS 4. Airspeed sensor 5. Wing rotation mechanism 6. Horizontal stab. Rotation mechanism	Notes: This test will be to take off vertically, and test the transition to forward flight.		
Frequencies: 2.4GHz 900Mhz	Weight & Balance: CG Measured (est.): 25% CG Calculated: 28%	TOW lbs: 11.6	

PROCEDURE

Start Time:	5:00pm	End Time:	5:15pm
1	Take off vertically in Q_STABILIZE mode		
2	Fly vertically up to about 5 ft AGL		
3	Switch aircraft to FBWA		
4	After transition is complete, switch to MANUAL mode		
5	Switch aircraft to FBWA		
6	Fly up to about 200 ft AGL		
7	Switch aircraft to Q_STABILIZE		
8	Descend		
9	Land		

# Takeoff/Landing	Comments	Issues
1	Aircraft took off, and started the transition perfectly. However became abruptly unstable and crashed.	Aircraft crashed after a couple oscillations. Aircraft visually did not appear to be attempting to correct itself.

VITA

Seabrook Randolph Whyte

Candidate for the Degree of

Master of Science

Thesis: FLIGHT CHARACTERISTICS OF A TILT-WING, DISTRIBUTED-PROPULSION, VERTICAL TAKE-OFF AND LANDING AIRCRAFT CONCEPT

Major Field: Aerospace Engineering

Education:

Completed the requirements for the Master of Science in Mechanical & Aerospace engineering with an Unmanned Aerial Systems Option at Oklahoma State University, Stillwater, Oklahoma in May 2018.

Completed the requirements for the Bachelor of Science in Aerospace Engineering at Oklahoma State University, Stillwater, Oklahoma in 2015.